EUROPEAN ORGANIZATION FOR PARTICLE PHYSICS

CERN-EP/99-15
8 Feb 1999

# A Combination of Preliminary Electroweak Measurements and Constraints on the Standard Model

**The LEP Collaborations* ALEPH, DELPHI, L3, OPAL, the LEP Electroweak Working Group† and the SLD Heavy Flavour and Electroweak Groups‡**

**Prepared from Contributions of the LEP and SLD experiments to the 1998 Summer conferences.**

**Abstract**

This note presents a combination of published and preliminary electroweak results from the four LEP collaborations and the SLD collaboration which were prepared for the 1998 summer conferences. Averages are derived for hadronic and leptonic cross-sections, the leptonic forward-backward asymmetries, the $\tau$ polarisation asymmetries, the $b\overline{b}$ and $c\overline{c}$ partial widths and forward-backward asymmetries and the $q\overline{q}$ charge asymmetry. The major changes with respect to results presented in summer 1997 are updates to the measurements of the Z lineshape, tau polarisation, W mass and triple-gauge-boson couplings from LEP, and $A_{\rm LR}$ from SLD. The results are compared with precise electroweak measurements from other experiments. A significant update here is a new measurement of the mixing angle from the NuTeV Collaboration. The parameters of the Standard Model are evaluated, first using the combined LEP electroweak measurements, and then using the full set of electroweak results.

*The LEP Collaborations each take responsibility for the preliminary data of their own experiment.

†D. Abbaneo, J. Alcaraz, P. Antilogus, T. Behnke, G. Bella, B. Bertucci, B. Bloch-Devaux, D. Bloch, A. Blondel, D.G. Charlton, R. Clare, G. Duckeck, M. Elsing, R. Faccini, D. Glenzinski, M.W. Grünewald, A. Gurtu, J.B. Hansen, R. Hawkings, R.W.L. Jones, P. de Jong, D. Karlen, T. Kawamoto, R.G. Kellogg, N. Kjaer, M. Kobel, E. Lançon, W. Lohmann, L. Malgeri, C. Mariotti, M. Martinez, C. Matteuzzi, M. McCubbin, M.N. Minard, K. Mönig, P. Molnar, F. Muheim, S. Olshevski, Ch. Paus, M. Pepe-Altarelli, S. Petzold, B. Pietrzyk, H. Przysiezniak, G. Quast, D. Reid, P. Renton, J.M. Roney, D. Strom, R. Sekulin, R. Tenchini, F. Teubert, M.A. Thomson, J. Timmermans, M. Verzocchi, H. Wahlen, N.K. Watson, P.S. Wells, S. Wynhoff.

‡K. Baird, S. Fahey, N. de Groot, P.C. Rowson, B. Schumm, D. Su.

# 1 Introduction

The four LEP experiments have previously presented [1] parameters derived from the Z resonance using published and preliminary results based on data recorded until the end of 1995. Since then additional results have become available. To allow a quick assessment, a box highlighting the updates is given at the beginning of each section. During 1996 LEP ran at energies of 161 and 172 GeV, allowing the production of W boson pairs for the first time in high energy $e^+e^-$ collisions. In 1997, the energy was further increased to approximately 183 GeV, and significantly more luminosity was collected. Using these data the measurements of W boson properties have been updated. Published and preliminary fermion pair production cross-section and asymmetry results from data taken in 1995 and 1996 at energies well above the Z resonance are also included which are particularly sensitive to the $\gamma$Z interference. These results are denoted as LEP-II results.

The LEP-I data (1990-1995) consist of the hadronic and leptonic cross-sections, the leptonic forward-backward asymmetries, the $\tau$ polarisation asymmetries, the $b\overline{b}$ and $c\overline{c}$ partial widths and forward-backward asymmetries and the $q\overline{q}$ charge asymmetry. The measurements of the $b\overline{b}$ and $c\overline{c}$ partial widths and left-right-forward-backward asymmetries for b and c quarks from SLD are treated consistently with the LEP data. Many technical aspects of their combination have already been described in References 2, 3 and references therein.

This note is organised as follows:

**Section 2** Z line shape and leptonic forward-backward asymmetries;

**Section 3** $\tau$ polarisation;

**Section 4** Heavy flavour analyses;

**Section 5** Inclusive hadronic charge asymmetry;

**Section 6** $A_{\mathrm{LR}}$ measurement at SLD;

**Section 7** W-boson properties, including $m_{\mathrm{W}}$, branching ratios, production cross-sections and anomalous triple-gauge-boson couplings;

**Section 8** Interpretation of the results, including the combination of results from LEP, SLD, neutrino interaction experiments and from CDF and DØ;

**Section 9** Prospects for the future.

## 2 Z Lineshape and Lepton Forward-Backward Asymmetries

**Updates with respect to last summer:**
ALEPH, DELPHI and OPAL have updated their results using the full data sets and the final LEP energies.

### 2.1 Results from the Z Peak Data

The results presented here are based on data accumulated through 1995. This includes the data taken during the energy scans in 1990 and 1991 in the range[1] $|\sqrt{s} - m_{\mathrm{Z}}| < 3$ GeV, the data collected at the Z peak in 1992 and preliminary analyses of the energy scans in 1993 and 1995 ($|\sqrt{s} - m_{\mathrm{Z}}| < 1.8$ GeV) and the peak running in 1994. The total statistics and the systematic errors on the individual analyses of the four LEP collaborations are given in Tables 1 and 2. Details of the individual analyses can be found in References 4–7.

| | | ALEPH | DELPHI | L3 | OPAL | LEP |
|---|---|---|---|---|---|---|
| $\mathrm{q\overline{q}}$ | '90-'91 | 433 | 357 | 416 | 454 | 1660 |
| | '92 | 633 | 697 | 678 | 733 | 2741 |
| | '93 prel. | 630 | 682 | 646 | 642 | 2600 |
| | '94 prel. | 1640 | 1310 | 1307 | 1585 | 5842 |
| | '95 prel. | 735 | 659 | 311 | 652 | 2357 |
| | total | 4071 | 3705 | 3358 | 4066 | 15200 |
| $\ell^+\ell^-$ | '90-'91 | 53 | 36 | 40 | 58 | 187 |
| | '92 | 77 | 70 | 58 | 88 | 293 |
| | '93 prel. | 78 | 75 | 64 | 79 | 296 |
| | '94 prel. | 202 | 137 | 127 | 191 | 657 |
| | '95 prel. | 90 | 66 | 28 | 81 | 265 |
| | total | 500 | 384 | 317 | 497 | 1698 |

Table 1: LEP statistics in units of $10^3$ events used for the analysis of the Z line shape and lepton forward-backward asymmetries. Not all experiments have used the full 1995 data set for the present results, in particular this applies to the data recorded before the start of the high precision energy scan.

For the averaging of results the LEP experiments provide a standard set of 9 parameters describing the information contained in hadronic and leptonic cross sections and leptonic forward-backward asymmetries [2, 10]. These parameters are convenient for fitting and averaging since they have small correlations. They are:

- The mass and total width of the Z boson, where the definition is based on the Breit-Wigner denominator ($s - m_{\mathrm{Z}}^2 + is\Gamma_{\mathrm{Z}}/m_{\mathrm{Z}}$) ($s$-dependent width) [11].
- The hadronic pole cross-section of Z exchange:

$$\sigma_{\mathrm{h}}^0 \equiv \frac{12\pi}{m_{\mathrm{Z}}^2}\frac{\Gamma_{\mathrm{ee}}\Gamma_{\mathrm{had}}}{\Gamma_{\mathrm{Z}}^2}\,. \tag{1}$$

Here $\Gamma_{\mathrm{ee}}$ and $\Gamma_{\mathrm{had}}$ are the partial widths of the Z for decays into electrons and hadrons.

[1] In this note $\hbar = c = 1$.

| | ALEPH | | | DELPHI | | | L3 | | | OPAL | | |
|---|---|---|---|---|---|---|---|---|---|---|---|---|
| | '93 prel. | '94 prel. | '95 prel. | '93 prel. | '94 prel. | '95 prel. | '93 prel. | '94 prel. | '95 prel. | '93 prel. | '94 prel. | '95 prel. |
| $\mathcal{L}^{\text{exp. }(a)}$ | 0.067% | 0.073% | 0.080% | 0.24% | 0.09% | 0.09% | 0.10% | 0.078% | 0.128% | 0.033% | 0.033% | 0.034% |
| $\sigma_{\text{had}}$ | 0.069% | 0.072% | 0.073% | 0.10% | 0.10% | 0.10% | 0.052% | 0.051% | 0.10% | 0.072% | 0.072% | 0.084% |
| $\sigma_{\text{e}}$ | 0.18% | 0.16% | 0.18% | 0.46% | 0.52% | 0.52% | 0.30% | 0.23% | 0.17% | 0.17% | 0.14% | 0.16 |
| $\sigma_{\mu}$ | 0.11% | 0.09% | 0.11% | 0.28% | 0.26% | 0.28% | 0.31% | 0.31% | 0.16% | 0.16% | 0.10% | 0.12 |
| $\sigma_{\tau}$ | 0.26% | 0.18% | 0.25% | 0.60% | 0.60% | 0.60% | 0.67% | 0.65% | 0.48% | 0.48% | 0.42% | 0.48 |
| $A_{\text{FB}}^{\text{e}}$ | 0.0012 | 0.0012 | 0.0012 | 0.0026 | 0.0021 | 0.0020 | 0.003 | 0.003 | 0.01 | 0.001 | 0.001 | 0.001 |
| $A_{\text{FB}}^{\mu}$ | 0.0005 | 0.0005 | 0.0005 | 0.0009 | 0.0005 | 0.0010 | 0.0008 | 0.0008 | 0.005 | 0.001 | 0.001 | 0.001 |
| $A_{\text{FB}}^{\tau}$ | 0.0009 | 0.0007 | 0.0009 | 0.0020 | 0.0020 | 0.0020 | 0.003 | 0.003 | 0.003 | 0.0012 | 0.0012 | 0.0012 |

Table 2: Experimental systematic errors for the analysis of the Z line shape and lepton forward-backward asymmetries at the Z peak. The errors quoted do not include the common uncertainty due to the LEP energy calibration. The treatment of correlations between the errors for different years is described in References 4–7.
$^{(a)}$In addition, there is a theoretical error for the calculation of the small angle Bhabha cross-section of 0.11% [8], which has been treated as common to all experiments. In the future, this error should be significantly smaller [9].

- The ratios:
$$R_{\text{e}} \equiv \Gamma_{\text{had}}/\Gamma_{\text{ee}}, \quad R_{\mu} \equiv \Gamma_{\text{had}}/\Gamma_{\mu\mu} \text{ and } R_{\tau} \equiv \Gamma_{\text{had}}/\Gamma_{\tau\tau}. \tag{2}$$
Here $\Gamma_{\mu\mu}$ and $\Gamma_{\tau\tau}$ are the partial widths of the Z for the decays $\text{Z} \to \mu^+\mu^-$ and $\text{Z} \to \tau^+\tau^-$. Due to the large mass of the $\tau$ lepton, a small difference of 0.2% is expected between the values for $R_{\text{e}}$ and $R_{\mu}$, and the value for $R_{\tau}$, even under the assumption of lepton universality [12].

- The pole asymmetries, $A_{\text{FB}}^{0,\text{e}}$, $A_{\text{FB}}^{0,\mu}$ and $A_{\text{FB}}^{0,\tau}$, for the processes $\text{e}^+\text{e}^- \to \text{e}^+\text{e}^-$, $\text{e}^+\text{e}^- \to \mu^+\mu^-$ and $\text{e}^+\text{e}^- \to \tau^+\tau^-$. In terms of the real parts of the effective vector and axial-vector neutral current couplings of fermions, $g_{V\text{f}}$ and $g_{A\text{f}}$, the pole asymmetries are expressed as:
$$A_{\text{FB}}^{0,\text{f}} \equiv \frac{3}{4}\mathcal{A}_{\text{e}}\mathcal{A}_{\text{f}} \tag{3}$$
with:
$$\mathcal{A}_{\text{f}} \equiv \frac{2g_{V\text{f}}g_{A\text{f}}}{g_{V\text{f}}^2 + g_{A\text{f}}^2}\,. \tag{4}$$

The imaginary parts of the vector and axial-vector coupling constants as well as real and imaginary parts of the photon vacuum polarisation are accounted for explicitly in the fitting formulae and are fixed to their Standard Model values.

The fitting procedure takes into account effects of initial-state radiation [11] as well as $t$-channel and $s/t$ interference contributions in the case of $\text{e}^+\text{e}^-$ final states. Corrections to $\mathcal{O}(\alpha^3)$ [13–15] have now been included in the procedure. These corrections modify the cross-sections by approximately one per-mille. As they are asymmetric around the Z peak, they also modify the mass and width of the Z boson. For the moment, these corrections are still under study, so the central values of the fits have not been modified. Instead, the full difference between including the corrections or not has been used as a systematic error. This amounts to 0.5 MeV on $m_{\text{Z}}$, 0.6 MeV on $\Gamma_{\text{Z}}$ and 0.021 nb on $\sigma_{\text{h}}^0$. The theoretical error on the $t$-channel contribution has also been evaluated [16]. This error source is now treated as a common systematic error. In addition, correlations are now considered between $A_{\text{FB}}^{0,\text{e}}$ and $R_{\text{e}}$. This effect is also still under study.

The set of 9 parameters does not describe hadron and lepton-pair production completely, because it does not include the interference of the $s$-channel Z exchange with the $s$-channel $\gamma$ exchange. For the results presented in this section and used in the rest of the note, the $\gamma$-exchange contributions and the hadronic $\gamma$Z interference terms are fixed to their Standard Model values. The leptonic $\gamma$Z

interference terms are expressed in terms of the effective couplings. An alternative analysis, where all $\gamma$Z interference terms are independently determined from the LEP data, is presented in Section 2.2.

The four sets of 9 parameters provided by the LEP experiments are presented in Table 3. The covariance matrix of these parameters is constructed as described in Reference 10. It is constructed from the covariance matrices of the individual LEP experiments and common systematic errors. These common errors arise from the theoretical uncertainty in the luminosity normalisation affecting the hadronic pole cross-section, $\Delta\sigma^0_{\rm h}/\sigma^0_{\rm h} = 0.11\%$, from the uncertainty of the LEP centre-of-mass energy spread of about 1 MeV [17], resulting in $\Delta\Gamma_{\rm Z} \approx 0.2$ MeV, and from the uncertainty in the LEP energy calibration. The combined parameter set and its correlation matrix are given in Tables 4 and 5.

| | ALEPH | DELPHI | L3[(a)] | OPAL |
|---|---|---|---|---|
| $m_{\rm Z}$(GeV) | 91.1884±0.0031 | 91.1866±0.0029 | 91.1883±0.0029 | 91.1848±0.0030 |
| $\Gamma_{\rm Z}$(GeV) | 2.4950±0.0043 | 2.4872±0.0041 | 2.4996±0.0043 | 2.4939±0.0040 |
| $\sigma^0_{\rm h}$(nb) | 41.519±0.067 | 41.553±0.079 | 41.411±0.074 | 41.474±0.068 |
| $R_{\rm e}$ | 20.688±0.074 | 20.87±0.12 | 20.78±0.11 | 20.924±0.095 |
| $R_\mu$ | 20.815±0.056 | 20.67±0.08 | 20.84±0.10 | 20.819±0.058 |
| $R_\tau$ | 20.719±0.063 | 20.78±0.13 | 20.75±0.14 | 20.855±0.086 |
| $A^{0,\,{\rm e}}_{\rm FB}$ | 0.0181±0.0033 | 0.0189±0.0048 | 0.0148±0.0063 | 0.0069±0.0051 |
| $A^{0,\,\mu}_{\rm FB}$ | 0.0170±0.0025 | 0.0160±0.0025 | 0.0176±0.0035 | 0.0156±0.0025 |
| $A^{0,\,\tau}_{\rm FB}$ | 0.0166±0.0028 | 0.0244±0.0037 | 0.0233±0.0049 | 0.0143±0.0030 |
| $\chi^2$/d.o.f. | 169/176 | 179/168 | 142/159 | 158/202 |

Table 3: Line shape and asymmetry parameters from 9-parameter fits to the data of the four LEP experiments.
[(a)]These results use the energies as given in Ref. [18]. L3 has estimated that using the new energies the mass would shift by +0.3 MeV and the width by +0.3 MeV, and these values have been used in subsequent fits.

| Parameter | Average Value |
|---|---|
| $m_{\rm Z}$(GeV) | 91.1867±0.0021 |
| $\Gamma_{\rm Z}$(GeV) | 2.4939±0.0024 |
| $\sigma^0_{\rm h}$(nb) | 41.491±0.058 |
| $R_{\rm e}$ | 20.783±0.052 |
| $R_\mu$ | 20.789±0.034 |
| $R_\tau$ | 20.764±0.045 |
| $A^{0,\,{\rm e}}_{\rm FB}$ | 0.0153±0.0025 |
| $A^{0,\,\mu}_{\rm FB}$ | 0.0164±0.0013 |
| $A^{0,\,\tau}_{\rm FB}$ | 0.0183±0.0017 |

Table 4: Average line shape and asymmetry parameters from the data of the four LEP experiments given in Table 3, without the assumption of lepton universality. The $\chi^2$/d.o.f. of the average is 28/27.

The measurement of the LEP beam energies, and the associated uncertainties, are important in the determination of the mass and width of the Z. In earlier notes the treatment of the LEP energies was based on Reference 18. Since then, the studies of the sources of uncertainty in the energy measurements have been finalized [19]. The ALEPH, DELPHI and OPAL collaborations have reanalysed their data using these new determinations of energies and errors. L3 have not yet updated their analyses, but have estimated the impact on $m_{\rm Z}$ and $\Gamma_{\rm Z}$ from changes in the overall energy scale; however, improvements due to reduced LEP energy errors have not been included in their results. The uncertainty causes errors of $\Delta m_{\rm Z} \approx 1.7$ MeV and $\Delta\Gamma_{\rm Z} \approx 1.3$ MeV [19].

| | $m_{\rm Z}$ | $\Gamma_{\rm Z}$ | $\sigma^0_{\rm h}$ | $R_{\rm e}$ | $R_\mu$ | $R_\tau$ | $A^{0,\rm e}_{\rm FB}$ | $A^{0,\mu}_{\rm FB}$ | $A^{0,\tau}_{\rm FB}$ |
|---|---|---|---|---|---|---|---|---|---|
| $m_{\rm Z}$ | 1.000 | 0.000 | −0.040 | 0.002 | −0.010 | −0.006 | 0.016 | 0.045 | 0.038 |
| $\Gamma_{\rm Z}$ | 0.000 | 1.000 | −0.184 | −0.007 | 0.003 | 0.003 | 0.009 | 0.000 | 0.003 |
| $\sigma^0_{\rm h}$ | −0.040 | −0.184 | 1.000 | 0.058 | 0.094 | 0.070 | 0.006 | 0.002 | 0.005 |
| $R_{\rm e}$ | 0.002 | −0.007 | 0.058 | 1.000 | 0.098 | 0.073 | −0.442 | 0.007 | 0.012 |
| $R_\mu$ | −0.010 | 0.003 | 0.094 | 0.098 | 1.000 | 0.105 | 0.001 | 0.010 | −0.001 |
| $R_\tau$ | −0.006 | 0.003 | 0.070 | 0.073 | 0.105 | 1.000 | 0.002 | 0.000 | 0.020 |
| $A^{0,\rm e}_{\rm FB}$ | 0.016 | 0.009 | 0.006 | −0.442 | 0.001 | 0.002 | 1.000 | −0.008 | −0.006 |
| $A^{0,\mu}_{\rm FB}$ | 0.045 | 0.000 | 0.002 | 0.007 | 0.010 | 0.000 | −0.008 | 1.000 | 0.029 |
| $A^{0,\tau}_{\rm FB}$ | 0.038 | 0.003 | 0.005 | 0.012 | −0.001 | 0.020 | −0.006 | 0.029 | 1.000 |

Table 5: The correlation matrix for the set of parameters given in Table 4.

The estimation of the common errors which arise from the LEP energy calibration is more complicated than in previous years because the energy was better determined in 1995 than in 1993. The procedure adopted changed with respect to the previous note [20] as it was found that the old method slightly underestimated the common uncertainties. As before, two fits are performed to the data from a single experiment. In one fit all errors except those due to the LEP energy uncertainty are scaled by a factor $\sqrt{1+\varepsilon}$ while in the other they are scaled by a factor $\sqrt{1-\varepsilon}$. The procedure results in two covariance matrices, $V_1 = V_E + V_O(1+\varepsilon)$ and $V_2 = V_E + V_O(1-\varepsilon)$, where $V_E$ contains the components due to energy and $V_O$ contains all other components. From this $V_E$ is obtained algebraically

$$V_E = (V_2(1+\varepsilon) - V_1(1-\varepsilon))/2\varepsilon$$

and is then used as a correlated part of the full covariance matrix when combining the data from experiments. This procedure ensures a proper weighting of statistical and systematic errors for small $\varepsilon$.

If lepton universality is assumed, the set of 9 parameters given above is reduced to a set of 5 parameters. $R_\ell$ is defined as $R_\ell \equiv \Gamma_{\rm had}/\Gamma_{\ell\ell}$, where $\Gamma_{\ell\ell}$ refers to the partial Z width for the decay into a pair of massless charged leptons. The data of each of the four LEP experiments are consistent with lepton universality (the difference in $\chi^2$ over the difference in d.o.f. with and without the assumption of lepton universality is 4/4, 4/4, 2/4 and 3/4 for ALEPH, DELPHI, L3 and OPAL, respectively). Table 6 gives the five parameters $m_{\rm Z}$, $\Gamma_{\rm Z}$, $\sigma^0_{\rm h}$, $R_\ell$ and $A^{0,\ell}_{\rm FB}$ for the individual LEP experiments, assuming lepton universality. Tables 7 and 8 give the combined result and the corresponding correlation matrix. Figure 1 shows, for each lepton species and for the combination assuming lepton universality, the resulting 68% probability contours in the $R_\ell$-$A^{0,\ell}_{\rm FB}$ plane. For completeness the partial decay widths of the Z boson are listed in Table 9.

| | ALEPH | DELPHI | L3[(a)] | OPAL |
|---|---|---|---|---|
| $m_{\rm Z}$(GeV) | 91.1883±0.0031 | 91.1864±0.0029 | 91.1883±0.0029 | 91.1843±0.0029 |
| $\Gamma_{\rm Z}$(GeV) | 2.4949±0.0043 | 2.4873±0.0041 | 2.4996±0.0043 | 2.4940±0.0040 |
| $\sigma^0_{\rm h}$(nb) | 41.519±0.067 | 41.553±0.079 | 41.411±0.074 | 41.474±0.068 |
| $R_\ell$ | 20.738±0.038 | 20.728±0.060 | 20.788±0.066 | 20.828±0.045 |
| $A^{0,\ell}_{\rm FB}$ | 0.0169±0.0016 | 0.0187±0.0019 | 0.0187±0.0026 | 0.0141±0.0017 |
| $\chi^2$/d.o.f. | 173/180 | 184/172 | 144/163 | 160/206 |

Table 6: Line shape and asymmetry parameters from 5-parameter fits to the data of the four LEP experiments, assuming lepton universality. $R_\ell$ is defined as $R_\ell \equiv \Gamma_{\rm had}/\Gamma_{\ell\ell}$, where $\Gamma_{\ell\ell}$ refers to the partial Z width for the decay into a pair of massless charged leptons.
[(a)]These results use the energies as given in Ref. [18]. L3 has estimated that using the new energies the mass would shift by +0.3 MeV and the width by +0.3 MeV, and these values have been used in subsequent fits.

| Parameter | Average Value |
|---|---|
| $m_{\rm Z}$(GeV) | 91.1867±0.0021 |
| $\Gamma_{\rm Z}$(GeV) | 2.4939±0.0024 |
| $\sigma^0_{\rm h}$(nb) | 41.491±0.058 |
| $R_\ell$ | 20.765±0.026 |
| $A^{0,\ell}_{\rm FB}$ | 0.01683±0.00096 |

Table 7: Average line shape and asymmetry parameters from the results of the four LEP experiments given in Table 6, assuming lepton universality. $R_\ell$ is defined as $R_\ell \equiv \Gamma_{\rm had}/\Gamma_{\ell\ell}$, where $\Gamma_{\ell\ell}$ refers to the partial Z width for the decay into a pair of massless charged leptons. The $\chi^2$/d.o.f. of the average is 31/31.

| | $m_{\rm Z}$ | $\Gamma_{\rm Z}$ | $\sigma^0_{\rm h}$ | $R_\ell$ | $A^{0,\ell}_{\rm FB}$ |
|---|---|---|---|---|---|
| $m_{\rm Z}$ | 1.000 | 0.000 | −0.040 | −0.010 | 0.062 |
| $\Gamma_{\rm Z}$ | 0.000 | 1.000 | −0.184 | 0.002 | 0.004 |
| $\sigma^0_{\rm h}$ | −0.040 | −0.184 | 1.000 | 0.123 | 0.006 |
| $R_\ell$ | −0.010 | 0.002 | 0.123 | 1.000 | −0.072 |
| $A^{0,\ell}_{\rm FB}$ | 0.062 | 0.004 | 0.006 | −0.072 | 1.000 |

Table 8: The correlation matrix for the set of parameters given in Table 7.

| Without Lepton Universality | | |
|---|---|---|
| $\Gamma_{\rm ee}$ | (MeV) | 83.87±0.14 |
| $\Gamma_{\mu\mu}$ | (MeV) | 83.84±0.18 |
| $\Gamma_{\tau\tau}$ | (MeV) | 83.94±0.22 |
| **With Lepton Universality** | | |
| $\Gamma_{\ell\ell}$ | (MeV) | 83.90±0.10 |
| $\Gamma_{\rm had}$ | (MeV) | 1742.3±2.3 |
| $\Gamma_{\rm inv}$ | (MeV) | 500.1±1.9 |

Table 9: Partial decay widths of the Z boson, derived from the results of the 9-parameter (Tables 4 and 5) and the 5-parameter fit (Tables 7 and 8). In the case of lepton universality, $\Gamma_{\ell\ell}$ refers to the partial Z width for the decay into a pair of massless charged leptons.

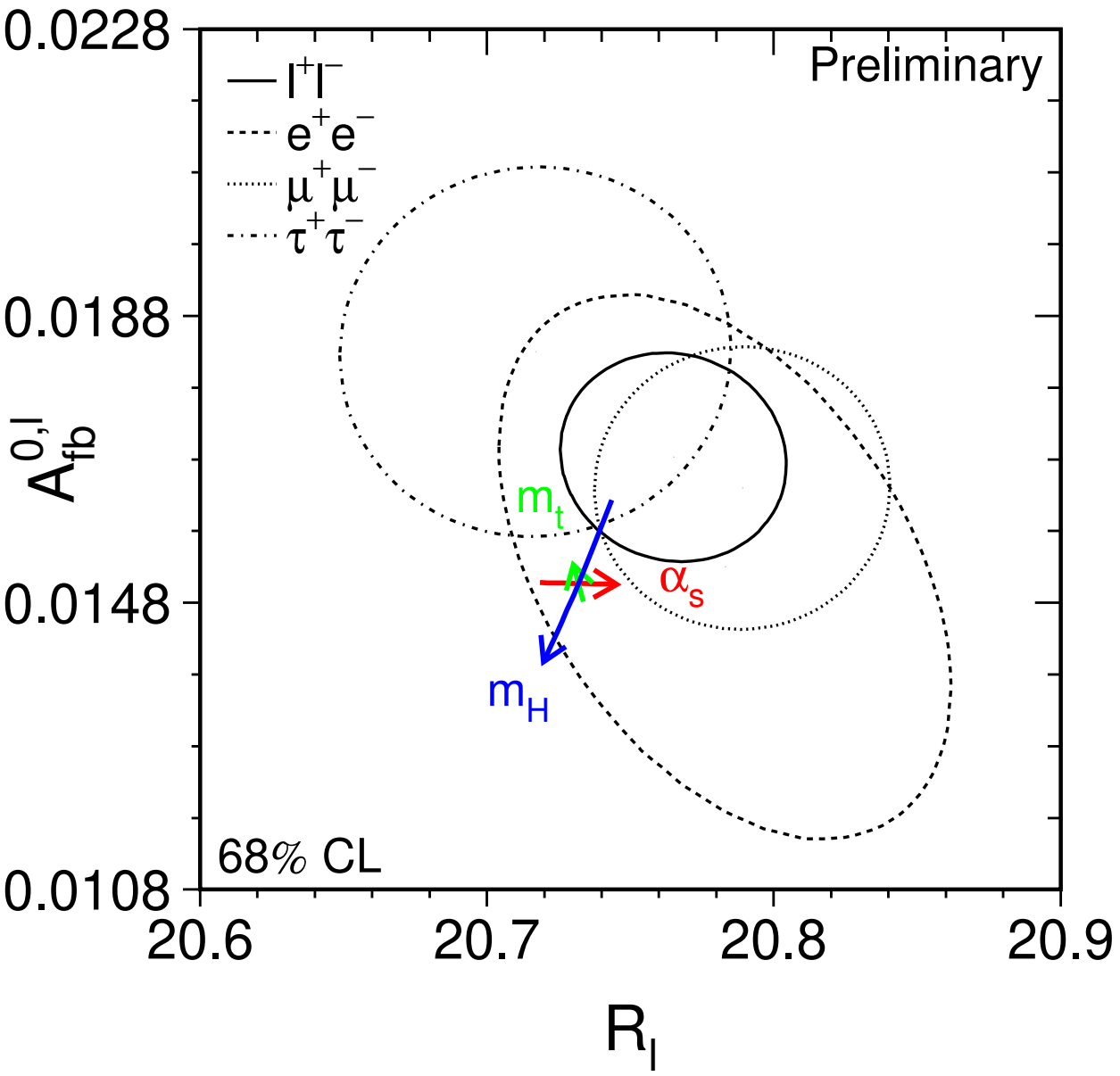


Figure 1: Contours of 68% probability in the $R_\ell$-$A_{\rm FB}^{0,\ell}$ plane. For better comparison the results for the $\tau$ lepton are corrected to correspond to the massless case. The Standard Model prediction for $m_{\rm Z} = 91.1867$ GeV, $m_{\rm t} = 173.8$ GeV, $m_{\rm H} = 300$ GeV, and $\alpha_{\rm s}(m_{\rm Z}^2) = 0.119$ is also shown. The lines with arrows correspond to the variation of the Standard Model prediction when $m_{\rm t}$, $m_{\rm H}$ or $\alpha_{\rm s}(m_{\rm Z}^2)$ are varied in the intervals $m_{\rm t} = 173.8 \pm 5.0$ GeV, $m_{\rm H} = 300^{+700}_{-210}$ GeV, and $\alpha_{\rm s}(m_{\rm Z}^2) = 0.119 \pm 0.002$, respectively. The arrows point in the direction of increasing values of $m_{\rm t}$, $m_{\rm H}$ and $\alpha_{\rm s}$.

## 2.2 Measurement of $\gamma$Z Interference including LEP-II Data

In Section 2.1 a model dependence is introduced into the parameterisation of the lineshape and asymmetries by the treatment of the $\gamma$Z interference contribution to the hadronic cross-section, because quark couplings to the Z are not individually measured for each flavour. This term is therefore taken from the Standard Model. A more general approach is to parameterise the $\gamma$Z interference term independently of the Z exchange amplitude. Several model independent formalisms exist [21, 22]. For the analysis performed here the framework described in Reference 22 based on the S-Matrix ansatz is used.

In addition to the measurements of cross-section and forward-backward asymmetry in the vicinity of the Z resonance (LEP-I) the results from the 1995 and 1996 LEP runs at centre-of-mass energies from 130 GeV to 172 GeV (LEP-II) are included [23–26]. For a large fraction of these high-energy events, initial-state radiation photons lower the effective centre-of-mass energy, $\sqrt{s'}$, of the annihilation process to values close to the Z mass, $m_{\mathrm{Z}}$ (radiative return to the Z). These radiative events dilute the sensitivity of the cross-section and forward-backward asymmetry measurements to the $\gamma$Z interference parameters. By applying a cut $\sqrt{s'} \gg m_{\mathrm{Z}}$, the high-energy events are isolated and used to constrain these parameters. The total statistics of these high-energy measurements of the four LEP collaborations are given in Table 10. These data are particularly important for the S-Matrix analysis, and significantly improve the precision of the results.

| | | ALEPH | DELPHI | L3 | OPAL | LEP |
|---|---|---|---|---|---|---|
| hadrons | total | 4439 | 4397 | 4305 | 4355 | 17496 |
| | $s'$ cut | 1096 | 1224 | 1179 | 1049 | 4548 |
| $\mu^+\mu^-$ & $\tau^+\tau^-$ | total | 519 | 412 | 379 | 450 | 1760 |
| | $s'$ cut | 254 | 190 | 181 | 225 | 850 |

Table 10: Number of hadronic and $\mu^+\mu^-$ plus $\tau^+\tau^-$ events collected by the LEP experiments at centre-of-mass energies between 130 and 172 GeV. The $s'$ cuts to separate events at high effective $s'$ of the experiments vary between $0.8 < \sqrt{s'/s} < 0.9$. For the selection of the total data sample the experiments also apply loose $s'$ cuts.

In the S-Matrix ansatz the lowest-order total cross-section, $\sigma^0_{\mathrm{tot}}$, and forward-backward asymmetry, $A^0_{\mathrm{fb}}$, for $\mathrm{e^+e^-}$ annihilation into a fermion-antifermion pair are given by [22]:

$$\sigma^0_a(s) = \frac{4}{3}\pi\alpha^2\left[\frac{g^a_{\mathrm{f}}}{s} + \frac{j^a_{\mathrm{f}}(s-\overline{m}^2_{\mathrm{Z}}) + r^a_{\mathrm{f}}\,s}{(s-\overline{m}^2_{\mathrm{Z}})^2 + \overline{m}^2_{\mathrm{Z}}\overline{\Gamma}^2_{\mathrm{Z}}}\right] \qquad \text{for } a = \mathrm{tot}, \mathrm{fb} \tag{5}$$

$$A^0_{\mathrm{fb}}(s) = \frac{3}{4}\frac{\sigma^0_{\mathrm{fb}}(s)}{\sigma^0_{\mathrm{tot}}(s)}\,. \tag{6}$$

The S-Matrix parameters $r_{\mathrm{f}}$, $j_{\mathrm{f}}$ and $g_{\mathrm{f}}$ are real numbers which express the size of the Z exchange, $\gamma$Z interference and photon exchange contributions. In the approach presented here, $r_{\mathrm{f}}$ and $j_{\mathrm{f}}$ are treated as free parameters while the photon exchange contribution, $g_{\mathrm{f}}$, is fixed to its QED prediction. Each final state is thus described by four free parameters: two for cross-sections, $r^{\mathrm{tot}}_{\mathrm{f}}$ and $j^{\mathrm{tot}}_{\mathrm{f}}$, and two for forward-backward asymmetries, $r^{\mathrm{fb}}_{\mathrm{f}}$ and $j^{\mathrm{fb}}_{\mathrm{f}}$. In models with only vector and axial-vector couplings of the Z boson, *e.g.* the Standard Model, these four S-Matrix parameters are not independent of each other and are approximately [22]:

$$r^{\mathrm{tot}}_{\mathrm{f}} \propto \left[g^2_{A\mathrm{e}} + g^2_{V\mathrm{e}}\right]\cdot\left[g^2_{A\mathrm{f}} + g^2_{V\mathrm{f}}\right] \tag{7}$$

$$j^{\mathrm{tot}}_{\mathrm{f}} \propto g_{V\mathrm{e}}g_{V\mathrm{f}} \tag{8}$$

$$r_{\rm f}^{\rm fb} \;\propto\; g_{Ae}g_{V{\rm e}}\cdot g_{Af}g_{V{\rm f}} \tag{9}$$
$$j_{\rm f}^{\rm fb} \;\propto\; g_{Ae}g_{Af}\,. \tag{10}$$

The S-Matrix ansatz is defined using a Breit-Wigner denominator with $s$-independent width for the Z resonance, $s-\overline{m}_{\rm Z}^2+i\overline{m}_{\rm Z}\overline{\Gamma}_{\rm Z}$. The results described in Section 2.1 used an $s$-dependent width. Because of this, there is a shift in the Z mass and width between the two parameterisations. These shifts are given by

$$\begin{aligned} m_{\rm Z} &\equiv \overline{m}_{\rm Z}\sqrt{1+\overline{\Gamma}_{\rm Z}^2/\overline{m}_{\rm Z}^2} \;\approx\; \overline{m}_{\rm Z}+34.1\text{ MeV and} \\ \Gamma_{\rm Z} &\equiv \overline{\Gamma}_{\rm Z}\sqrt{1+\overline{\Gamma}_{\rm Z}^2/\overline{m}_{\rm Z}^2} \;\approx\; \overline{\Gamma}_{\rm Z}+\;\;0.9\text{ MeV}, \end{aligned} \tag{11}$$

such that $\Gamma_{\rm Z}/m_{\rm Z}=\overline{\Gamma}_{\rm Z}/\overline{m}_{\rm Z}$. These transformations have been applied to the results shown in this section, so that results are comparable to those in the rest of this note. QED radiative corrections are included by convoluting with a radiator function [11].

The experiments fit their data with a set of 16 parameters: one set of the above 4 parameters for each lepton species, $r_{\rm had}^{\rm tot}$ and $j_{\rm had}^{\rm tot}$ for the hadronic final states (asymmetries are not used), and $m_{\rm Z}$ and $\Gamma_{\rm Z}$. These results are presented in Table 33 in Appendix A. For the averaging the procedure defined in the previous section is used. The correlated luminosity error is 0.25% at the LEP-II energies and is still negligible compared with the statistical errors. A correlated error of 0.11% relevant for the Z peak data is taken into account. The common errors originating from the LEP centre-of-mass energy calibration are determined following the procedure described in the previous section.

The data of each of the four LEP experiments are consistent with lepton universality (see the tables in Appendix A). If lepton universality is assumed, the set of 16 S-Matrix parameters is reduced to a set of 8 parameters. In Table 11 the 8 parameters of the individual LEP experiments are shown. In Tables 12 and 13 the LEP averages and their correlation matrix are provided. The Standard Model predictions agree well with the LEP averages of the S-Matrix parameters.

Large correlations appear between the S-Matrix parameters. The correlations between $\Gamma_{\rm Z}$ and the $r_{\rm f}$ parameters are a consequence of the parameter definition and were not visible in the previous section because there the parameters were chosen to be as uncorrelated as possible. A large correlation ($-75\%$) arises between the Z mass, $m_{\rm Z}$, and the hadronic $\gamma$Z interference term, $j_{\rm had}^{\rm tot}$. The latter is fixed to its Standard Model value in the analysis presented in Section 2.1. This now observable correlation leads to a sizeable increase in the error on the Z mass in fits where $j_{\rm had}^{\rm tot}$ is left free. In Figure 2 the 68% probability contour in the $m_{\rm Z}$-$j_{\rm had}^{\rm tot}$ plane is depicted for the complete data set and for the LEP-I data only as shown at the EPS conference in Brussels 1995 [27]. The error on the hadronic $\gamma$Z interference term, and consequently the error on $m_{\rm Z}$, are reduced by using total cross-section measurements at centre-of-mass energies far away from the Z pole [22, 28]. By now the LEP-II data constrain $j_{\rm had}^{\rm tot}$ well enough that the inclusion of data taken far below the Z peak improves the errors only slightly. The TOPAZ collaboration at TRISTAN (KEK) has performed a measurement of the total hadronic cross section at $\sqrt{s}=57.77$ GeV, $\sigma_{\rm tot}^0=143.6\pm1.5(stat.)\pm4.5(syst.)$ pb [29]. Combining this measurement with the LEP results yields:

$$m_{\rm Z} \;=\; 91.1882\pm0.0029\text{ GeV} \tag{12}$$
$$j_{\rm had}^{\rm tot} \;=\; 0.14\pm0.12\,, \tag{13}$$

and the correlation between $m_{\rm Z}$ and $j_{\rm had}^{\rm tot}$ is reduced to $-71\%$.

The results presented here are consistent with the results obtained in Section 2.1 where the leptonic $\gamma$Z interference terms are constrained by the effective couplings and the hadronic $\gamma$Z interference term is fixed to its Standard Model value.

| S-Matrix fit | | | | |
|---|---|---|---|---|
| | ALEPH | DELPHI | L3[a] | OPAL[a] |
| $m_{\rm Z}$ [GeV] | 91.1951±0.0056 | 91.1837±0.0056 | 91.1854±0.0056 | 91.1861±0.0054 |
| $\Gamma_{\rm Z}$ [GeV] | 2.4939±0.0044 | 2.4896±0.0041 | 2.4999±0.0043 | 2.4945±0.0044 |
| $r^{\rm tot}_{\rm had}$ | 2.966±0.010 | 2.956±0.010 | 2.971±0.010 | 2.962±0.010 |
| $r^{\rm tot}_{\ell}$ | 0.14293±0.00055 | 0.14211±0.00061 | 0.14264±0.00066 | 0.14188±0.00060 |
| $j^{\rm tot}_{\rm had}$ | -0.18±0.27 | 0.38±0.28 | 0.34±0.28 | 0.08±0.27 |
| $j^{\rm tot}_{\ell}$ | -0.012±0.022 | 0.024±0.023 | 0.031±0.025 | -0.013±0.027 |
| $r^{\rm fb}_{\ell}$ | 0.00292±0.00033 | 0.00306±0.00040 | 0.00327±0.00050 | 0.00264±0.00037 |
| $j^{\rm fb}_{\ell}$ | 0.840±0.025 | 0.761±0.026 | 0.788±0.033 | 0.733±0.025 |
| $\chi^2$/d.o.f. | 183/197 | 241/203 | 164/191 | 116/163 |

Table 11: S-Matrix parameters from 8-parameter fits to the data of the four LEP experiments, assuming lepton universality.
[a]For the averaging procedure the L3 values of $m_{\rm Z}$ and $\Gamma_{\rm Z}$ are shifted by +0.3 MeV and the OPAL value of $m_{\rm Z}$ by +0.5 MeV to account for the new energy calibration.

| S-Matrix fit | | |
|---|---|---|
| Parameter | Average Value | SM Prediction |
| $m_{\rm Z}$ [GeV] | 91.1882±0.0031 | — |
| $\Gamma_{\rm Z}$ [GeV] | 2.4945±0.0024 | 2.4935 |
| $r^{\rm tot}_{\rm had}$ | 2.9637±0.0062 | 2.9608 |
| $r^{\rm tot}_{\ell}$ | 0.14245±0.00032 | 0.14250 |
| $j^{\rm tot}_{\rm had}$ | 0.14±0.14 | 0.22 |
| $j^{\rm tot}_{\ell}$ | 0.004±0.012 | 0.004 |
| $r^{\rm fb}_{\ell}$ | 0.00292±0.00019 | 0.00265 |
| $j^{\rm fb}_{\ell}$ | 0.780±0.013 | 0.799 |

Table 12: Average S-Matrix parameters from the data of the four LEP experiments given in Table 33, assuming lepton universality. The $\chi^2$/d.o.f. of the average is 59/56. The Standard-Model predictions are listed for $m_{\rm Z} = 91.1882$ GeV, $m_{\rm t} = 173.8$ GeV, $m_{\rm H} = 300$ GeV, $\alpha_s(m^2_{\rm Z}) = 0.119$, and $1/\alpha(m^2_{\rm Z})^5 = 128.878$.

| S-Matrix fit | | | | | | | | |
|---|---|---|---|---|---|---|---|---|
| | $m_{\rm Z}$ | $\Gamma_{\rm Z}$ | $r^{\rm tot}_{\rm had}$ | $r^{\rm tot}_{\ell}$ | $j^{\rm tot}_{\rm had}$ | $j^{\rm tot}_{\ell}$ | $r^{\rm fb}_{\ell}$ | $j^{\rm fb}_{\ell}$ |
| $m_{\rm Z}$ | 1.00 | -0.13 | -0.09 | -0.08 | -0.75 | -0.43 | 0.14 | -0.02 |
| $\Gamma_{\rm Z}$ | -0.13 | 1.00 | 0.80 | 0.61 | 0.16 | 0.09 | 0.00 | 0.07 |
| $r^{\rm tot}_{\rm had}$ | -0.09 | 0.80 | 1.00 | 0.77 | 0.13 | 0.06 | 0.02 | 0.09 |
| $r^{\rm tot}_{\ell}$ | -0.08 | 0.61 | 0.77 | 1.00 | 0.12 | 0.12 | 0.03 | 0.12 |
| $j^{\rm tot}_{\rm had}$ | -0.75 | 0.16 | 0.13 | 0.12 | 1.00 | 0.47 | -0.14 | 0.03 |
| $j^{\rm tot}_{\ell}$ | -0.43 | 0.09 | 0.06 | 0.12 | 0.47 | 1.00 | -0.05 | 0.02 |
| $r^{\rm fb}_{\ell}$ | 0.14 | 0.00 | 0.02 | 0.03 | -0.14 | -0.05 | 1.00 | 0.15 |
| $j^{\rm fb}_{\ell}$ | -0.02 | 0.07 | 0.09 | 0.12 | 0.03 | 0.02 | 0.15 | 1.00 |

Table 13: The correlation matrix for the set of parameters given in Table 12.

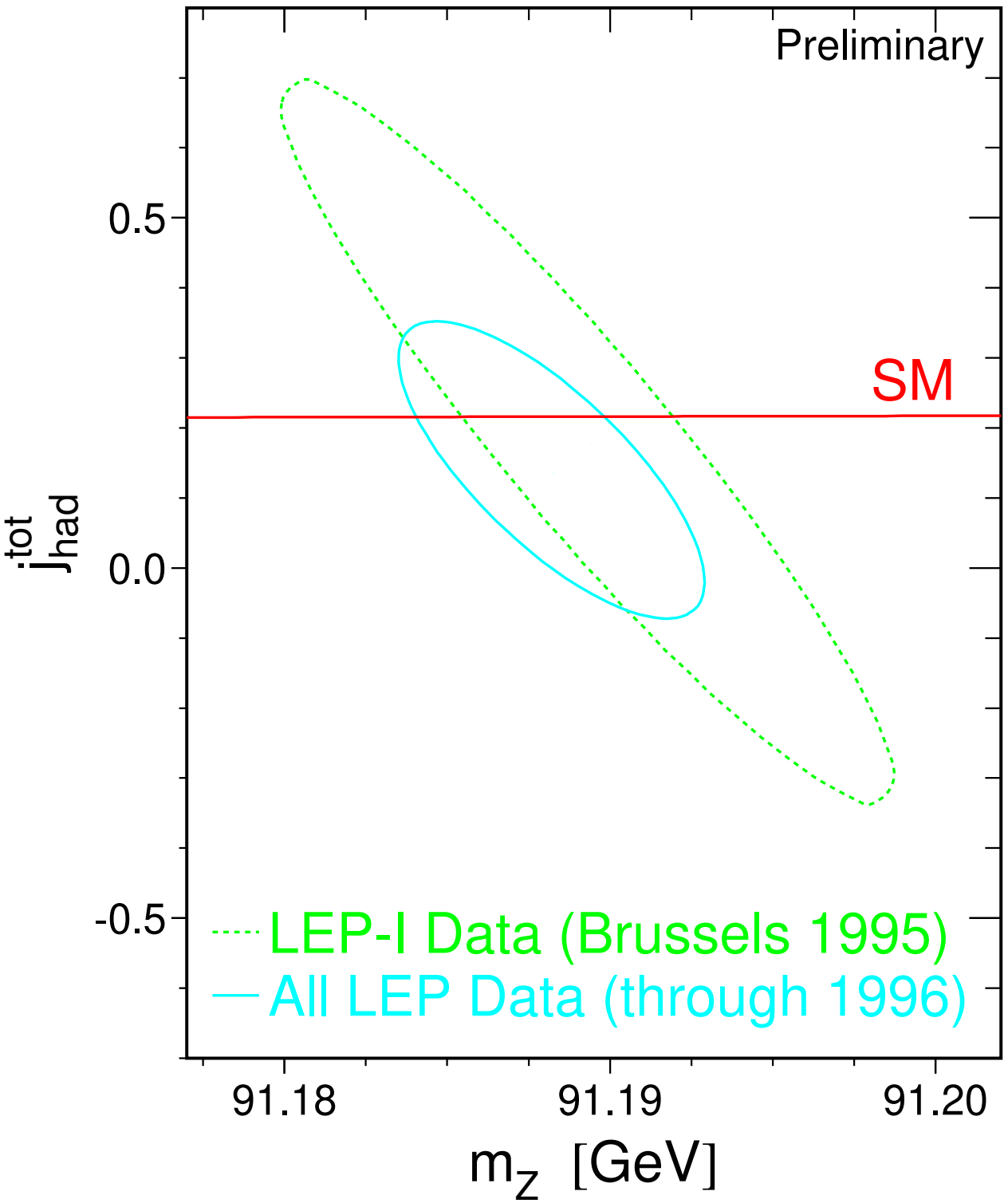


Figure 2: Contours of 68% confidence level between the mass of the Z boson, $m_Z$, and the hadronic $\gamma$Z interference term for total cross sections, $j^{tot}_{had}$. Lepton universality is assumed. The solid contour corresponds to all LEP data (except the 183 GeV data) while the dashed contour is obtained using only LEP-I results as presented at the EPS in Brussels 1995 [27]. The Standard-Model prediction for $j^{tot}_{had}$ is shown as the solid line.

# 3 The $\tau$ Polarisation

**Updates with respect to last summer:**
L3 have finalized their analysis of the complete data. ALEPH and DELPHI have updated their results with new preliminary measurements from the complete data.

The longitudinal $\tau$ polarisation, $\mathcal{P}_\tau$, of $\tau$ pairs produced in Z decays is defined as:

$$\mathcal{P}_\tau \equiv \frac{\sigma_{\mathrm{R}} - \sigma_{\mathrm{L}}}{\sigma_{\mathrm{R}} + \sigma_{\mathrm{L}}}, \tag{14}$$

where $\sigma_{\mathrm{R}}$ and $\sigma_{\mathrm{L}}$ are the $\tau$-pair cross-sections for the production of a right-handed and left-handed $\tau^-$, respectively. The distribution of $\mathcal{P}_\tau$ as a function of the polar scattering angle $\theta$ between the $\mathrm{e}^-$ and the $\tau^-$, at $\sqrt{s} = m_{\mathrm{Z}}$, is given by:

$$\mathcal{P}_\tau(\cos\theta) = -\frac{\mathcal{A}_\tau(1+\cos^2\theta) + 2\mathcal{A}_{\mathrm{e}}\cos\theta}{1+\cos^2\theta + 2\mathcal{A}_\tau\mathcal{A}_{\mathrm{e}}\cos\theta}, \tag{15}$$

with $\mathcal{A}_{\mathrm{e}}$ and $\mathcal{A}_\tau$ as defined in Equation (4). Equation (15) neglects the effects of $\gamma$ exchange, $\gamma$Z interference and electromagnetic radiative corrections for initial-state and final-state radiation. These effects are taken into account in the experimental analyses. In particular, these corrections account for the $\sqrt{s}$ dependence of the $\tau$ polarisation, $\mathcal{P}_\tau(\cos\theta)$, which is important since the off-peak data are included in the event samples for all experiments. When averaged over all production angles $\mathcal{P}_\tau$ is a measurement of $\mathcal{A}_\tau$. As a function of $\cos\theta$, $\mathcal{P}_\tau(\cos\theta)$ provides nearly independent determinations of both $\mathcal{A}_\tau$ and $\mathcal{A}_{\mathrm{e}}$, thus allowing a test of the universality of the couplings of the Z to e and $\tau$.

Each experiment makes separate $\mathcal{P}_\tau$ measurements using the five $\tau$ decay modes $\mathrm{e}\nu\overline{\nu}$, $\mu\nu\overline{\nu}$, $\pi\nu$, $\rho\nu$ and $a_1\nu$ [30–33]. The $\rho\nu$ and $\pi\nu$ are the most sensitive channels, contributing weights of about 40% each in the average. DELPHI and L3 have also used an inclusive hadronic analysis. The combination is made using the results from each experiment already averaged over the $\tau$ decay modes.

## 3.1 Results

Tables 14 and 15 show the most recent results for $\mathcal{A}_\tau$ and $\mathcal{A}_{\mathrm{e}}$ obtained by the four LEP collaborations [30–33] and their combination. Common systematic errors arise from uncertainties in the decay radiation in the $\pi\nu$ and $\rho\nu$ channels, and in the modelling of the $a_1$ decays [2]. These errors need further investigation and might need to be taken into account for the final results (see Reference 32). For the current combination the systematic errors on $\mathcal{A}_\tau$ and $\mathcal{A}_{\mathrm{e}}$ are treated as uncorrelated between the experiments. The statistical correlation between the extracted values of $\mathcal{A}_\tau$ and $\mathcal{A}_{\mathrm{e}}$ is small ($\leq$ 5%), and is neglected.

The average values for $\mathcal{A}_\tau$ and $\mathcal{A}_{\mathrm{e}}$:

$$\mathcal{A}_\tau = 0.1431 \pm 0.0045 \tag{16}$$

$$\mathcal{A}_{\mathrm{e}} = 0.1479 \pm 0.0051, \tag{17}$$

are compatible, in agreement with lepton universality. Assuming $\mathrm{e}-\tau$ universality, the values for $\mathcal{A}_\tau$ and $\mathcal{A}_{\mathrm{e}}$ can be combined. This combination is performed neglecting any possible common systematic error between $\mathcal{A}_\tau$ and $\mathcal{A}_{\mathrm{e}}$ within a given experiment, as these errors are also estimated to be small. The combined result of $\mathcal{A}_\tau$ and $\mathcal{A}_{\mathrm{e}}$ is:

$$\mathcal{A}_\ell = 0.1452 \pm 0.0034. \tag{18}$$

| Experiment | | $\mathcal{A}_\tau$ |
|---|---|---|
| ALEPH | (90 - 95), prel. | $0.1452 \pm 0.0052 \pm 0.0032$ |
| DELPHI | (90 - 95), prel. | $0.1381 \pm 0.0079 \pm 0.0067$ |
| L3 | (90 - 95), final | $0.1476 \pm 0.0088 \pm 0.0062$ |
| OPAL | (90 - 94), final | $0.134 \pm 0.009 \pm 0.010$ |
| LEP Average | | $0.1431 \pm 0.0045$ |

Table 14: LEP results for $\mathcal{A}_\tau$. The $\chi^2$/d.o.f. for the average is 1.0/3. The first error is statistical and the second systematic. In the LEP average, statistical and systematic errors are combined in quadrature. The systematic component of the error is $\pm 0.0027$.

| Experiment | | $\mathcal{A}_{\mathrm{e}}$ |
|---|---|---|
| ALEPH | (90 - 95), prel. | $0.1505 \pm 0.0069 \pm 0.0010$ |
| DELPHI | (90 - 95), prel. | $0.1353 \pm 0.0116 \pm 0.0033$ |
| L3 | (90 - 95), final | $0.1678 \pm 0.0127 \pm 0.0030$ |
| OPAL | (90 - 94), final | $0.129 \pm 0.014 \pm 0.005$ |
| LEP Average | | $0.1479 \pm 0.0051$ |

Table 15: LEP results for $\mathcal{A}_{\mathrm{e}}$. The $\chi^2$/d.o.f. for the average is 5.2/3. The first error is statistical and the second systematic. In the LEP average, statistical and systematic errors are combined in quadrature. The systematic component of the error is $\pm 0.0010$.

# 4 Results from b and c Quarks

**Updates with respect to last summer:**
DELPHI and OPAL have updated their $R_b$ measurements with the full LEP1-dataset, SLD has included data up to spring 1998.
DELPHI, OPAL and SLD have updated some of their $R_c$ measurements with more data.
ALEPH has presented a new $A_{FB}^b$ measurement with jet charge and DELPHI has updated $A_{FB}^b$ with leptons and jet charge with the full data set.
$A_{FB}^c$ measurements by ALEPH, DELPHI and OPAL have been updated.
SLD have updated most of their $\mathcal{A}_b$ and $\mathcal{A}_c$ analyses with new data.
Many preliminary analyses have been published.

The relevant quantities in the heavy quark sector at LEP/SLD which are currently determined by the combination procedure are:

- The ratios of the b and c quark partial widths of the Z to its total hadronic partial width: $R_b^0 \equiv \Gamma_{b\bar{b}}/\Gamma_{had}$ and $R_c^0 \equiv \Gamma_{c\bar{c}}/\Gamma_{had}$.
- The forward-backward asymmetries, $A_{FB}^{b\bar{b}}$ and $A_{FB}^{c\bar{c}}$.
- The final state coupling parameters $\mathcal{A}_b$, $\mathcal{A}_c$ obtained from the left-right-forward-backward asymmetry at SLD.
- The semileptonic branching ratios, BR($b \to \ell$) and BR($b \to c \to \bar{\ell}$), and the average $B^0\overline{B^0}$ mixing parameter, $\overline{\chi}$. These are often determined at the same time or with similar methods as the asymmetries. Including them in the combination reduces the errors.
- The probability that a c quark produces a $D^+$, $D_s$, $D^{*+}$ meson[2] or a charmed baryon. The probability that a c quark fragments into a $D^0$ is calculated from the constraint that the probabilities for the weakly decaying charmed hadrons add up to one. These quantities are determined now with good accuracy by the LEP experiments. The interpretation of the $D^*$ rate in terms of $R_c$ and the determination of the charm background in the lifetime tag $R_b$ measurements can now be made without assumptions on the energy dependence of the D-meson production rates.

There are several motivations for the averaging procedure [3] presented here. Several analyses measure more than one parameter simultaneously, for example the asymmetry measurements with leptons or D-mesons. Some of the measurements of electroweak parameters depend explicitly on the values of other parameters, for example $R_b$ depends on $R_c$. The common tagging and analysis techniques lead to common sources of systematic uncertainty, in particular for the double-tag measurements of $R_b$. The starting point for the combination is to ensure that all the analyses use a common set of assumptions for input parameters which give rise to systematic uncertainties. A full description of the averaging procedure has been published in Reference 3. The input parameters have been updated and extended [34] to accommodate new analyses and more recent measurements. The correlations and interdependences of the input measurements are then taken into account in a $\chi^2$ minimisation which results in the combined electroweak parameters and their correlation matrix.

In a first fit the asymmetry measurements on peak, above peak and below peak are combined at each centre-of-mass energy. The results of this fit, including the SLD results, are given in Appendix B.

[2] Actually the product $P(c \to D^{*+}) \times BR(D^{*+} \to \pi^+ D^0)$ is fitted since this quantity is needed and measured by the LEP experiments.

The dependence of the average asymmetries on centre-of-mass energy agrees with the prediction of the Standard Model. A second fit is made to derive the pole asymmetries, $A_{\rm FB}^{0,\,{\rm q}}$, from the measured quark asymmetries, in which all the off-peak asymmetry measurements are corrected to the peak energy before combining. This fit determines a total of 13 parameters: the two partial widths, two LEP-asymmetries, two coupling parameters from SLD, two semileptonic branching ratios, the average mixing parameter and the probabilities for c quark to fragment into a $\rm D^+$, a $\rm D_s$, a $\rm D^{*+}$, or a charmed baryon. If the SLD measurements are excluded from the fit there are 11 parameters to be determined.

## 4.1 Summary of Measurements and Averaging Procedure

All measurements are presented by the LEP and SLD collaborations in a consistent manner for the purpose of combination [3]. The tables prepared by the experiments include a detailed breakdown of the systematic error of each measurement and its dependence on other electroweak parameters. Where necessary, the experiments apply small corrections to their results in order to use agreed values and ranges for the input parameters to calculate systematic errors. The measurements, corrected where necessary, are summarised in Appendix B in Tables 37-54, where the statistical and systematic errors are quoted separately. The correlated systematic entries are from sources shared with one or more other results in the table and are derived from the full breakdown of common systematic uncertainties. The uncorrelated systematic entries come from the remaining sources.

All collaborations now present precise $R_{\rm b}$ measurements using lifetime tags and measurements of $\rm BR(b \to \ell)$ using b-tagging in the opposite hemisphere. The old measurements of $R_{\rm b}$, $\rm BR(b \to \ell)$ and some other quantities with fits to the single- and double lepton spectra [35–38] are no longer competitive in their errors and have been excluded from the combination. The same is true for the L3 measurement of $R_{\rm b}$ using event shape variables [39].

### 4.1.1 Averaging procedure

A $\chi^2$ minimisation procedure is used to derive the values of the heavy-flavour electroweak parameters as published in Reference 3. The full statistical and systematic covariance matrix for all measurements is calculated. This correlation matrix takes correlations between different measurements of one experiment and between different experiments into account. The explicit dependences of each measurement on the other parameters are also accounted for. The most important example is the dependence of the value of $R_{\rm b}$ on the assumed value of $R_{\rm c}$.

Since c-quark events form the main background in the $R_{\rm b}$ analyses, the value of $R_{\rm b}$ depends on the value of $R_{\rm c}$. If $R_{\rm b}$ and $R_{\rm c}$ are measured in the same analysis, this is reflected in the correlation matrix for the results. However most analyses do not determine $R_{\rm b}$ and $R_{\rm c}$ simultaneously but instead measure $R_{\rm b}$ for an assumed value of $R_{\rm c}$. In this case the dependence is parameterised as:

$$R_{\rm b} \;=\; R_{\rm b}^{\rm meas} + a(R_{\rm c})\frac{(R_{\rm c} - R_{\rm c}^{\rm used})}{R_{\rm c}}. \tag{19}$$

In this expression, $R_{\rm b}^{\rm meas}$ is the result of the analysis assuming a value of $R_{\rm c} = R_{\rm c}^{\rm used}$. The values of $R_{\rm c}^{\rm used}$ and the coefficients $a(R_{\rm c})$ are given in Table 37 where appropriate. The dependences of all other measurements on other electroweak parameters are treated in the same way, with coefficients $a(x)$ describing the dependence on parameter $x$.

### 4.1.2 Partial width measurements

The measurements of the partial widths fall into two categories. In the first, called a single-tag measurement, a method to select b or c events is devised, and the number of tagged events is counted. This number must then be corrected for backgrounds from other flavours and for the tagging efficiency to calculate the true fraction of hadronic Z decays of that flavour. The dominant systematic errors come from understanding the branching ratios and detection efficiencies which give the overall tagging efficiency. For the current set of measurements, this method is only used to determine $R_{\mathrm{c}}$. For the second technique, called a double-tag measurement, the event is divided into two hemispheres. With $N_{\mathrm{t}}$ being the number of tagged hemispheres, $N_{\mathrm{tt}}$ the number of events with both hemispheres tagged and $N_{\mathrm{had}}$ the total number of hadronic Z decays one has:

$$\frac{N_{\mathrm{t}}}{2N_{\mathrm{had}}} = \varepsilon_{\mathrm{b}}R_{\mathrm{b}} + \varepsilon_{\mathrm{c}}R_{\mathrm{c}} + \varepsilon_{\mathrm{uds}}(1 - R_{\mathrm{b}} - R_{\mathrm{c}}), \tag{20}$$

$$\frac{N_{\mathrm{tt}}}{N_{\mathrm{had}}} = \mathcal{C}_{\mathrm{b}}\varepsilon_{\mathrm{b}}^2R_{\mathrm{b}} + \mathcal{C}_{\mathrm{c}}\varepsilon_{\mathrm{c}}^2R_{\mathrm{c}} + \mathcal{C}_{\mathrm{uds}}\varepsilon_{\mathrm{uds}}^2(1 - R_{\mathrm{b}} - R_{\mathrm{c}}), \tag{21}$$

where $\varepsilon_{\mathrm{b}}$, $\varepsilon_{\mathrm{c}}$ and $\varepsilon_{\mathrm{uds}}$ are the tagging efficiencies per hemisphere for b, c and light-quark events, and $\mathcal{C}_{\mathrm{q}} \neq 1$ accounts for the fact that the tagging efficiencies between the hemispheres may be correlated. In the case of $R_{\mathrm{b}}$ one has $\varepsilon_{\mathrm{b}} \gg \varepsilon_{\mathrm{c}} \gg \varepsilon_{\mathrm{uds}}$, $\mathcal{C}_{\mathrm{b}} \approx 1$. The correlations for the other flavours can be neglected. These equations can be solved to give $R_{\mathrm{b}}$ and $\varepsilon_{\mathrm{b}}$. Neglecting the c and uds backgrounds and the correlations they are approximately given by:

$$\varepsilon_{\mathrm{b}} \approx 2N_{\mathrm{tt}}/N_{\mathrm{t}}, \tag{22}$$

$$R_{\mathrm{b}} \approx N_{\mathrm{t}}^2/(4N_{\mathrm{tt}}N_{\mathrm{had}}). \tag{23}$$

The double-tagging method has the advantage that the b tagging efficiency is derived directly from the data, reducing the systematic error. The residual background of other flavours in the sample, and the evaluation of the correlation between the tagging efficiencies in the two hemispheres of the event are the main sources of systematic uncertainty in such an analysis.

In some analyses, this method is enhanced by including different kinds of tags. All additional efficiencies are determined from data, reducing the statistical uncertainties without adding new systematics.

In the past the cross section ratios $R_{\mathrm{b}}$ and $R_{\mathrm{c}}$ have been combined and small corrections have been applied to the results to obtain the partial width ratios $R_{\mathrm{b}}^0$ and $R_{\mathrm{c}}^0$. However these corrections depend slightly on the invariant mass cut-off of the simulations used by the experiments, so that now these corrections are applied by the experiments before the combination.

The partial width measurements included are:

- Lifetime (and lepton) double tag measurements for $R_{\mathrm{b}}$ from ALEPH [40], DELPHI [41], L3 [42], OPAL [43] and SLD [44]. The basic features of the double-tag technique were discussed above. In the ALEPH, DELPHI, OPAL and SLD measurements the charm rejection has been enhanced by using the invariant mass information. DELPHI also adds information from the energy of all particles at the secondary vertex and their rapidity. The ALEPH and DELPHI measurements make use of several different tags; this improves the statistical accuracy and reduces the systematic errors due to hemisphere correlations and charm contamination, compared with the simple single/double tag.

- Analyses with $D/D^{*\pm}$ mesons to measure $R_c$ from ALEPH, DELPHI and OPAL. All measurements are constructed in a way that no assumptions on the energy dependence of charm fragmentation are necessary. The available measurements can be divided into four groups:
  - inclusive/exclusive double tag (ALEPH [45], DELPHI [46], OPAL [47]): In a first step $D^{*\pm}$ mesons are reconstructed in several decay channels and their production rate is measured, which depends on the product $R_c \times P(c \to D^{*+}) \times BR(D^{*+} \to \pi^+ D^0)$. This sample of $c\overline{c}$ (and $b\overline{b}$) events is then used to measure $P(c \to D^{*+}) \times BR(D^{*+} \to \pi^+ D^0)$ using a slow pion tag in the opposite hemisphere. In the ALEPH measurement $R_c$ is unfolded internally in the analysis so that no explicit $P(c \to D^{*+}) \times BR(D^{*+} \to \pi^+ D^0)$ is available.
  - inclusive single/double tag (DELPHI [46]): This measurement measures the single and double tag rate using a slow pion tag. It takes advantage of the higher efficiency of the inclusive slow pion tag compared with the exclusive reconstruction. The high background, however, limits the precision of this measurement.
  - exclusive double tag (ALEPH [45]): This analysis uses exclusively reconstructed $D^{*+}$, $D^0$ and $D^+$ mesons in different decay channels. It has lower statistics but better purity than the inclusive analyses.
  - Reconstruction of all weakly decaying D states (ALEPH [48], DELPHI [49], OPAL [50]): These analyses make the assumption that the production rates of $D^0$, $D^+$, $D_s$ and $\Lambda_c$ saturate the fragmentation of $c\overline{c}$ with small corrections applied for the unobserved baryonic states. This is a single tag measurement, relying only on knowing the decay branching ratios of the charm hadrons. These analyses are also used to measure the c hadron production ratios which are needed for the $R_b$ analyses.
- A lifetime plus mass double tag from SLD to measure $R_c$ [51]. This analysis uses the same tagging algorithm as the SLD $R_b$ analysis, but requiring that the mass of the secondary vertex is smaller than the D-meson mass. Although the charm tag has a purity of about 67%, most of the background is from b which can be measured from the b/c mixed tag rate.
- A measurement of $R_c$ using single leptons assuming $BR(c \to \ell)$ from ALEPH [45].

#### 4.1.3 Asymmetry measurements

For the 11- and 13-parameter fits described above, the LEP peak and off-peak asymmetries are corrected to $\sqrt{s} = 91.26$ GeV using the predicted dependence from ZFITTER [52]. The slope of the asymmetry around $m_Z$ depends only on the axial coupling and the charge of the initial and final state fermions and is thus independent of the value of the asymmetry itself.

The QCD corrections to the forward-backward asymmetries depend strongly on the experimental analyses. For this reason the numbers given by the collaborations are already corrected to full acceptance and for QCD effects. A detailed description of the procedure can be found in Reference 53.

After calculating the overall averages, the quark pole asymmetries, $A_{FB}^{0,q}$, as defined in Eqn. 3, are derived by applying the corrections summarised in Table 16. These corrections are the effects of the energy shift from 91.26 GeV to $m_Z$, initial state radiation, $\gamma$ exchange and $\gamma Z$ interference. A very small correction due to the finite value of the b-quark mass is included in the correction called $\gamma Z$ interference. All corrections are calculated using ZFITTER.

The SLD left-right-forward-backward asymmetries are also corrected for all radiative effects and are directly presented in terms of $\mathcal{A}_b$ and $\mathcal{A}_c$.

| Source | $\delta A_{\rm FB}^{\rm b}$ | $\delta A_{\rm FB}^{\rm c}$ |
|---|---|---|
| $\sqrt{s} = m_{\rm Z}$ | $-0.0013$ | $-0.0034$ |
| QED corrections | $+0.0041$ | $+0.0104$ |
| $\gamma$, $\gamma$Z | $-0.0003$ | $-0.0008$ |
| Total | $+0.0025$ | $+0.0062$ |

Table 16: Corrections to be applied to the quark asymmetries. The corrections are to be understood as $A_{\rm FB}^{0,\,{\rm q}} = A_{\rm FB}^{meas} + \sum_i (\delta A_{\rm FB})_i$.

The measurements used are:

- Measurements of $A_{\rm FB}^{\rm b\bar{b}}$ and $A_{\rm FB}^{\rm c\bar{c}}$ using leptons from ALEPH [54], DELPHI [55], L3 [56] and OPAL [57]. These analyses measure either $A_{\rm FB}^{\rm b\bar{b}}$ only from a high $p_t$ lepton sample or they obtain $A_{\rm FB}^{\rm b\bar{b}}$ and $A_{\rm FB}^{\rm c\bar{c}}$ from a fit to the lepton spectra. In the case of OPAL the lepton information has been combined with hadronic variables in a neural net. Some asymmetry analyses also measure $\overline{\chi}$.
- Measurements of $A_{\rm FB}^{\rm b\bar{b}}$ based on lifetime tagged events with a hemisphere charge measurement from ALEPH [58], DELPHI [59], L3 [60] and OPAL [61]. These measurements contribute roughly the same weight to the combined result as the lepton fits.
- Analyses with D mesons to measure $A_{\rm FB}^{\rm c\bar{c}}$ from ALEPH [62] or $A_{\rm FB}^{\rm c\bar{c}}$ and $A_{\rm FB}^{\rm b\bar{b}}$ from DELPHI [63] and OPAL [64].
- Measurements of $\mathcal{A}_{\rm b}$ and $\mathcal{A}_{\rm c}$ from SLD. These results include measurements using lepton [65], D meson [66] and vertex mass plus hemisphere charge [67] tags, which have similar sources of systematic errors as the LEP asymmetry measurements. SLD also uses vertex mass for b or charm tags in conjunction with a Kaon tag for an $\mathcal{A}_{\rm b}$ measurement [68], or with a vertex charge and Kaon tag for an $\mathcal{A}_{\rm c}$ measurement [69].

#### 4.1.4 Other measurements

The measurements of the charmed hadron fractions $f({\rm D}^+)$, $f({\rm D_s})$, $f({\rm c_{baryon}})$ and ${\rm P(c \to D^{*+}) \times BR(D^{*+} \to \pi^+ D^0)}$ are included in the $R_{\rm c}$ measurements and are described there.

In addition ALEPH [70], DELPHI [71], L3 [72] and OPAL [73] measure ${\rm BR(b \to \ell)}$, ${\rm BR(b \to c \to \bar{\ell})}$ and $\overline{\chi}$ or a subset of them from a sample of leptons opposite to a b-tagged hemisphere and from a double lepton sample.

### 4.2 Results

Using the full averaging procedure gives the following combined results from LEP for the electroweak parameters:

$$\begin{aligned} R_{\rm b}^0 &= 0.21664 \pm 0.00076 \\ R_{\rm c}^0 &= 0.1724 \pm 0.0048 \\ A_{\rm FB}^{0,\,{\rm b}} &= 0.0991 \pm 0.0021 \\ A_{\rm FB}^{0,\,{\rm c}} &= 0.0712 \pm 0.0045\,, \end{aligned} \tag{24}$$

where all corrections to the asymmetries and partial widths have been applied. The $\chi^2$/d.o.f. is $42/(80-11)$. The corresponding correlation matrix is given in Table 17.

| | $R_{\rm b}^0$ | $R_{\rm c}^0$ | $A_{\rm FB}^{0,\,\rm b}$ | $A_{\rm FB}^{0,\,\rm c}$ |
|---|---|---|---|---|
| $R_{\rm b}^0$ | 1.00 | −0.17 | −0.06 | 0.02 |
| $R_{\rm c}^0$ | −0.17 | 1.00 | 0.06 | −0.05 |
| $A_{\rm FB}^{0,\,\rm b}$ | −0.06 | 0.06 | 1.00 | 0.13 |
| $A_{\rm FB}^{0,\,\rm c}$ | 0.02 | −0.05 | 0.13 | 1.00 |

Table 17: The correlation matrix for the four electroweak parameters from the 11-parameter fit.

### 4.2.1 Results of the 13-Parameter Fit to LEP and SLD Data

Including the SLD results on $R_{\rm c}$, $R_{\rm b}$, $\mathcal{A}_{\rm b}$ and $\mathcal{A}_{\rm c}$ into the fit the following results are obtained:

$$\begin{aligned} R_{\rm b}^0 &= 0.21656 \pm 0.00074 \\ R_{\rm c}^0 &= 0.1735 \pm 0.0044 \\ A_{\rm FB}^{0,\,\rm b} &= 0.0990 \pm 0.0021 \\ A_{\rm FB}^{0,\,\rm c} &= 0.0709 \pm 0.0044 \\ \mathcal{A}_{\rm b} &= 0.867 \pm 0.035 \\ \mathcal{A}_{\rm c} &= 0.647 \pm 0.040\,, \end{aligned} \tag{25}$$

with a $\chi^2$/d.o.f. of $44/(88-13)$. The corresponding correlation matrix is given in Table 18. In deriving these results the parameters $\mathcal{A}_{\rm b}$ and $\mathcal{A}_{\rm c}$ have been treated as independent of the forward-backward asymmetries $A_{\rm FB}^{0,\,\rm b}$ and $A_{\rm FB}^{0,\,\rm c}$. In Figure 3 the results on $R_{\rm b}^0$ and $R_{\rm c}^0$ are shown compared with the Standard Model expectation.

| | $R_{\rm b}^0$ | $R_{\rm c}^0$ | $A_{\rm FB}^{0,\,\rm b}$ | $A_{\rm FB}^{0,\,\rm c}$ | $\mathcal{A}_{\rm b}$ | $\mathcal{A}_{\rm c}$ |
|---|---|---|---|---|---|---|
| $R_{\rm b}^0$ | 1.00 | −0.17 | −0.06 | 0.02 | −0.02 | 0.02 |
| $R_{\rm c}^0$ | −0.17 | 1.00 | 0.05 | −0.04 | 0.01 | −0.04 |
| $A_{\rm FB}^{0,\,\rm b}$ | −0.06 | 0.05 | 1.00 | 0.13 | 0.03 | 0.02 |
| $A_{\rm FB}^{0,\,\rm c}$ | 0.02 | −0.04 | 0.13 | 1.00 | −0.01 | 0.07 |
| $\mathcal{A}_{\rm b}$ | −0.02 | 0.01 | 0.03 | −0.01 | 1.00 | 0.04 |
| $\mathcal{A}_{\rm c}$ | 0.02 | −0.04 | 0.02 | 0.07 | 0.04 | 1.00 |

Table 18: The correlation matrix for the six electroweak parameters from the 13-parameter fit.

The dominant errors for the electroweak parameters are listed in table 19.

The branching ratio $\rm b \to \ell$ from the 13 parameter fit is

$$\mathrm{BR}(\mathrm{b} \to \ell) \;=\; 0.1086 \pm 0.0024. \tag{26}$$

The dominant error on this quantity is the dependence on the semileptonic decay model with

$$\Delta\mathrm{BR}(\mathrm{b} \to \ell)(\mathrm{model}) \;=\; 0.0013.$$

Extensive studies have been made to understand the size of this error. If only the measurements of $\mathrm{BR}(\mathrm{b} \to \ell)$ are combined a consistent result is obtained with a modelling error of 0.0018. The reduction of the modelling uncertainty is due to the inclusion of asymmetry measurements using different

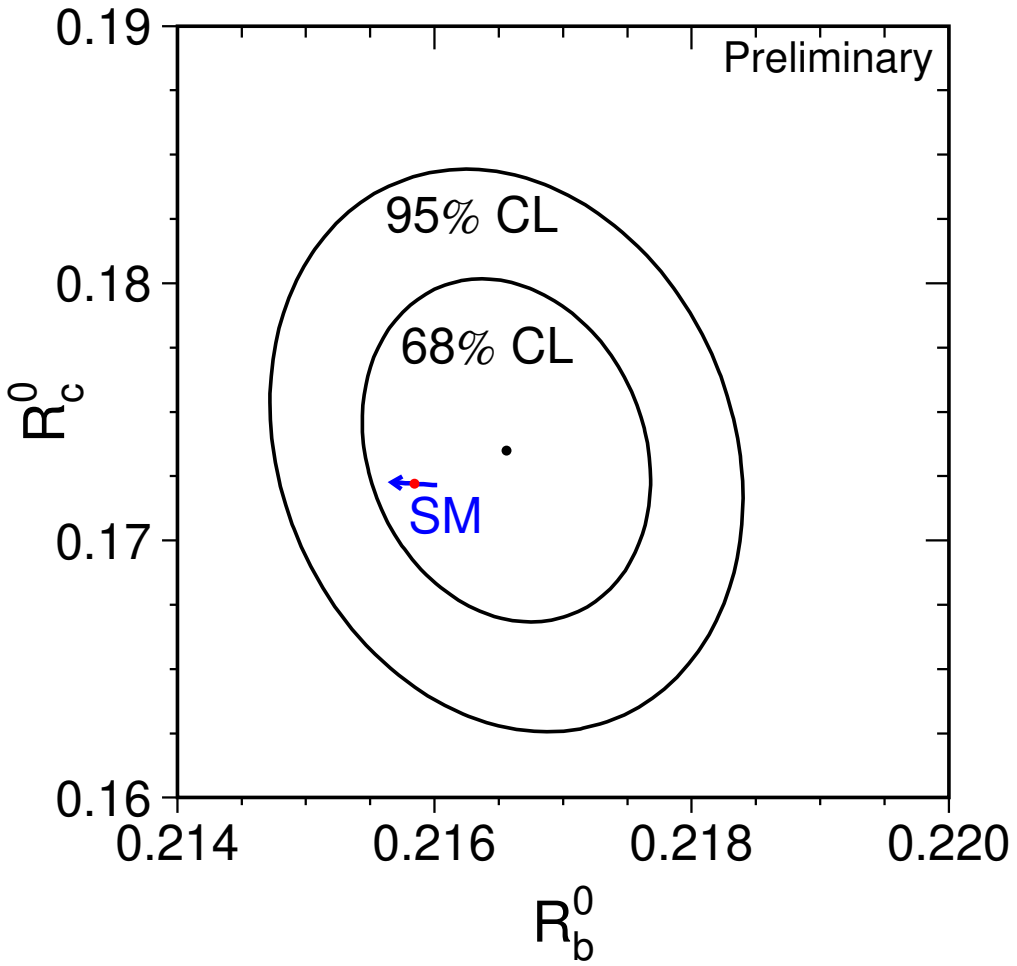


Figure 3: Contours in the $R_b^0$-$R_c^0$ plane derived from the LEP+SLD data, corresponding to 68% and 95% confidence levels assuming Gaussian systematic errors. The Standard Model prediction assuming $m_t = 173.8 \pm 5.0$ GeV is also shown. The arrow points in the direction of increasing values of $m_t$.

methods. Those using leptons depend on the semileptonic decay model while those using a lifetime tag and jet charge or D-mesons do not. The mutual consistency of the asymmetry measurements effectively constrains the semileptonic decay model, and reduces the uncertainty in the semileptonic branching ratio.

The value from the full fit was presented at the Vancouver conference [74]. Further studies of the sensitivity of BR($b \to \ell$) to the averaging procedure will be made in future, to improve the reliability of the LEP combined branching ratio results.

The result of the full fit to the LEP+SLC results including the off-peak asymmetries and the non-electroweak parameters can be found in Appendix B. It should be noted that the result on the non-electroweak parameters is independent of the treatment of the off-peak asymmetries and the SLD data.

| | $R_b^0$ $[10^{-3}]$ | $R_c^0$ $[10^{-3}]$ | $A_{FB}^{0,b}$ $[10^{-3}]$ | $A_{FB}^{0,c}$ $[10^{-3}]$ | $\mathcal{A}_b$ $[10^{-2}]$ | $\mathcal{A}_c$ $[10^{-2}]$ |
|---|---|---|---|---|---|---|
| statistics | 0.47 | 2.7 | 1.8 | 3.8 | 2.5 | 3.3 |
| internal systematics | 0.32 | 2.4 | 0.8 | 1.9 | 2.4 | 2.2 |
| QCD effects | 0.23 | 0.2 | 0.3 | 0 | 0.7 | 0.3 |
| BR(D $\rightarrow$ neut.) | 0.17 | 0.1 | 0 | 0 | 0 | 0 |
| D decay multiplicity | 0.09 | 0.5 | 0.1 | 0.1 | 0 | 0 |
| BR($D^+ \rightarrow K^-\pi^+\pi^+$) | 0.10 | 0.4 | 0 | 0 | 0 | 0.1 |
| BR($D_s \rightarrow \phi\pi^+$) | 0.02 | 1.2 | 0 | 0 | 0 | 0 |
| BR($\Lambda_c \rightarrow pK^-\pi^+$) | 0.04 | 0.6 | 0 | 0 | 0 | 0.1 |
| BR(c $\rightarrow \ell$) | 0.02 | 1.2 | 0.3 | 0.1 | 0 | 0 |
| D lifetimes | 0.07 | 0.2 | 0.1 | 0.1 | 0 | 0 |
| gluon splitting | 0.29 | 0.9 | 0 | 0 | 0.1 | 0.2 |
| c fragmentation | 0.07 | 0.8 | 0.1 | 0 | 0.1 | 0.1 |
| light quarks | 0.10 | 0.6 | 0.5 | 0 | 0 | 0.1 |
| Total | 0.74 | 4.4 | 2.1 | 4.4 | 3.5 | 4.0 |

Table 19: The dominant error sources for the electroweak parameters from the 13-parameter fit. The internal systematics contain errors that are uncorrelated among the experiments; the rest of the systematic errors are fully correlated among the experiments.

# 5 The Hadronic Charge Asymmetry $\langle Q_{\rm FB} \rangle$

**Updates with respect to last summer:**
L3 has a new preliminary result based on 1991-1995 data.

The LEP experiments ALEPH [75–77], DELPHI [78, 79], L3 [80] and OPAL [81, 82] have provided measurements of the hadronic charge asymmetry based on the mean difference in jet charges measured in the forward and backward event hemispheres, $\langle Q_{\rm FB} \rangle$. DELPHI has also provided a related measurement of the total charge asymmetry by making a charge assignment on an event-by-event basis and performing a likelihood fit [78]. The experimental values quoted for the average forward-backward charge difference, $\langle Q_{\rm FB} \rangle$, cannot be directly compared as some of them include detector dependent effects such as acceptances and efficiencies. Therefore the effective electroweak mixing angle, $\sin^2\theta^{\rm lept}_{\rm eff}$, as defined in Section 8.4, is used as a means of combining the experimental results summarised in Table 20.

| Experiment | | $\sin^2\theta^{\rm lept}_{\rm eff}$ |
|---|---|---|
| ALEPH | (90-94), final | $0.2322 \pm 0.0008 \pm 0.0011$ |
| DELPHI | (91-94), prel. | $0.2311 \pm 0.0010 \pm 0.0014$ |
| L3 | (91-95), prel. | $0.2327 \pm 0.0012 \pm 0.0013$ |
| OPAL | (91-94), prel. | $0.2326 \pm 0.0012 \pm 0.0013$ |
| LEP Average | | $0.2321 \pm 0.0010$ |

Table 20: Summary of the determination of $\sin^2\theta^{\rm lept}_{\rm eff}$ from inclusive hadronic charge asymmetries at LEP. For each experiment, the first error is statistical and the second systematic. The latter is dominated by fragmentation and decay modelling uncertainties.

The dominant source of systematic error arises from the modelling of the charge flow in the fragmentation process for each flavour. All experiments measure the required charge properties for $\mathrm{Z} \to \mathrm{b\overline{b}}$ events from the data. ALEPH also determines the charm charge properties from the data. The fragmentation model implemented in the JETSET Monte Carlo program [83] is used by all experiments as reference; the one of the HERWIG Monte Carlo program [84] is used for comparison. The JETSET fragmentation parameters are varied to estimate the systematic errors. The central values chosen by the experiments for these parameters are, however, not the same. The smaller of the two fragmentation errors in any pair of results is treated as common to both. The present average of $\sin^2\theta^{\rm lept}_{\rm eff}$ from $\langle Q_{\rm FB} \rangle$ and its associated error are not very sensitive to the treatment of common uncertainties. The ambiguities due to QCD corrections may cause changes in the derived value of $\sin^2\theta^{\rm lept}_{\rm eff}$. These are, however, well below the fragmentation uncertainties and experimental errors. The effect of fully correlating the estimated systematic uncertainties from this source between the experiments has a negligible effect upon the average and its error.

There is also some correlation between these results and those for $A^{\rm b\bar{b}}_{\rm FB}$ using jet charges. The dominant source of correlation is again through uncertainties in the fragmentation and decay models used. The typical correlation between the derived values of $\sin^2\theta^{\rm lept}_{\rm eff}$ between the $\langle Q_{\rm FB} \rangle$ and the $A^{\rm b\bar{b}}_{\rm FB}$ jet charge measurement has been estimated to be between 20% and 25%. This leads to only a small change in the relative weights for the $A^{\rm b\bar{b}}_{\rm FB}$ and $\langle Q_{\rm FB} \rangle$ results when averaging their $\sin^2\theta^{\rm lept}_{\rm eff}$ values (Section 8.4). Furthermore, the jet charge method contributes at most half of the weight of the $A^{\rm b\bar{b}}_{\rm FB}$ measurement. Thus, the correlation between $\langle Q_{\rm FB} \rangle$ and $A^{\rm b\bar{b}}_{\rm FB}$ from jet charge will have little impact on the overall Standard Model fit, and is neglected at present.

# 6 Measurement of $A_{\rm LR}$ at SLC

**Updates with respect to last summer:**
This is a new section.

The measurement of the left-right cross-section asymmetry ($A_{\rm LR}$) by SLD [85] at the SLC provides a systematically precise, statistics dominated, determination of the coupling $\mathcal{A}_{\rm e}$, and is presently the most precise single measurement, with the smallest systematic error, of this quantity. In principle the analysis is straightforward: one counts the numbers of Z bosons produced by left and right longitudinally polarised electrons, forms an asymmetry, and then divides by the luminosity-weighted $e^-$ beam polarisation magnitude (the $e^+$ beam is not polarised). Since the advent of high polarisation "strained lattice" GaAs photocathodes (1994), the average electron polarisation at the interaction point has been in the range 73% to 77%. The method requires no detailed final state event identification ($e^+e^-$ final state events are removed, as are non-Z backgrounds) and is insensitive to all acceptance and efficiency effects. The small total systematic error of typically 0.75% relative is completely dominated by the 0.7% relative systematic error in the determination of the $e^-$ polarisation. We note that the present statistical error on $A_{\rm LR}$ is about 1.3% relative.

The precision Compton polarimeter detects beam electrons that have been scattered by photons from a circularly polarised laser. Two additional polarimeters that are sensitive to the Compton-scattered photons have verified the precision polarimeter result to within their estimated errors of about 1%. In 1998, a dedicated experiment was performed in order to directly test the expectation that accidental polarisation of the positron beam was negligible – the $e^+$ polarisation was found to be consistent with zero ($-0.02 \pm 0.07\%$).

The $A_{\rm LR}$ analysis includes several very small corrections. The polarimeter result is corrected for higher order QED and accelerator related effects (a total of $0.16 \pm 0.07\%$), and the event asymmetry is corrected for backgrounds and accelerator asymmetries (a total of $0.02 \pm 0.07\%$). The translation of the $A_{\rm LR}$ result to a "Z-pole" value is a $1.8 \pm 0.4\%$ effect, where the uncertainty arises from the precision of the centre-of-mass energy determination. This small error due to beam energy measurement is slightly larger than seen previously (it was closer to 0.3%) and reflects the results of a scan of the Z peak used to calibrate the energy spectrometers to LEP data, which was performed for the first time during the most recent SLC run. The Z-pole value, $A^0_{\rm LR}$, is equivalent to a measurement of $\mathcal{A}_{\rm e}$.

The 1998 preliminary result is included in a running average of all of the SLD $A_{\rm LR}$ measurements (1992, 1993, 1994/1995, 1996, 1997 and 1998), which taken together yield a $\chi^2$ of 6.9 for 5 degrees of freedom. This preliminary result for $A^0_{\rm LR}$ ($\mathcal{A}_{\rm e}$) is $0.1510 \pm 0.0025$. Assuming lepton universality, this result can be combined with preliminary measurements of lepton left-right forward-backward asymmetries ($\mathcal{A}_\ell = 0.1459 \pm 0.0063$) and earlier measurements of the hadronic polarised asymmetry to arrive at the combined result of $\mathcal{A}_\ell = 0.1504 \pm 0.0023$.

# 7 Measurement of W-Boson Properties at LEP-II

**Updates with respect to last summer:**
WW cross-section at 183 GeV(prel.), update of W decay branching ratios (prel.), W Mass at 183 GeV(prel.), DELPHI 172 WW cross-section(final), and W TGC's at 183 GeV(prel.)

In 1996 the energy of LEP was increased in two steps to 161 GeV and 172 GeV, allowing the production of W boson pairs. In 1997, the energy was further increased to 183 GeV. The data recorded at 161 GeV, which is just above the pair production threshold, was used to determine the W mass by comparing the measured cross-section with the predicted cross-section behaviour. At higher energies, the mass is determined by directly reconstructing the decay products of the W boson. In addition, the data at all energies have been used to determine other properties, such as the W decay branching ratios and the couplings of the W to other bosons.

In 1997, at an average centre-of-mass energy of 183 GeV [86], each experiment collected approximately 55 $\mathrm{pb}^{-1}$. Examples of the invariant mass distributions from the four experiments are shown in Figure 4. The W mass values determined [87–90], from semi-leptonic and hadronic WW decays have been combined separately and are shown in Table 21. Systematic uncertainties arising from ISR and fragmentation effects have been considered as correlated between experiments.

| Experiment | $m_{\mathrm{W}}$ (GeV) | | |
|---|---|---|---|
| | $\mathrm{q\bar{q}}\ell\nu$ | $\mathrm{q\bar{q}q\bar{q}}$ | combined |
| ALEPH (prel.) | $80.34 \pm 0.19 \pm 0.04$ | $80.41 \pm 0.18 \pm 0.10$ | $80.37 \pm 0.13 \pm 0.06$ |
| DELPHI (prel.) | $80.50 \pm 0.26 \pm 0.07$ | $80.02 \pm 0.20 \pm 0.10$ | $80.23 \pm 0.16 \pm 0.07$ |
| L3 (prel.) | $80.03 \pm 0.24 \pm 0.07$ | $80.51 \pm 0.21 \pm 0.12$ | $80.32 \pm 0.16 \pm 0.09$ |
| OPAL (prel.) | $80.25 \pm 0.18 \pm 0.08$ | $80.48 \pm 0.23 \pm 0.12$ | $80.34 \pm 0.14 \pm 0.07$ |
| LEP Average | $80.28 \pm 0.12$ | $80.34 \pm 0.14$ | $80.32 \pm 0.10$ |

Table 21: The (preliminary) measurements of $m_{\mathrm{W}}$ at 183 GeV in the $\mathrm{q\bar{q}}\ell\nu$, $\mathrm{q\bar{q}q\bar{q}}$ and combined channels, for the four experiments and the LEP average. In this table, the first error is statistical and the second is the total systematic error. The $\chi^2$/d.o.f. for the three combinations is 1.8/3, 3.6/3 and 0.5/3.

The combined W mass value, derived from the semi-leptonic channels, is $80.28 \pm 0.11 \pm 0.02$ GeV, where the first error includes statistics and systematics, the latter corresponding to the uncertainty on the LEP beam energy [86]. The total common error is 0.04 GeV and the $\chi^2$ per degree of freedom is 1.8/3.

The combined W mass value from the fully hadronic channel is $80.34 \pm 0.11 \pm 0.09(\mathrm{FSI}) \pm 0.02(\mathrm{LEP})$ GeV, with a $\chi^2$ per degree of freedom is 3.6/3. FSI stands for Final State Interactions, and includes effects due to Bose-Einstein correlations and Colour-Reconnection. ALEPH quotes a 56 MeV error on the W mass due to FSI effects, while the other three experiments assign 100 MeV. Conservatively a common systematic error of 90 MeV has been assigned in performing the average. The total common error amounts to 0.10 GeV.

The averaged W mass from semi-leptonic and hadronic final states has been derived from the combined mass of the individual experiments, as the treatment of error correlations is better controlled by each experiment. The average W mass value is $80.32 \pm 0.08 \pm 0.05(\mathrm{FSI}) \pm 0.02(\mathrm{LEP})$ GeV, with a $\chi^2$ per degree of freedom of 0.5/3. The total common error amounts to 0.06 GeV.

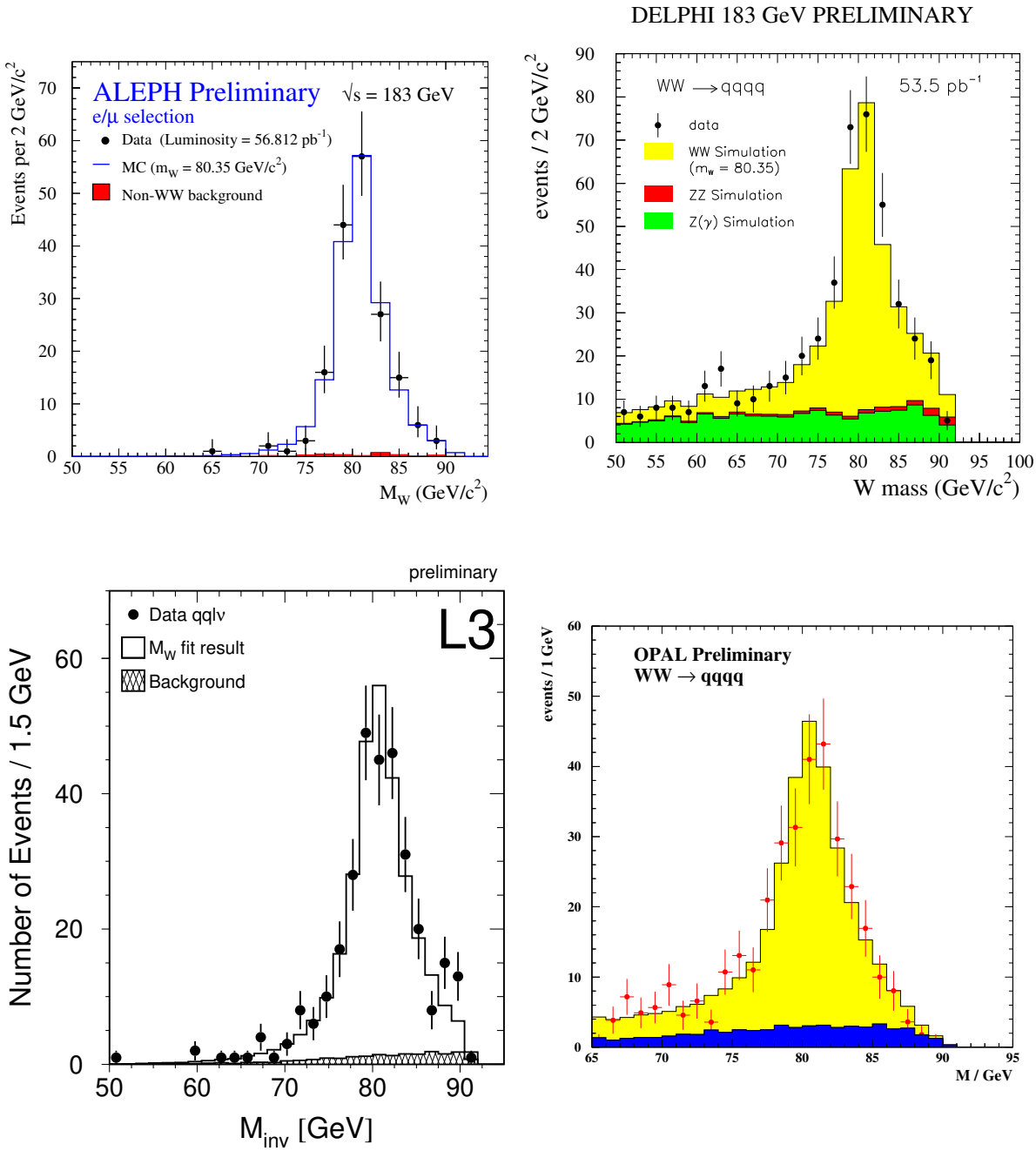


Figure 4: W mass distributions from the four LEP experiments at 183 GeV.

Earlier direct W mass reconstruction (172 GeV) results have been combined by each experiments with the 183 GeV result, for each channel. The same method has been used to combine the measurements of the four experiments; the results are summarised in table 22.

The combined four-experiment W mass value in the semi-leptonic channel is

$$m_{\mathrm{W}}^{\mathrm{leptonic}} \quad = \quad 80.31 \pm 0.11 \pm 0.02(\mathrm{LEP})\ \mathrm{GeV}, \tag{27}$$

and in the hadronic channel is measured to be

$$m_{\mathrm{W}}^{\mathrm{hadronic}} \quad = \quad 80.39 \pm 0.10 \pm 0.09(\mathrm{FSI}) \pm 0.02(\mathrm{LEP})\ \mathrm{GeV}. \tag{28}$$

| Experiment | $m_{\mathrm{W}}$ (GeV) | | |
|---|---|---|---|
| | $\mathrm{q\overline{q}}\ell\nu$ | $\mathrm{q\overline{q}q\overline{q}}$ | combined |
| ALEPH (prel.) | $80.34 \pm 0.18$ | $80.53 \pm 0.18$ | $80.44 \pm 0.13$ |
| DELPHI (prel.) | $80.50 \pm 0.24$ | $80.01 \pm 0.22$ | $80.24 \pm 0.17$ |
| L3 (prel.) | $80.09 \pm 0.24$ | $80.59 \pm 0.23$ | $80.40 \pm 0.18$ |
| OPAL (prel.) | $80.29 \pm 0.19$ | $80.40 \pm 0.24$ | $80.34 \pm 0.15$ |
| LEP Average | $80.31 \pm 0.11$ | $80.39 \pm 0.14$ | $80.36 \pm 0.09$ |

Table 22: Summary of W mass measurements by direct reconstruction (172 and 183 GeV) from the four LEP experiments in the semi-leptonic channel, the hadronic channel and the combined $m_{\mathrm{W}}$. The last row is the combination of the four measurements for the different channels. The errors include statistic and systematic uncertainties. The $\chi^2$/d.o.f. for the three combinations is 1.6/3, 5.6/3 and 1.1/3.

At the current level of accuracy there is no significant difference between the W mass determined in the fully hadronic and semi-leptonic channel. The combined mass value[3] from all channels is

$$m_{\mathrm{W}} \quad = \quad 80.36 \pm 0.08 \pm 0.05(\mathrm{FSI}) \pm 0.02(\mathrm{LEP}) \ \mathrm{GeV}. \tag{29}$$

This W mass measurement from direct reconstruction is combined with the W mass determination from the WW cross-section at threshold ($80.40 \pm 0.22$ GeV) [1] with a common error between the two measurements of 0.02 GeV(LEP), yielding

$$m_{\mathrm{W}} \quad = \quad 80.37 \pm 0.09 \ \mathrm{GeV} \tag{30}$$

as the current LEP-II average W mass.

| Experiment | 172.12 GeV $\sigma_{\mathrm{W^+W^-}}$ (pb) (final) | 182.67 GeV $\sigma_{\mathrm{W^+W^-}}$ (pb) (preliminary) |
|---|---|---|
| ALEPH | $11.7 \pm 1.2 \pm 0.3$ | $15.5 \pm 0.6 \pm 0.4$ |
| DELPHI | $11.58^{+1.44}_{-1.35} \pm 0.32$ | $16.0 \pm 0.7 \pm 0.4$ |
| L3 | $12.27^{+1.41}_{-1.32} \pm 0.23$ | $16.5 \pm 0.7 \pm 0.3$ |
| OPAL | $12.3 \pm 1.3 \pm 0.3$ | $15.5 \pm 0.6 \pm 0.4$ |
| LEP Average | $12.0 \pm 0.7$ | $15.9 \pm 0.4$ |

Table 23: The measurements of the W pair cross-sections at 172.12 and 182.67 GeV.

In addition, the LEP experiments have determined the W pair cross-section at 183 GeV. Table 23 summarises the cross section values, assuming standard model decay branching ratios for the W decay, obtained by ALEPH [91], DELPHI [92], L3 [93] and OPAL [94]. In the averaging procedure, the QCD component of the systematic errors has been taken as a correlated systematic uncertainty between experiments. The average is $15.86 \pm 0.40$ pb, with a $\chi^2$ per degree of freedom of 1.4/3; the common error amounts to 0.18 pb. Figure 5 shows the evolution of the W pair cross-section with centre-of-mass energy.

[3]It should be noted that this method of combination of the two channels is optimal for taking into account correlations within one experiment. However, correlations between experiments, such as the FSI error for the fully hadronic channel, are not fully reflected in the weights for the total average. At the current level of accuracy, this effect is sufficiently small to be neglected.

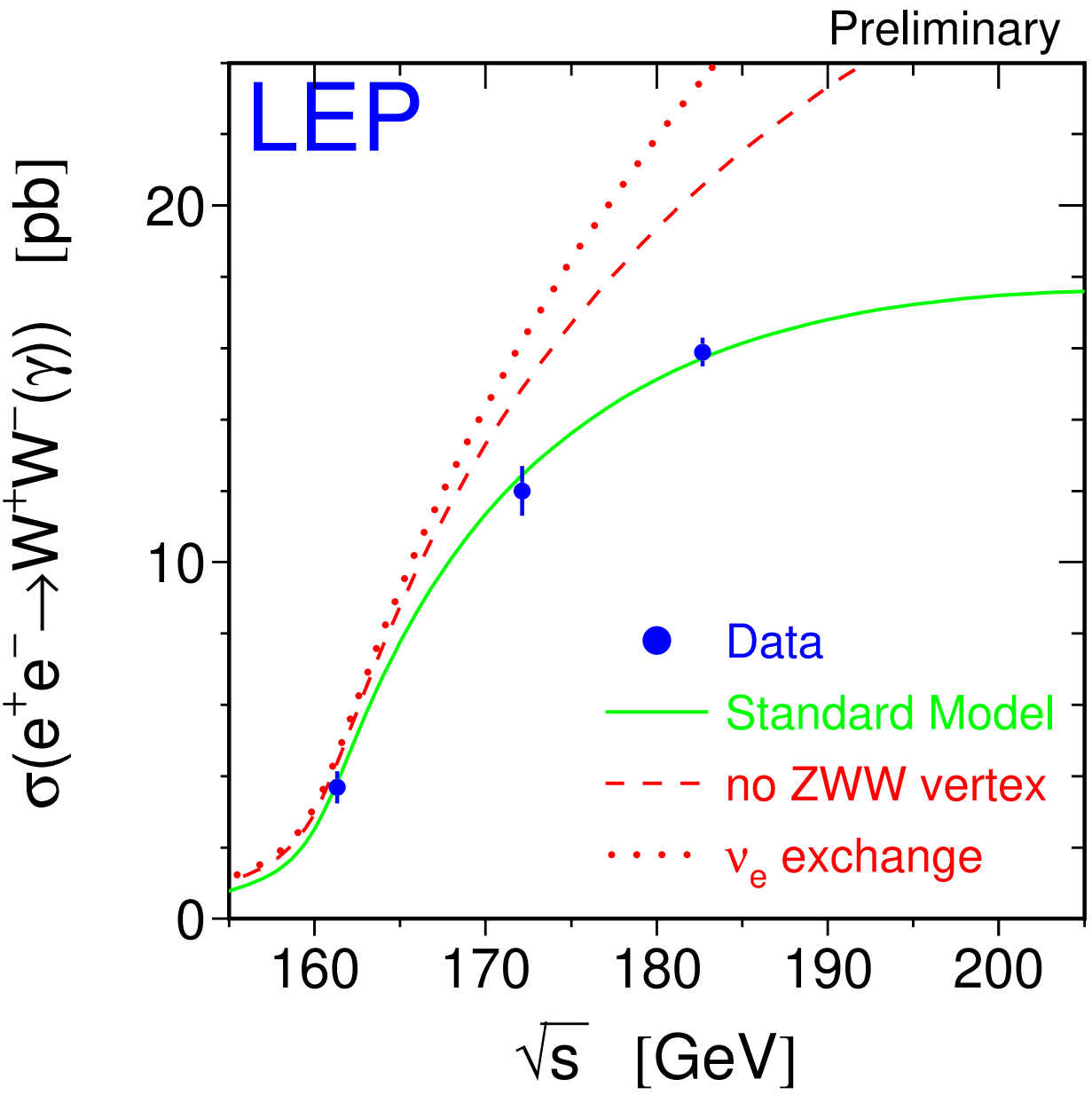


Figure 5: The W-pair cross-section as a function of the centre-of-mass energy. The data points are the LEP averages. Also shown is the Standard Model prediction (solid line), and for comparison the cross-section if the ZWW coupling did not exist (dashed line), or if only the $t$-channel $\nu_e$ exchange diagram existed (dotted line).

The W decay branching ratios have been determined from individual channels cross-section values measured by the four experiments (at all centre-of-mass energies [91–94]), with and without lepton universality assumption and are shown in Table 24. Correlated errors between the individual channels have been taken into account. $B(W \to \tau\nu)$ is 25% anti-correlated with the other two leptonic branching ratios, $B(W \to \mu\nu)$ and $B(W \to e\nu)$ are 1.0% correlated. Under the assumption of lepton universality,

the measured hadronic W decay branching ratio is $68.8 \pm 0.8\%$.

| Experiment | Br(W→e$\nu$) | Br(W→ $\mu\nu$) | Br(W→ $\tau\nu$) | Br(W→hadrons) |
|---|---|---|---|---|
| ALEPH | $11.2 \pm 0.8 \pm 0.3$ | $9.9 \pm 0.8 \pm 0.2$ | $9.7 \pm 1.0 \pm 0.3$ | $69.0 \pm 1.2 \pm 0.6$ |
| DELPHI | $9.9 \pm 1.1 \pm 0.5$ | $11.4 \pm 1.1 \pm 0.5$ | $11.2 \pm 1.7 \pm 0.7$ | $67.5 \pm 1.5 \pm 0.9$ |
| L3 | $10.5 \pm 0.9 \pm 0.2$ | $10.2 \pm 0.9 \pm 0.2$ | $9.0 \pm 1.2 \pm 0.3$ | $70.1 \pm 1.3 \pm 0.4$ |
| OPAL | $11.7 \pm 0.9 \pm 0.3$ | $10.1 \pm 0.8 \pm 0.3$ | $10.3 \pm 1.0 \pm 0.3$ | $67.9 \pm 1.2 \pm 0.6$ |
| LEP Average | $10.9 \pm 0.5$ | $10.3 \pm 0.5$ | $10.0 \pm 0.6$ | $68.8 \pm 0.8$ |

Table 24: Preliminary measurements of the W decay branching ratios in percent. The hadronic branching ratio is determined assuming lepton universality. There are large correlations between the individual leptonic branching ratios, which have been taken into account in determining the hadronic branching ratio.

Within the Standard Model the branching ratios of the W boson depend on the six elements of the Cabibbo-Kobayashi-Maskawa quark-mixing matrix ($V_{\rm CKM}$) not involving the top quark and on $\alpha_{\rm s}$. Using the current world-average values and errors of the other matrix elements not assuming the unitarity of $V_{\rm CKM}$ [95], and from the world average value of $\alpha_{\rm s}(m_{\rm Z}^2) = 0.119 \pm 0.002$ [95] evolved to $m_{\rm W}^2$, a constraint on the least well measured CKM matrix element is obtained :

$$|V_{\rm cs}| \quad = \quad 1.04 \pm 0.04. \tag{31}$$

The error includes the errors on $\alpha_{\rm s}$ and the other $V_{\rm CKM}$ elements but is dominated by the statistical error on the W branching fractions. The element $V_{\rm cs}$ is also determined by counting charm and strange jets in W decays; details are given in References 96–99.

The $\rm W^+W^-$ production process also involves the triple-gauge-boson vertices between the $\rm W^+W^-$ and the Z or photon. The measurement of these triple gauge boson couplings (TGC's) and the search for possible anomalous values is one of the main physics goal at LEP-II.

The parameterisation of anomalous TGC's is described in References 100–105. The most general Lorentz invariant Lagrangian which describes the triple gauge boson interaction has fourteen independent terms, seven describing the WW$\gamma$ vertex and seven describing the WWZ vertex. Assuming electromagnetic gauge invariance and C and P conservation the number of parameters is reduced to five. One common set is $\{\Delta g_1^{\rm z}, \Delta\kappa_{\rm z}, \Delta\kappa_\gamma, \lambda_{\rm z}, \lambda_\gamma\}$ [101] which are all zero in the Standard Model. With the further assumption of global SU(2) symmetry, this set can be further reduced to three independent parameters, $\Delta g_1^{\rm z}$, $\Delta\kappa_\gamma$ and $\lambda_\gamma$ with the constraints $\Delta\kappa_{\rm z} = -\Delta\kappa_\gamma \tan^2\theta_{\rm W} + \Delta g_1^{\rm z}$ and $\lambda_{\rm z} = \lambda_\gamma$. A slightly different parameterisation which embodied the same physics was used in the previous note [1].

Anomalous TGC's can affect both the total production cross-section and the shape of the differential cross-section as a function of the $\rm W^-$ production angle in W pair production. The relative contributions of each helicity state of the W bosons are also changed, which in turn affects the distributions of their decay products. In addition to W pair production, results from e$\nu$W ("single W") and $\nu\nu\gamma$ ("single photon") production have also been included. Single W production is particularly sensitive to $\Delta\kappa_\gamma$, thus providing complementary information to that of W pair production. The analyses presented by each experiment make use of different combinations of these quantities. The results presented here use measurements of all three parameters $\Delta g_1^{\rm z}$, $\Delta\kappa_\gamma$ and $\lambda_\gamma$, by DELPHI [106], L3 [107] and OPAL [108], and of $\Delta\kappa_\gamma$ and $\lambda_\gamma$ by ALEPH [109] and DØ [110] . In each case, the individual references should be consulted for details.

The measurements are combined by adding the log-likelihood curves provided by the experiments. This is performed both in one dimension, where only one of the parameters is allowed to vary from its

Standard Model value, as well as in two dimensions where two parameters are allowed to vary. In all cases, correlated systematic errors have been estimated to be small and thus the correlations among experiments have been neglected.

The results of fits to $\Delta g_1^z$, $\Delta\kappa_\gamma$ and $\lambda_\gamma$, assuming in each case that the other two anomalous couplings are zero, are shown in Table 25 for each experiment and for the LEP+DØ combined results. The values are all consistent with zero.

| Experiment | $\Delta g_1^z$ | $\Delta\kappa_\gamma$ | $\lambda_\gamma$ |
|---|---|---|---|
| ALEPH [109] | | $-0.02^{+0.28}_{-0.33}$ | $0.05^{+0.50}_{-0.51}$ |
| DELPHI [106] | $0.04^{+0.14}_{-0.14}$ | $0.34^{+0.26}_{-0.28}$ | $-0.07^{+0.19}_{-0.16}$ |
| L3 [107] | $-0.03^{+0.18}_{-0.16}$ | $0.16^{+0.40}_{-0.35}$ | $0.01^{+0.19}_{-0.17}$ |
| OPAL [108] | $-0.02^{+0.12}_{-0.11}$ | $0.19^{+0.47}_{-0.37}$ | $-0.08^{+0.13}_{-0.12}$ |
| DØ [110] | | $-0.08^{+0.34}_{-0.34}$ | $0.00^{+0.10}_{-0.10}$ |
| 68% C.L. | $0.00^{+0.08}_{-0.08}$ | $0.13^{+0.14}_{-0.14}$ | $-0.03^{+0.07}_{-0.07}$ |
| 95% C.L. interval | $[-0.15,\ 0.16]$ | $[-0.14,\ 0.48]$ | $[-0.22,\ 0.13]$ |

Table 25: The measured values obtained by the four LEP and DØ experiments for the anomalous TGC parameters. Both statistical and systematic errors are included. For the fits to each coupling, the values of the other two are set to zero. For the combined results, the 95% confidence level interval is also shown.

| | $\Delta g_1^z$<br>$\Delta\kappa_\gamma$ | $\Delta g_1^z$<br>$\lambda_\gamma$ | $\Delta\kappa_\gamma$<br>$\lambda_\gamma$ |
|---|---|---|---|
| ALEPH [109] | | | $0.05^{+1.2}_{-1.1}$<br>$-0.05^{+1.6}_{-1.5}$ |
| DELPHI [106] | $0.06^{+0.21}_{-0.18}$<br>$0.31^{+0.50}_{-0.39}$ | $0.17^{+0.16}_{-0.18}$<br>$-0.23^{+0.22}_{-0.19}$ | $0.27^{+0.39}_{-0.36}$<br>$-0.10^{+0.36}_{-0.31}$ |
| L3 [107] | $-0.06^{+0.20}_{-0.16}$<br>$0.33^{+0.62}_{-0.52}$ | $-0.06^{+0.23}_{-0.21}$<br>$0.04^{+0.24}_{-0.23}$ | $0.35^{+0.64}_{-0.53}$<br>$-0.04^{+0.21}_{-0.19}$ |
| OPAL [108] | $0.01^{+0.15}_{-0.17}$<br>$0.00^{+0.60}_{-0.30}$ | $-0.15^{+0.34}_{-0.20}$<br>$0.23^{+0.26}_{-0.43}$ | $-0.01^{+0.46}_{-0.34}$<br>$0.03^{+0.22}_{-0.18}$ |
| 68% C.L. | $0.00^{+0.12}_{-0.11}$<br>$0.28^{+0.33}_{-0.27}$ | $0.05^{+0.13}_{-0.13}$<br>$-0.07^{+0.16}_{-0.15}$ | $0.09^{+0.17}_{-0.15}$<br>$0.02^{+0.13}_{-0.12}$ |
| Correlation | $-0.54$ | $-0.79$ | $-0.50$ |
| 95% C.L. interval | $[-0.19,\ 0.22]$<br>$[-0.19,\ 0.89]$ | $[-0.21,\ 0.29]$<br>$[-0.34,\ 0.26]$ | $[-0.19,\ 0.44]$<br>$[-0.22,\ 0.27]$ |

Table 26: The measured values obtained by the four LEP experiments for the anomalous TGC parameters. Both statistical and systematic errors are included. In each column, the two listed parameters are allowed to vary while the third one is fixed to its SM value. For the combined results, the correlations as well as the 95% confidence level intervals are also shown.

The results of the two parameter fits are shown in Table 26 and an example of a two-dimensional contour is shown in Figure 6. In all cases, there is very good agreement with the Standard Model. It is interesting to note, that these results can be used to completely exclude [111] the Kaluza-Klein theory [112] in which $\Delta\kappa_\gamma = -3$.

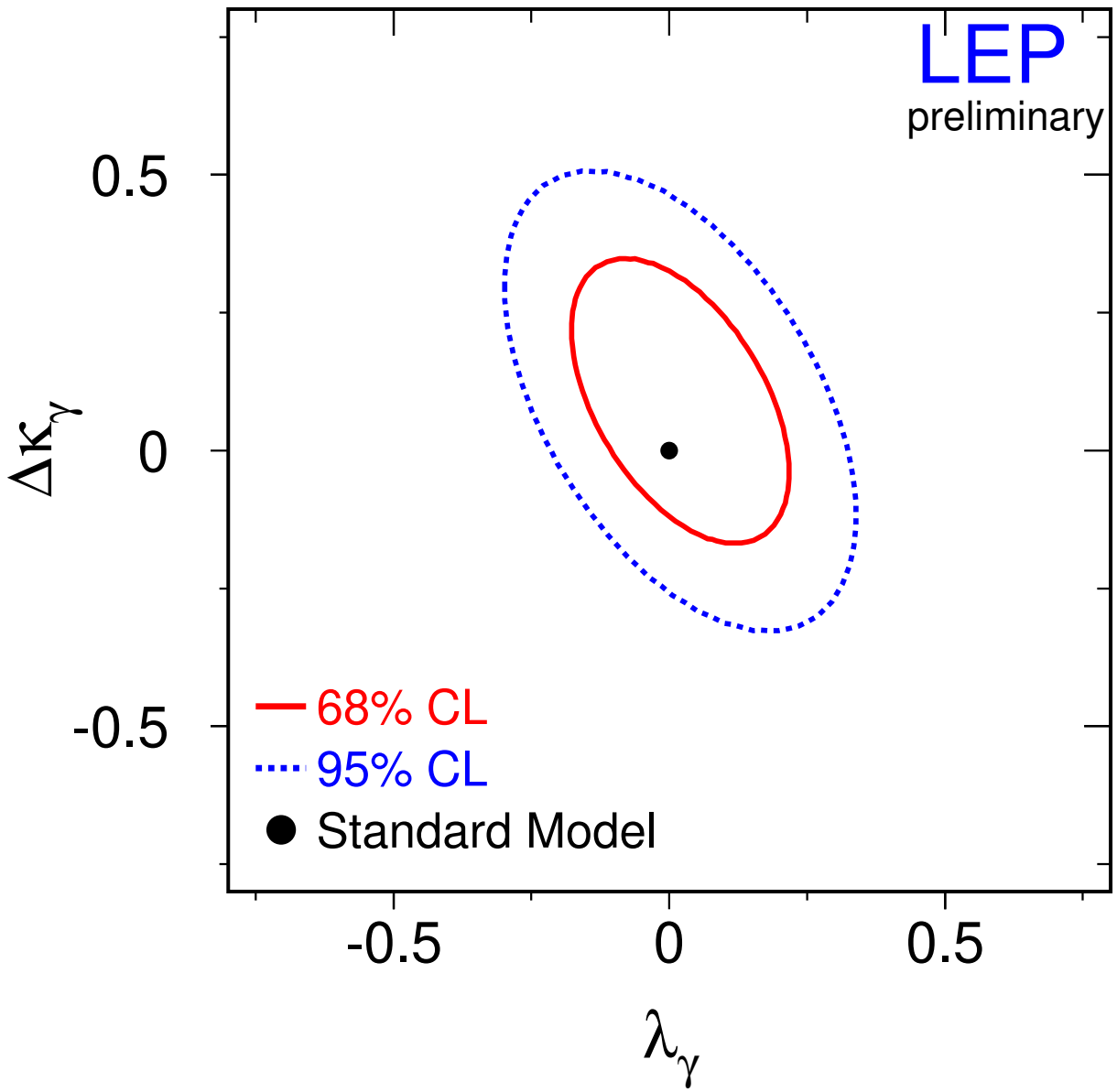


Figure 6: The contour curves for 68% C.L. and 95% C.L. in the parameter space $\Delta\kappa_\gamma$ *vs.* $\lambda_\gamma$, obtained from the sum of the curves from the individual LEP experiments and plotting the parameter at $\Delta \log \mathcal{L} = 1.15$ and $\Delta \log \mathcal{L} = 3.0$ respectively.

# 8 Interpretation of Results

**Updates with respect to last summer:**
For the Standard Model fits, new versions of the analytical programs which incorporate higher-order corrections have been used.

## 8.1 Number of Neutrino Species

An important aspect of our measurement concerns the information related to Z decays into invisible channels. Using the results of Tables 7 and 8, the ratio of the Z decay width into invisible particles and the leptonic decay width is determined:

$$\Gamma_{\rm inv}/\Gamma_{\ell\ell} \;=\; 5.961 \pm 0.023\,. \tag{32}$$

The Standard Model value for the ratio of the partial widths to neutrinos and charged leptons is:

$$(\Gamma_{\nu\nu}/\Gamma_{\ell\ell})_{\rm SM} \;=\; 1.991 \pm 0.001\,. \tag{33}$$

The central value is evaluated for $m_{\rm Z} = 91.1867$ GeV and the error quoted accounts for a variation of $m_{\rm t}$ in the range $m_{\rm t} = 173.8 \pm 5.0$ GeV and a variation of $m_{\rm H}$ in the range 90 GeV $\leq m_{\rm H} \leq$ 1000 GeV. The number of light neutrino species is given by the ratio of the two expressions listed above:

$$N_\nu \;=\; 2.994 \pm 0.011\,. \tag{34}$$

Alternatively, one can assume 3 neutrino species and determine the width from additional invisible decays of the Z. This yields

$$\Delta\Gamma_{\rm inv} \;=\; -1.6 \pm 1.9 \text{ MeV}. \tag{35}$$

The negative additional width results from a measured total width that is slightly below the Standard Model expectation. This is also seen in the number of neutrino families which is slightly lower than 3. If a conservative approach is taken to limit the result to only positive values of $\Delta\Gamma_{\rm inv}$, then the 95% CL upper limit on additional invisible decays of the Z is

$$\Delta\Gamma_{\rm inv} \;<\; 2.8 \text{ MeV}. \tag{36}$$

The uncertainties on $N_\nu$ and $\Delta\Gamma_{\rm inv}$ are dominated by the theoretical error on the luminosity. These results will therefore improve when the improved theoretical calculations on Bhabha scattering [9] are incorporated in the fits.

## 8.2 The Coupling Parameters $\mathcal{A}_{\rm f}$

The coupling parameters $\mathcal{A}_{\rm f}$ are defined in terms of the effective vector and axial-vector neutral current couplings of fermions (Equation (4)). The LEP measurements of the forward-backward asymmetries of charged leptons (Section 2) and b and c quarks (Section 4) determine the products $A_{\rm FB}^{0,\,\rm f} = \frac{3}{4}\mathcal{A}_{\rm e}\mathcal{A}_{\rm f}$ (Equation (3)). The LEP measurements of the $\tau$ polarisation (Section 3), $\mathcal{P}_\tau(\cos\theta)$, determine $\mathcal{A}_\tau$ and $\mathcal{A}_{\rm e}$ separately (Equation (15)).

Table 27 shows the results for the leptonic coupling parameter $\mathcal{A}_\ell$ from the LEP and SLD measurements, assuming lepton universality.

| | $\mathcal{A}_\ell$ | Cumulative Average | $\chi^2$/d.o.f. |
|---|---|---|---|
| $A_{\rm FB}^{0,\ell}$ | $0.1498 \pm 0.0043$ | | |
| $\mathcal{P}_\tau(\cos\theta)$ | $0.1452 \pm 0.0034$ | $0.1469 \pm 0.0027$ | 0.7/1 |
| $A_{\rm LR}^0$ (SLD) | $0.1504 \pm 0.0023$ | $0.1489 \pm 0.0017$ | 1.7/2 |

Table 27: Determinations of the leptonic coupling parameter $\mathcal{A}_\ell$ assuming lepton universality. The second column lists the $\mathcal{A}_\ell$ values derived from the quantities listed in the first column. The third column contains the cumulative averages of these $\mathcal{A}_\ell$ results. The averages are derived assuming no correlations between the measurements. The $\chi^2$ per degree of freedom for the cumulative averages is given in the last column.

| | LEP ($\mathcal{A}_\ell = 0.1469 \pm 0.0027$) | SLD | LEP+SLD ($\mathcal{A}_\ell = 0.1489 \pm 0.0017$) |
|---|---|---|---|
| $\mathcal{A}_{\rm b}$ | $0.899 \pm 0.025$ | $0.867 \pm 0.035$ | $0.881 \pm 0.018$ |
| $\mathcal{A}_{\rm c}$ | $0.646 \pm 0.043$ | $0.647 \pm 0.040$ | $0.641 \pm 0.028$ |

Table 28: Determinations of the quark coupling parameters $\mathcal{A}_{\rm b}$ and $\mathcal{A}_{\rm c}$ from LEP data alone (using the LEP average for $\mathcal{A}_\ell$), from SLD data alone, and from LEP+SLD data (using the LEP+SLD average for $\mathcal{A}_\ell$) assuming lepton universality.

Using the measurements of $\mathcal{A}_\ell$ one can extract $\mathcal{A}_{\rm b}$ and $\mathcal{A}_{\rm c}$ from the LEP measurements of the b and c quark asymmetries. The SLD measurements of the left-right forward-backward asymmetries for b and c quarks are direct determinations of $\mathcal{A}_{\rm b}$ and $\mathcal{A}_{\rm c}$. Table 28 shows the results on the quark coupling parameters $\mathcal{A}_{\rm b}$ and $\mathcal{A}_{\rm c}$ derived from LEP or SLD measurements separately (Equations 24 and 25) and from the combination of LEP+SLD measurements (Equation 25). The LEP extracted values of $\mathcal{A}_{\rm b}$ and $\mathcal{A}_{\rm c}$ are in excellent agreement with the SLD measurements, and in reasonable agreement with the Standard Model predictions (0.935 and 0.668, respectively, essentially independent of $m_{\rm t}$ and $m_{\rm H}$) However, the combination of LEP and SLD of $\mathcal{A}_{\rm b}$ is 3.0 sigma below the Standard Model. This is due to three independent results: the SLD measurement of $\mathcal{A}_{\rm b}$ is low compared to the Standard Model, while the LEP measurement of $A_{\rm FB}^{0,\rm b}$ and the combined LEP+SLD measurement of $\mathcal{A}_\ell$ are respectively low and high compared with the Standard Model fit of Table 31. This can be seen in Figure 7.

### 8.3 The Effective Vector and Axial-Vector Coupling Constants

The partial widths of the Z into leptons and the lepton forward-backward asymmetries (Section 2), the $\tau$ polarisation and the $\tau$ polarisation asymmetry (Section 3) can be combined to determine the effective vector and axial-vector couplings for e, $\mu$ and $\tau$. The asymmetries (Equations (3) and (15)) determine the ratio $g_{V\ell}/g_{A\ell}$ (Equation (4)), while the leptonic partial widths determine the sum of the squares of the couplings:

$$\Gamma_{\ell\ell} \;=\; \frac{G_{\rm F} m_{\rm Z}^3}{6\pi\sqrt{2}}(g_{V\ell}^2 + g_{A\ell}^2)(1+\delta_\ell^{QED})\,, \tag{37}$$

where $\delta_\ell^{QED} = 3q_\ell^2\alpha(m_{\rm Z}^2)/(4\pi)$ accounts for final state photonic corrections. Corrections due to lepton masses, neglected in Equation 37, are taken into account for the results presented below.

The averaged results for the effective lepton couplings are given in Table 29. Figure 8 shows the 68% probability contours in the $g_{A\ell}$-$g_{V\ell}$ plane. The signs of $g_{A\ell}$ and $g_{V\ell}$ are based on the convention $g_{A{\rm e}} < 0$. With this convention the signs of the couplings of all charged leptons follow from LEP data

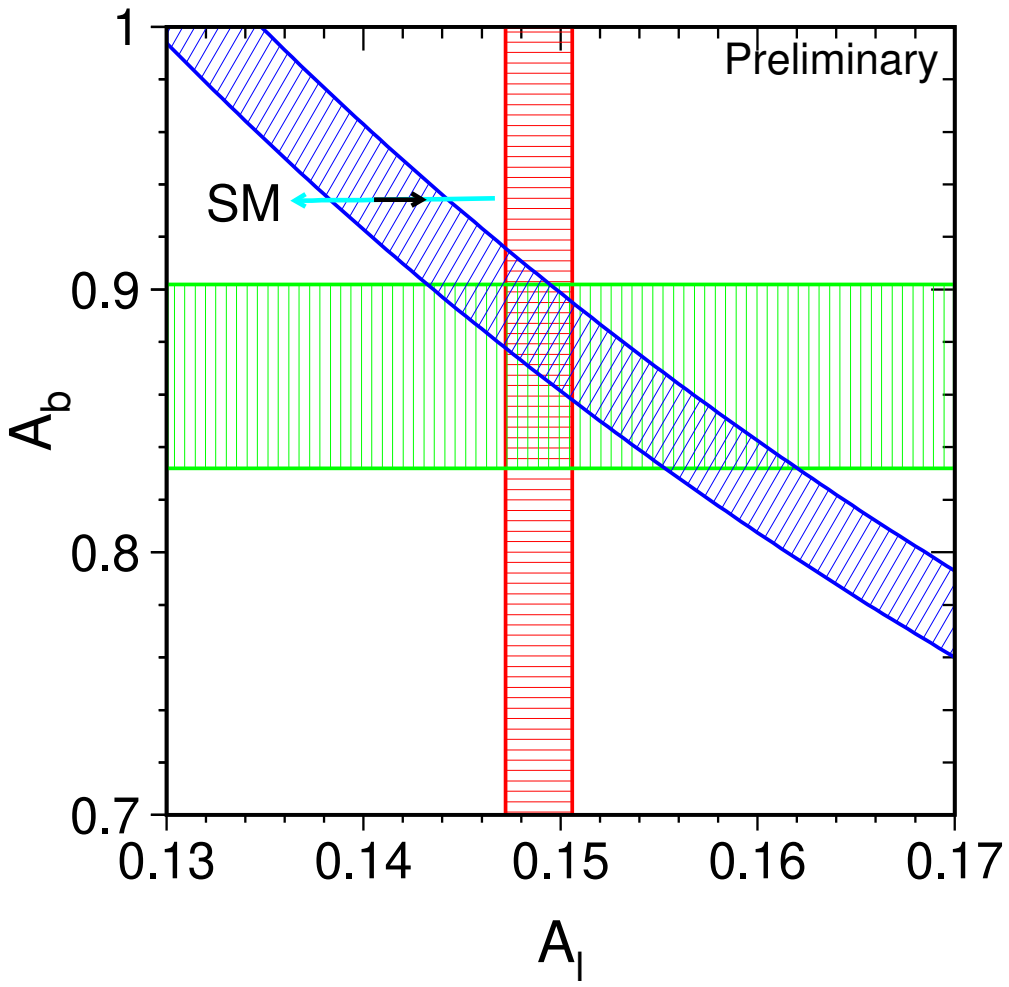


Figure 7: The measurements of the combined LEP+SLD $\mathcal{A}_\ell$ (vertical band), SLD $\mathcal{A}_\mathrm{b}$ (horizontal band) and LEP $A_\mathrm{FB}^{0,\mathrm{b}}$ (diagonal band), compared to the Standard Model expectations (arrows). The arrow pointing to the left shows the variation in the SM prediction for $m_\mathrm{H}$ in the range $300^{+700}_{-210}$ GeV, and the arrow pointing to the right for $m_\mathrm{t}$ in the range $173.8 \pm 5.0$ GeV. It should be noted that although the $A_\mathrm{FB}^{0,\mathrm{b}}$ measurement prefer a high Higgs mass, the Standard Model fit to the full set of measurements prefers a low Higgs mass.

alone. For comparison, the $g_{V\ell}$-$g_{A\ell}$ relation following from the measurement of $A_\mathrm{LR}$ from SLD [85] is indicated as a band in the $g_{A\ell}$-$g_{V\ell}$-plane of Figure 8. It is consistent with the LEP data. The information on the leptonic couplings from LEP can therefore be combined with the $A_\mathrm{LR}$ measurement of SLD. The results for this combination are given in the right column of Table 29. The measured ratios of the e, $\mu$ and $\tau$ couplings provide a test of lepton universality and are also given in Table 29.

The neutrino couplings to the Z can be derived from the measured value of the invisible width of the Z, $\Gamma_\mathrm{inv}$ (see Table 9), attributing it exclusively to the decay into three identical neutrino generations ($\Gamma_\mathrm{inv} = 3\Gamma_{\nu\nu}$) and assuming $g_{A\nu} \equiv g_{V\nu} \equiv g_\nu$. The relative sign of $g_\nu$ is chosen to be in agreement with neutrino scattering data [113], resulting in $g_\nu = +0.50123 \pm 0.00095$.

| | Without Lepton Universality: | |
|---|---|---|
| | LEP | LEP+SLD |
| $g_{V\mathrm{e}}$ | $-0.0375 \pm 0.0011$ | $-0.03781 \pm 0.00052$ |
| $g_{V\mu}$ | $-0.0369 \pm 0.0031$ | $-0.0366 \pm 0.0030$ |
| $g_{V\tau}$ | $-0.0365 \pm 0.0011$ | $-0.0365 \pm 0.0011$ |
| $g_{A\mathrm{e}}$ | $-0.50099 \pm 0.00038$ | $-0.50098 \pm 0.00038$ |
| $g_{A\mu}$ | $-0.50081 \pm 0.00058$ | $-0.50082 \pm 0.00058$ |
| $g_{A\tau}$ | $-0.50173 \pm 0.00065$ | $-0.50171 \pm 0.00065$ |
| | Ratios of couplings: | |
| | LEP | LEP+SLD |
| $g_{V\mu}/g_{V\mathrm{e}}$ | $0.984 \pm 0.098$ | $0.967 \pm 0.082$ |
| $g_{V\tau}/g_{V\mathrm{e}}$ | $0.974 \pm 0.043$ | $0.965 \pm 0.032$ |
| $g_{A\mu}/g_{A\mathrm{e}}$ | $0.9996 \pm 0.0014$ | $0.9997 \pm 0.0014$ |
| $g_{A\tau}/g_{A\mathrm{e}}$ | $1.0015 \pm 0.0015$ | $1.0015 \pm 0.0015$ |
| | With Lepton Universality: | |
| | LEP | LEP+SLD |
| $g_{V\ell}$ | $-0.03703 \pm 0.00068$ | $-0.03753 \pm 0.00044$ |
| $g_{A\ell}$ | $-0.50105 \pm 0.00030$ | $-0.50102 \pm 0.00030$ |
| $g_{\nu}$ | $+0.50123 \pm 0.00095$ | $+0.50123 \pm 0.00095$ |

Table 29: Results for the effective vector and axial-vector couplings derived from the combined LEP data without and with the assumption of lepton universality. For the right column the SLD measurement of $A_{\mathrm{LR}}$ is also included.

### 8.4 The Effective Electroweak Mixing Angle $\sin^2\theta^{\mathrm{lept}}_{\mathrm{eff}}$

The asymmetry measurements from LEP can be combined into a single observable, the effective electroweak mixing angle, $\sin^2\theta^{\mathrm{lept}}_{\mathrm{eff}}$, defined as:

$$\sin^2\theta^{\mathrm{lept}}_{\mathrm{eff}} \equiv \frac{1}{4}\left(1 - \frac{g_{V\ell}}{g_{A\ell}}\right), \tag{38}$$

without making any strong model-specific assumptions.

For a combined average of $\sin^2\theta^{\mathrm{lept}}_{\mathrm{eff}}$ from $A^{0,\ell}_{\mathrm{FB}}$, $\mathcal{A}_\tau$ and $\mathcal{A}_{\mathrm{e}}$ only the assumption of lepton universality, already inherent in the definition of $\sin^2\theta^{\mathrm{lept}}_{\mathrm{eff}}$, is needed. We can also include the hadronic forward-backward asymmetries if we assume the quark couplings to be given by the Standard Model. This is justified within the Standard Model as the hadronic asymmetries $A^{0,\mathrm{b}}_{\mathrm{FB}}$ and $A^{0,\mathrm{c}}_{\mathrm{FB}}$ have a reduced sensitivity to corrections particular to the quark vertex. The results of these determinations of $\sin^2\theta^{\mathrm{lept}}_{\mathrm{eff}}$ and their combination are shown in Table 30 and in Figure 9. Also the measurement of the left-right asymmetry, $A_{\mathrm{LR}}$, from SLD [85] is given. Compared with the results presented in our previous note [1], the $\chi^2$ of the average of all determinations has decreased by 4.7. This is due almost entirely to new results from tau polarisation, $A^{0,\mathrm{b}}_{\mathrm{FB}}$ and $A_{\mathrm{LR}}$.

| | $\sin^2\theta^{\rm lept}_{\rm eff}$ | Average by Group of Observations | Cumulative Average | $\chi^2$/d.o.f. |
|---|---|---|---|---|
| $A^{0,\ell}_{\rm FB}$ | $0.23117 \pm 0.00054$ | | | |
| $\mathcal{A}_\tau$ | $0.23141 \pm 0.00065$ | | | |
| $\mathcal{A}_{\rm e}$ | $0.23202 \pm 0.00057$ | $0.23153 \pm 0.00034$ | $0.23153 \pm 0.00034$ | 1.2/2 |
| $A^{0,{\rm b}}_{\rm FB}$ | $0.23225 \pm 0.00038$ | | | |
| $A^{0,{\rm c}}_{\rm FB}$ | $0.2322 \pm 0.0010$ | $0.23224 \pm 0.00035$ | $0.23187 \pm 0.00025$ | 3.3/4 |
| $\langle Q_{\rm FB} \rangle$ | $0.2321 \pm 0.0010$ | $0.2321 \pm 0.0010$ | $0.23189 \pm 0.00024$ | 3.3/5 |
| $A_{\rm LR}$ (SLD) | $0.23109 \pm 0.00029$ | $0.23109 \pm 0.00029$ | $0.23157 \pm 0.00018$ | 7.8/6 |

Table 30: Determinations of $\sin^2\theta^{\rm lept}_{\rm eff}$ from asymmetries. The second column lists the $\sin^2\theta^{\rm lept}_{\rm eff}$ values derived from the quantities listed in the first column. The third column contains the averages of these numbers by groups of observations, where the groups are separated by the horizontal lines. The fourth column shows the cumulative averages. The $\chi^2$ per degree of freedom for the cumulative averages is also given. The averages have been performed ignoring the small correlation between $A^{0,{\rm b}}_{\rm FB}$ and $A^{0,{\rm c}}_{\rm FB}$.

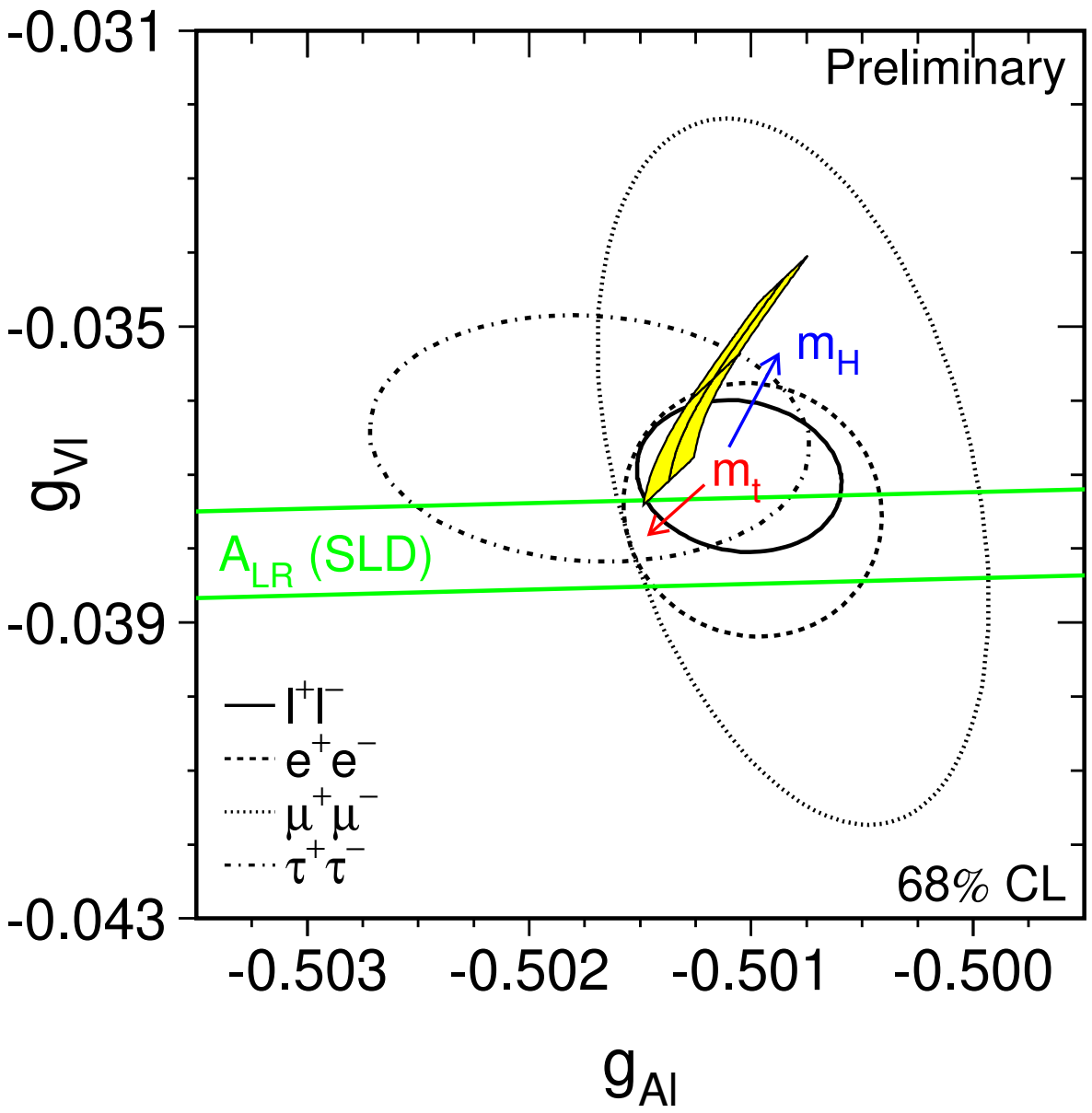


Figure 8: Contours of 68% probability in the $g_{V\ell}$-$g_{A\ell}$ plane from LEP measurements. The solid contour results from a fit assuming lepton universality. Also shown is the one standard deviation band resulting from the $A_{\rm LR}$ measurement of SLD. The shaded region corresponds to the Standard Model prediction for $m_{\rm t} = 173.8 \pm 5.0$ GeV and $m_{\rm H} = 300^{+700}_{-210}$ GeV. The arrows point in the direction of increasing values of $m_{\rm t}$ and $m_{\rm H}$.

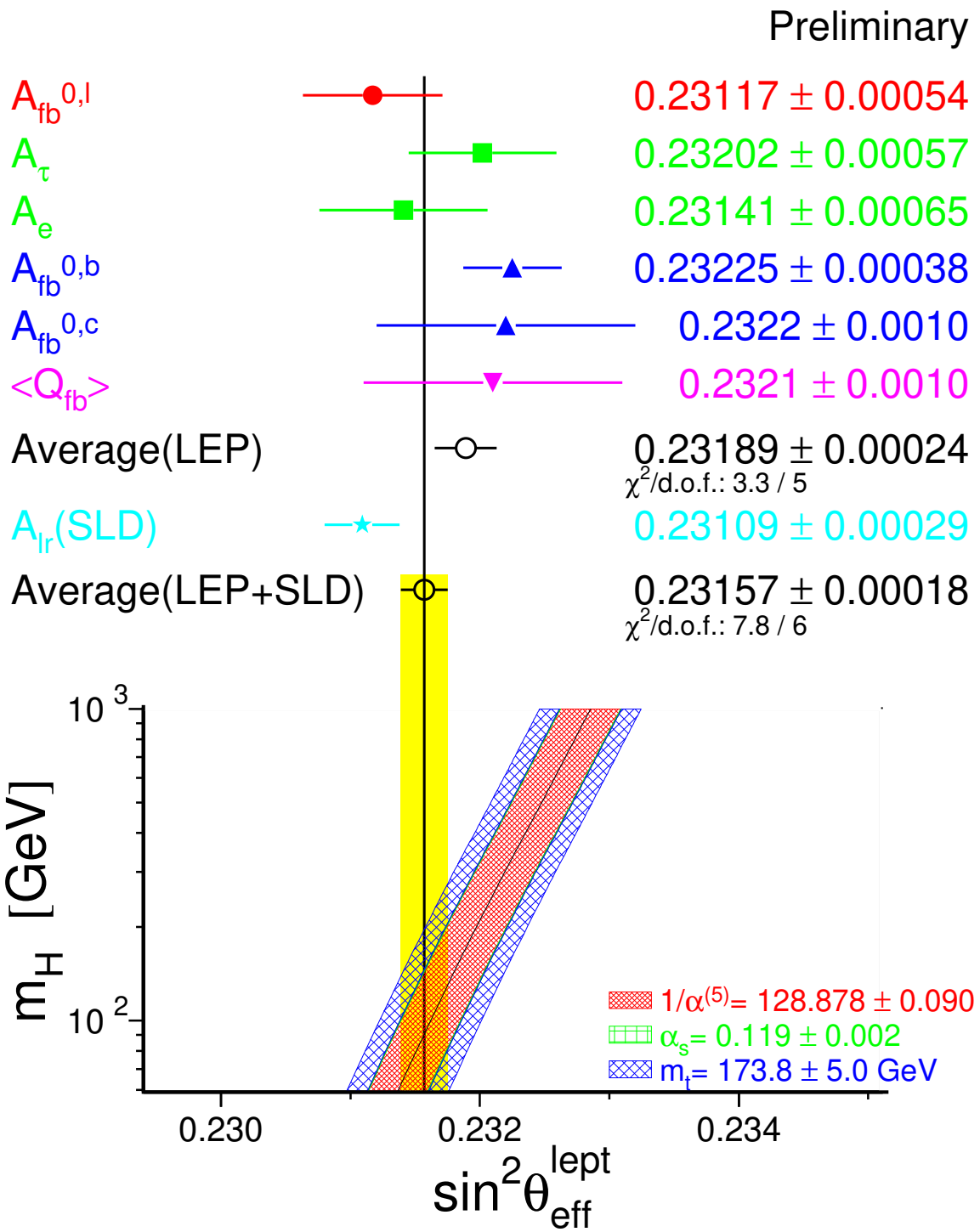


Figure 9: Comparison of several determinations of $\sin^2\theta_{\rm eff}^{\rm lept}$ from asymmetries. In the average, the small correlation between $A_{\rm FB}^{0,\rm b}$ and $A_{\rm FB}^{0,\rm c}$ has been ignored. Also shown is the prediction of the Standard Model as a function of $m_{\rm H}$. The width of the Standard Model band is due to the uncertainties in $\alpha(m_{\rm Z}^2)$, $\alpha_{\rm s}(m_{\rm Z}^2)$ and $m_{\rm t}$. The total width of the band is the linear sum of these effects.

## 8.5 Constraints on the Standard Model

The precise electroweak measurements performed at LEP and elsewhere can be used to check the validity of the Standard Model and, within its framework, to infer valuable information about its fundamental parameters. The accuracy of the measurements makes them sensitive to the top-quark mass, $m_{\rm t}$, and to the mass of the Higgs boson, $m_{\rm H}$, through loop corrections. While the leading $m_{\rm t}$ dependence is quadratic, the leading $m_{\rm H}$ dependence is logarithmic. Therefore, the inferred constraints on $m_{\rm H}$ are not very strong.

The LEP measurements used are summarised in Table 31 together with the results of the Standard Model fit. Also shown are the results from the SLD collaboration [85] as well as measurements of $m_{\rm W}$ from UA2 [114], CDF [115, 116], and DØ [117][4], measurements of the top quark mass by CDF [119] and DØ [120][5], and measurements of the neutrino-nucleon neutral to charged current ratios from CCFR [122] and NuTeV [123]. It should be noted that although these latter results are quoted in terms of $\sin^2\theta_W = 1 - m_{\rm W}^2/m_{\rm Z}^2$, radiative corrections result in small $m_{\rm t}$ and $m_{\rm H}$ dependences[6] that are included in the fit. In addition, the value of the electromagnetic coupling constant, $\alpha(m_{\rm Z}^2)$, which is used in the fits, is shown. An additional input parameter, not shown in the table, is the Fermi constant, $G_F$, determined from the $\mu$ lifetime, $G_F = (1.16639 \pm 0.00002) \times 10^{-5}\,\mathrm{GeV}^{-2}$ [95]. Although the relative error of $G_F$ is comparable to that of $m_{\rm Z}$, this uncertainty is neglected in the fits, as $G_F$ occurs in terms such as $G_F m_{\rm Z}^2$.

Detailed studies of the theoretical uncertainties in the Standard Model predictions due to missing higher-order electroweak corrections and their interplay with QCD corrections have been carried out in the working group on 'Precision calculations for the Z resonance' [126]. Theoretical uncertainties are evaluated by comparing different but, within our present knowledge, equivalent treatments of aspects such as resummation techniques, momentum transfer scales for vertex corrections and factorisation schemes. The effects of these theoretical uncertainties have been reduced by the inclusion of higher-order corrections [127, 128] in the electroweak libraries [129]. The use of the new QCD corrections [128] increases the value of $\alpha_{\rm s}(m_{\rm Z}^2)$ by 0.001, as expected. The effects of missing higher-order QCD corrections on $\alpha_{\rm s}(m_{\rm Z}^2)$ covers missing higher-order electroweak corrections and uncertainties in the interplay of electroweak and QCD corrections and has been estimated to be about 0.002 [130]. A discussion of theoretical uncertainties in the determination of $\alpha_{\rm s}$ can be found in References 126 and 130. For the moment, the determination of the size of remaining theoretical uncertainties is still under study. All theoretical errors discussed in this paragraph have been neglected for the results presented in Table 32.

At present the impact of theoretical uncertainties on the determination of SM parameters from the precise electroweak measurements is small compared with the error due to the uncertainty in the value of $\alpha(m_{\rm Z}^2)$. The uncertainty in $\alpha(m_{\rm Z}^2)$ arises from the contribution of light quarks to the photon vacuum polarisation ($\Delta\alpha^{(5)}_{\rm had}(m_{\rm Z}^2)$):

$$\alpha(m_{\rm Z}^2) = \frac{\alpha(0)}{1 - \Delta\alpha_\ell(m_{\rm Z}^2) - \Delta\alpha^{(5)}_{\rm had}(m_{\rm Z}^2) - \Delta\alpha_{\rm top}(m_{\rm Z}^2)}$$

The top contribution depends on the mass of the top quark, and is therefore determined inside the electroweak libraries [129]. The leptonic contribution has been recently calculated to third order [125] to be 0.031498. For the hadronic contribution, we use the value $0.02804 \pm 0.00065$ [124], which results

[4] See Reference 118 for a combination of these $m_{\rm W}$ measurements.

[5] See Reference 121 for a combination of these $m_{\rm t}$ measurements.

[6] The formula used is $\delta \sin^2\theta_W = -0.00142 \frac{m_{\rm t}^2 - (175\mathrm{GeV})^2}{(100\mathrm{GeV})^2} + 0.00048 \ln(\frac{m_{\rm H}}{150\mathrm{GeV}})$. See Reference 123 for details.

| | | Measurement with Total Error | Systematic Error | Standard Model fit | Pull |
|---|---|---|---|---|---|
| | $\alpha^{(5)}(m_{\rm Z}^2)^{-1}$ [124, 125] | $128.878 \pm 0.090$ | 0.083 | 128.878 | 0.0 |
| a) | LEP | | | | |
| | line-shape and | | | | |
| | lepton asymmetries: | | | | |
| | $m_{\rm Z}$ [GeV] | $91.1867 \pm 0.0021$ | [(a)]0.0017 | 91.1865 | 0.1 |
| | $\Gamma_{\rm Z}$ [GeV] | $2.4939 \pm 0.0024$ | [(a)]0.0013 | 2.4958 | −0.8 |
| | $\sigma_{\rm h}^0$ [nb] | $41.491 \pm 0.058$ | 0.057 | 41.473 | 0.3 |
| | $R_\ell$ | $20.765 \pm 0.026$ | 0.020 | 20.748 | 0.7 |
| | $A_{\rm FB}^{0,\ell}$ | $0.01683 \pm 0.00096$ | 0.00060 | 0.01613 | 0.7 |
| | + correlation matrix Table 8 | | | | |
| | $\tau$ polarisation: | | | | |
| | $\mathcal{A}_\tau$ | $0.1431 \pm 0.0045$ | 0.0027 | 0.1467 | −0.8 |
| | $\mathcal{A}_{\rm e}$ | $0.1479 \pm 0.0051$ | 0.0010 | 0.1467 | 0.2 |
| | $q\overline{q}$ charge asymmetry: | | | | |
| | $\sin^2\theta_{\rm eff}^{\rm lept}$ ($\langle Q_{\rm FB}\rangle$) | $0.2321 \pm 0.0010$ | 0.0008 | 0.23157 | 0.5 |
| | $m_{\rm W}$ [GeV] | $80.37 \pm 0.09$ | 0.06 | 80.37 | 0.0 |
| b) | SLD [85] | | | | |
| | $\sin^2\theta_{\rm eff}^{\rm lept}$ ($A_{\rm LR}$) | $0.23109 \pm 0.00029$ | 0.00018 | 0.23157 | −1.7 |
| c) | LEP and SLD Heavy Flavour | | | | |
| | $R_{\rm b}^0$ | $0.21656 \pm 0.00074$ | 0.00057 | 0.21590 | 0.9 |
| | $R_{\rm c}^0$ | $0.1735 \pm 0.0044$ | 0.0034 | 0.1722 | 0.3 |
| | $A_{\rm FB}^{0,\rm b}$ | $0.0990 \pm 0.0021$ | 0.0010 | 0.1028 | −1.8 |
| | $A_{\rm FB}^{0,\rm c}$ | $0.0709 \pm 0.0044$ | 0.0022 | 0.0734 | −0.6 |
| | $\mathcal{A}_{\rm b}$ | $0.867 \pm 0.035$ | 0.025 | 0.935 | −1.9 |
| | $\mathcal{A}_{\rm c}$ | $0.647 \pm 0.040$ | 0.023 | 0.668 | −0.5 |
| | + correlation matrix Table 18 | | | | |
| d) | $p\overline{p}$ and $\nu$N | | | | |
| | $m_{\rm W}$ [GeV] ($p\overline{p}$ [118]) | $80.41 \pm 0.09$ | 0.07 | 80.37 | 0.4 |
| | $1 - m_{\rm W}^2/m_{\rm Z}^2$ ($\nu$N [122, 123]) | $0.2254 \pm 0.0021$ | 0.0010 | 0.2232 | 1.1 |
| | $m_{\rm t}$ [GeV] ($p\overline{p}$ [121]) | $173.8 \pm 5.0$ | 3.9 | 171.1 | 0.5 |

Table 31: Summary of measurements included in the combined analysis of Standard Model parameters. Section a) summarises LEP averages, Section b) SLD results ($\sin^2\theta_{\rm eff}^{\rm lept}$ includes $A_{\rm LR}$ and the polarised lepton asymmetries), Section c) the LEP and SLD heavy flavour results and Section d) electroweak measurements from $p\overline{p}$ colliders and $\nu$N scattering. The total errors in column 2 include the systematic errors listed in column 3. Although the systematic errors include both correlated and uncorrelated sources, the determination of the systematic part of each error is approximate. The Standard Model results in column 4 and the pulls (difference between measurement and fit in units of the total measurement error) in column 5 are derived from the Standard Model fit including all data (Table 32, column 5) with the Higgs mass treated as a free parameter.

[(a)]The systematic errors on $m_{\rm Z}$ and $\Gamma_{\rm Z}$ contain the errors arising from the uncertainties in the LEP energy only.

in $1/\alpha^{(5)}(m_Z^2) = 128.878 \pm 0.090$. This uncertainty causes an error of 0.00023 on the Standard Model prediction of $\sin^2\theta_{\rm eff}^{\rm lept}$, an error of 1 GeV on $m_t$, and 0.2 on $\log(m_H)$, which are included in the results. The effect on the Standard Model prediction for $\Gamma_{\ell\ell}$ is negligible. The $\alpha_s(m_Z^2)$ values for the Standard Model fits presented in this Section are stable against a variation of $\alpha(m_Z^2)$ in the interval quoted. Recently there have been several reevaluations of $\Delta\alpha^{(5)}_{\rm had}(m_Z^2)$ [124, 131–137]. To show the effects of the uncertainty of $\alpha(m_Z^2)$, we also use the evaluation of $\Delta\alpha^{(5)}_{\rm had}(m_Z^2) = 0.02784 \pm 0.00026$ [135] which results in $1/\alpha^{(5)}(m_Z^2) = 128.905 \pm 0.036$.

Figure 10 shows a comparison of the leptonic partial width from LEP (Table 9) and the effective electroweak mixing angle from asymmetries measured at LEP and SLD (Table 30), with the Standard Model. Good agreement with the Standard Model prediction is observed. The point with the arrow shows the prediction if among the electroweak radiative corrections only the photon vacuum polarisation is included, which shows an example of evidence that LEP+SLD data are sensitive to electroweak corrections. Note that the error due to the uncertainty on $\alpha(m_Z^2)$ (shown as the length of the arrow) is larger than the experimental error on $\sin^2\theta_{\rm eff}^{\rm lept}$ from LEP and SLD. This underlines the growing importance of a precise measurement of $\sigma(e^+e^- \to \text{hadrons})$ at low centre-of-mass energies.

Of the measurements given in Table 31, $R_\ell$ is the most sensitive to QCD corrections. Thus, it can be used to determine the value of $\alpha_s(m_Z^2)$. For $m_Z = 91.1867$ GeV, and imposing $m_t = 173.8 \pm 5.0$ GeV as a constraint, $\alpha_s = 0.122 \pm 0.004 \pm 0.001$ is obtained, where the second error accounts for varying $m_H$ in the range $m_H = 76^{+85}_{-47}$ GeV. This result is in very good agreement with the world average ($\alpha_s(m_Z^2) = 0.119 \pm 0.002$ [95]).

To test the agreement between the LEP data and the Standard Model, we first perform a fit to the data (including the LEP-II $m_W$ determination) leaving the top quark mass and the Higgs mass as free parameters. The result is shown in Table 32, column 2. This fit shows that the LEP data prefer a light top quark and a light Higgs, albeit with very large errors. The strongly asymmetric errors on $m_H$ are due to the fact that to first order, the radiative corrections in the Standard Model are proportional to $\log(m_H)$. The correlation between the top quark mass and the Higgs mass is 0.72 (see Figure 11).

The data can also be used within the Standard Model to determine the top quark and W masses indirectly, which can be compared to the direct measurements performed at the Tevatron and LEP. For this, we perform several fits. In the first fit, we use all the results in Table 31, except the LEP-II and Tevatron $m_W$ and $m_t$ results. The results are shown in column 3 of Table 32. The indirect measurements of $m_W$ and $m_t$ from this data sample are shown in Figure 12, compared with the direct measurements. Also shown is the Standard Model predictions for Higgs masses between 90 and 1000 GeV. As can be seen in the figure, the indirect and direct measurements of $m_W$ and $m_t$ are in good agreement, and both sets prefer a low Higgs mass. For the second fit, we include the direct $m_W$ measurements from LEP and Tevatron to obtain $m_t = 161.1^{+8.2}_{-7.1}$ GeV, in good agreement with the direct measurement of $m_t = 173.8 \pm 5.0$ GeV. For the next fit, we use the direct $m_t$ measurements to obtain the best indirect determination of $m_W$. The result is shown in column 4 of Table 32. Also here, the direct measurements of $m_W$ are in excellent agreement with the indirect one.

Finally, the best constraints on $m_H$ are obtained when all data are used in the fit. The results of this fit are shown in column 5 of Table 32 and in Figure 11. In Figures 13 and 14 the sensitivity of the LEP and SLD measurements to the Higgs mass is shown. As can be seen, the most sensitive measurements are the asymmetries. A reduced uncertainty for the value of $\alpha(m_Z^2)$ would therefore result in an improved constraint on $m_H$, as shown in Figure 10.

In Figure 15 the observed value of $\Delta\chi^2 \equiv \chi^2 - \chi^2_{\rm min}$ as a function of $m_H$ is plotted for the fit

including all data. The solid curve is the result using ZFITTER, and corresponds to the last column of Table 32. The shaded band represents the uncertainty due to uncalculated higher-order corrections, as estimated by ZFITTER and TOPAZ0. This band is significantly narrower than last year's band [1], which shows the importance of the recent calculations [127, 128]. The 95% confidence level upper limit on $m_{\rm H}$ (taking the band into account) is 262 GeV. The lower limit on $m_{\rm H}$ of approximately 90 GeV obtained from direct searches [138] has not been used in this limit determination. Also shown is the curve (dashed curve) obtained when using a new evaluation of $\alpha^{(5)}(m_{\rm Z}^2)$. The fit results in $\log(m_{\rm H}) = 1.96^{+0.23}_{-0.26}$, a 30% reduction of the error.

| | LEP including LEP-II $m_{\rm W}$ | all data except $m_{\rm W}$ and $m_{\rm t}$ | all data except $m_{\rm W}$ | all data |
|---|---|---|---|---|
| $m_{\rm t}$ [GeV] | $160^{+13}_{-9}$ | $158^{+9}_{-8}$ | $171.0 \pm 4.9$ | $171.1 \pm 4.9$ |
| $m_{\rm H}$ [GeV] | $60^{+127}_{-35}$ | $32^{+41}_{-15}$ | $82^{+95}_{-51}$ | $76^{+85}_{-47}$ |
| $\log(m_{\rm H}/{\rm GeV})$ | $1.78^{+0.49}_{-0.37}$ | $1.51^{+0.36}_{-0.28}$ | $1.92^{+0.33}_{-0.42}$ | $1.88^{+0.33}_{-0.41}$ |
| $\alpha_{\rm s}(m_{\rm Z}^2)$ | $0.121 \pm 0.003$ | $0.120 \pm 0.003$ | $0.120 \pm 0.003$ | $0.119 \pm 0.003$ |
| $\chi^2$/d.o.f. | 4/9 | 13/12 | 15/13 | 15/15 |
| $\sin^2\theta^{\rm lept}_{\rm eff}$ | $0.23182 \pm 0.00023$ | $0.23157 \pm 0.00018$ | $0.23159 \pm 0.00020$ | $0.23157 \pm 0.00019$ |
| $1 - m_{\rm W}^2/m_{\rm Z}^2$ | $0.2243 \pm 0.0007$ | $0.2239 \pm 0.0007$ | $0.2232 \pm 0.0006$ | $0.2232 \pm 0.0005$ |
| $m_{\rm W}$ [GeV] | $80.314 \pm 0.038$ | $80.332 \pm 0.037$ | $80.367 \pm 0.029$ | $80.371 \pm 0.026$ |

Table 32: Results of the fits to LEP data alone, to all data except the direct determinations of $m_{\rm t}$ and $m_{\rm W}$ (Tevatron and LEP-II), to all data except direct $m_{\rm W}$ determinations, and to all data. As the sensitivity to $m_{\rm H}$ is logarithmic, both $m_{\rm H}$ as well as $\log(m_{\rm H}/{\rm GeV})$ are quoted. The bottom part of the table lists derived results for $\sin^2\theta^{\rm lept}_{\rm eff}$, $1 - m_{\rm W}^2/m_{\rm Z}^2$ and $m_{\rm W}$. See text for a discussion of theoretical errors not included in the errors above.

# 9 Prospects for the Future

Since 1996, the LEP energy has been increased; the Z phase of LEP has come to an end. However, the analyses of the LEP-I data are not yet finished. The improvements which should happen in the near future will be the completion of the lineshape analysis and the $\tau$ polarisation measurements. In the longer term the heavy flavor results will be finalised. SLAC has approved an additional SLC run to reach an accumulated total for the programme of one million Z events. This effort, which is presently pending funding, would result in a significant reduction on the errors of the SLD measurements.

In addition, the anticipated increase in statistics at LEP-II to 500 $\mathrm{pb}^{-1}$ per experiment will lead to substantially improved measurements of certain electroweak parameters. As a result, the measurements of $m_{\mathrm{W}}$ are likely to match the error obtained via the radiative corrections of the Z data, providing a further important test of the Standard Model. In the measurement of the WW$\gamma$ and WWZ triple-gauge-boson couplings the increase in LEP-II statistics, together with the improved precision per event obtained at higher beam energy, will lead to an improvement in the current precision by a factor approaching an order of magnitude.

# 10 Conclusions

The combination of the many precise electroweak results yields stringent constraints on the Standard Model. All measurements agree with the predictions. In addition, the results are sensitive to the Higgs mass.

The LEP experiments wish to stress that this report reflects a preliminary status at the time of the 1998 summer conferences. A definitive statement on these results has to wait for publication by each collaboration.

# Acknowledgements

We would like to thank the CERN accelerator divisions for the efficient operation of the LEP accelerator, the precise information on the absolute energy scale and their close cooperation with the four experiments. We would also like to thank members of the CDF, DØ, NuTeV, and SLD Collaborations for making results available to us in advance of the conferences and for useful discussions concerning their combination. Finally, the results of the section on Standard Model constraints would not have been possible without the close collaboration of many theorists. We especially thank the ZFITTER and TOPAZ0 teams.

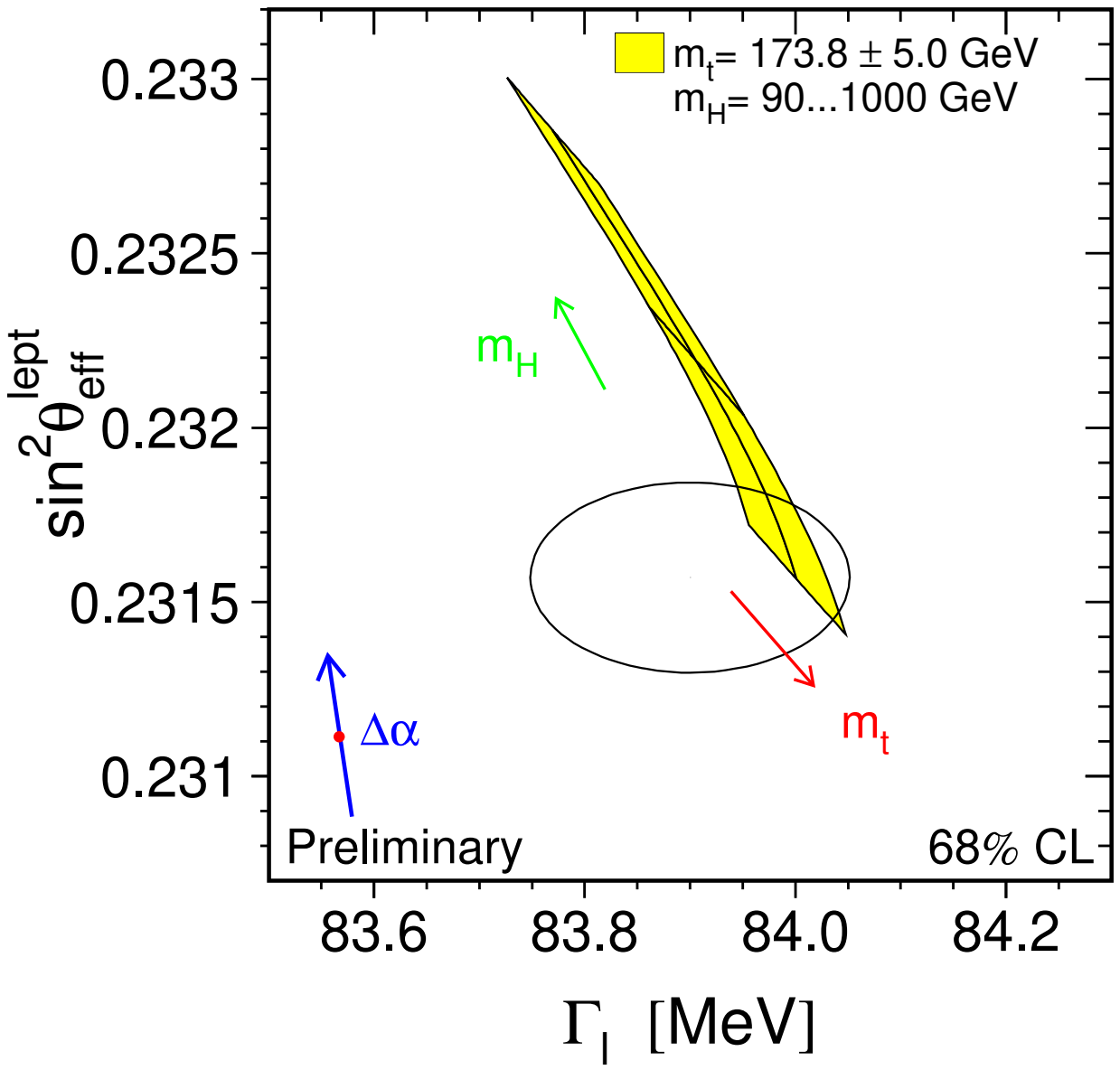


Figure 10: LEP-I+SLD measurements of $\sin^2\theta^{\rm lept}_{\rm eff}$ (Table 30) and $\Gamma_{\ell\ell}$ (Table 9) and the Standard Model prediction. The point shows the predictions if among the electroweak radiative corrections only the photon vacuum polarisation is included. The corresponding arrow shows variation of this prediction if $\alpha(m_{\rm Z}^2)$ is changed by one standard deviation. This variation gives an additional uncertainty to the Standard Model prediction shown in the figure.

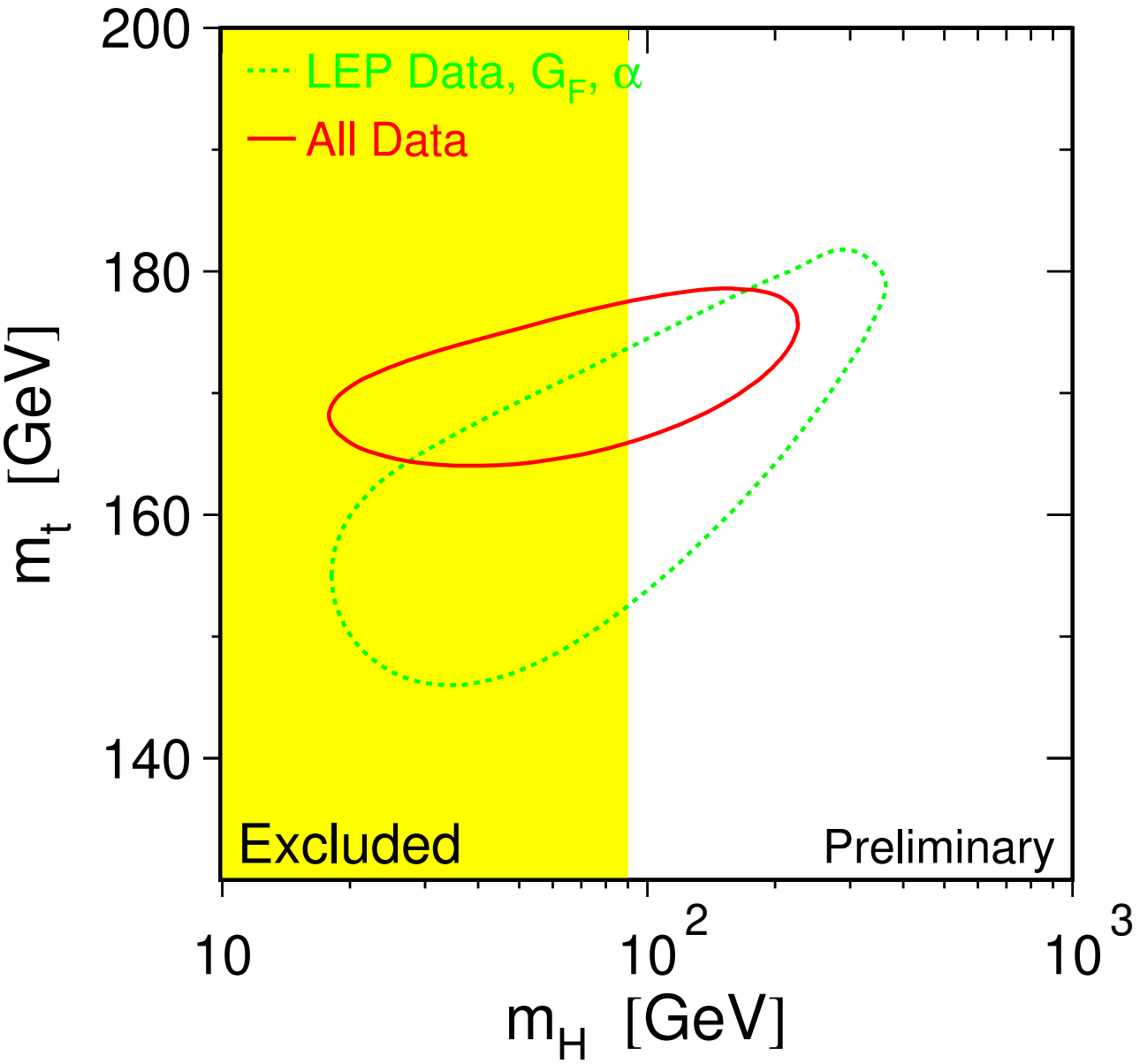


Figure 11: The 68% confidence level contours in $m_{\mathrm{t}}$ and $m_{\mathrm{H}}$ for the fits to LEP data only (dashed curve) and to all data including the CDF/DØ $m_{\mathrm{t}}$ measurement (solid curve). The vertical band shows the 95% CL exclusion limit on $m_{\mathrm{H}}$ from the direct search.

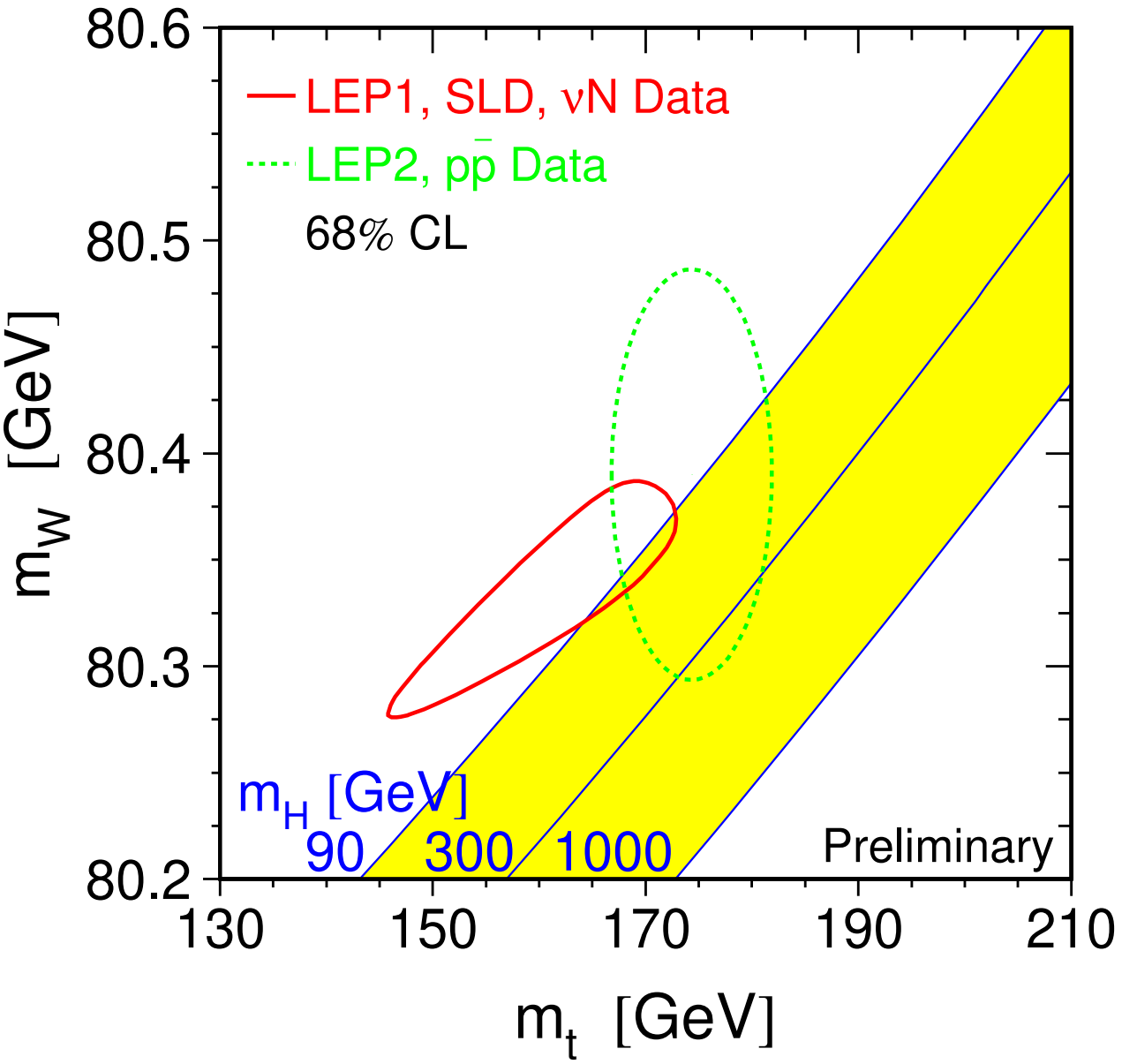


Figure 12: The comparison of the indirect measurements of $m_{\rm W}$ and $m_{\rm t}$ (LEP-I+SLD+$\nu$N data) (solid contour) and the direct measurements (Tevatron and LEP-II data) (dashed contour). In both cases the 68% CL contours are plotted. Also shown is the Standard Model relationship for the masses as a function of the Higgs mass.

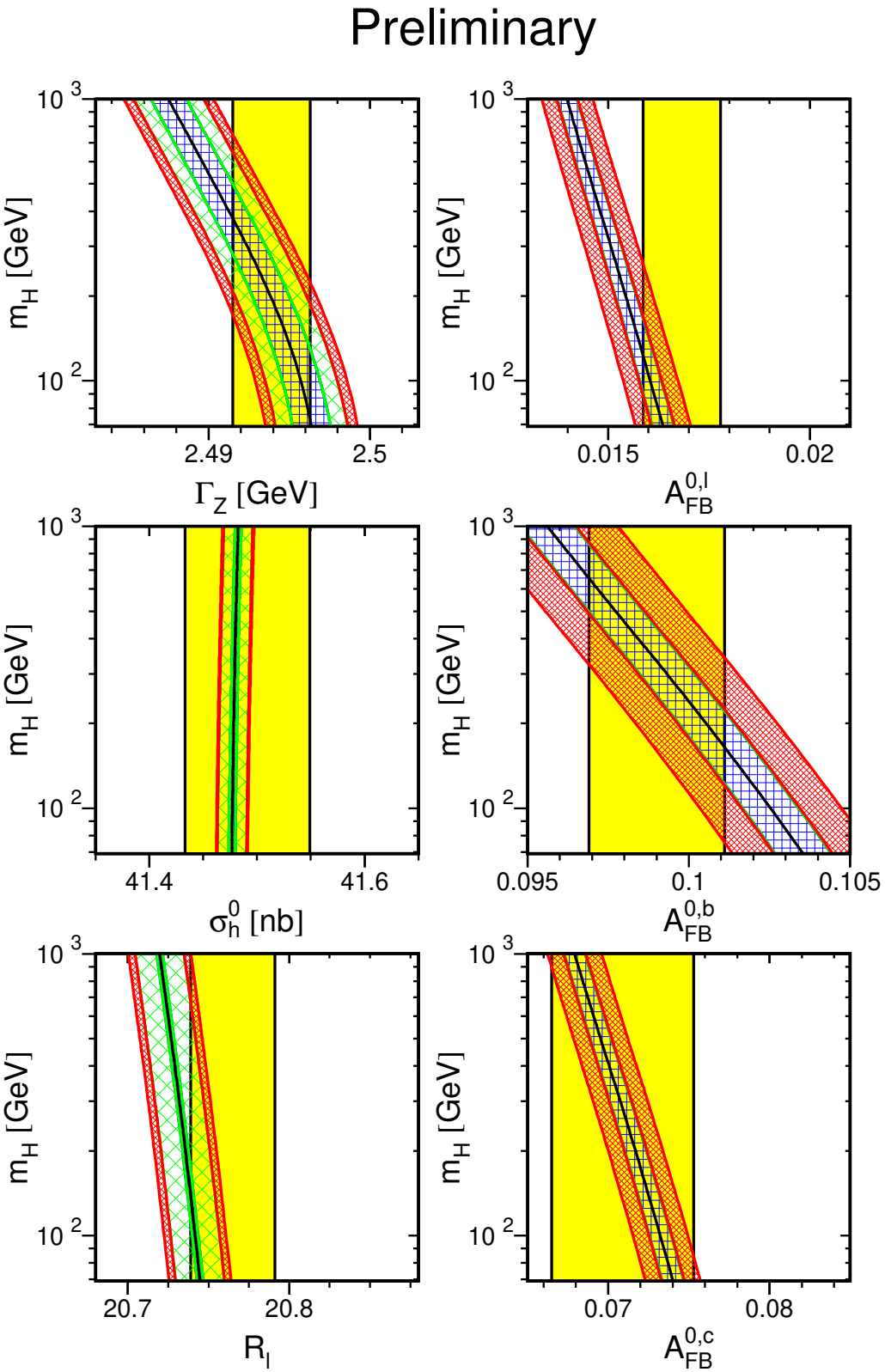


Figure 13: Comparison of LEP-I measurements with the Standard Model prediction as a function of $m_{\mathrm{H}}$. The measurement with its error is shown as the vertical band. The width of the Standard Model band is due to the uncertainties in $\alpha(m_{\mathrm{Z}}^2)$, $\alpha_{\mathrm{s}}(m_{\mathrm{Z}}^2)$ and $m_{\mathrm{t}}$. The total width of the band is the linear sum of these effects. See Figure 14 for the definition of these uncertainties.

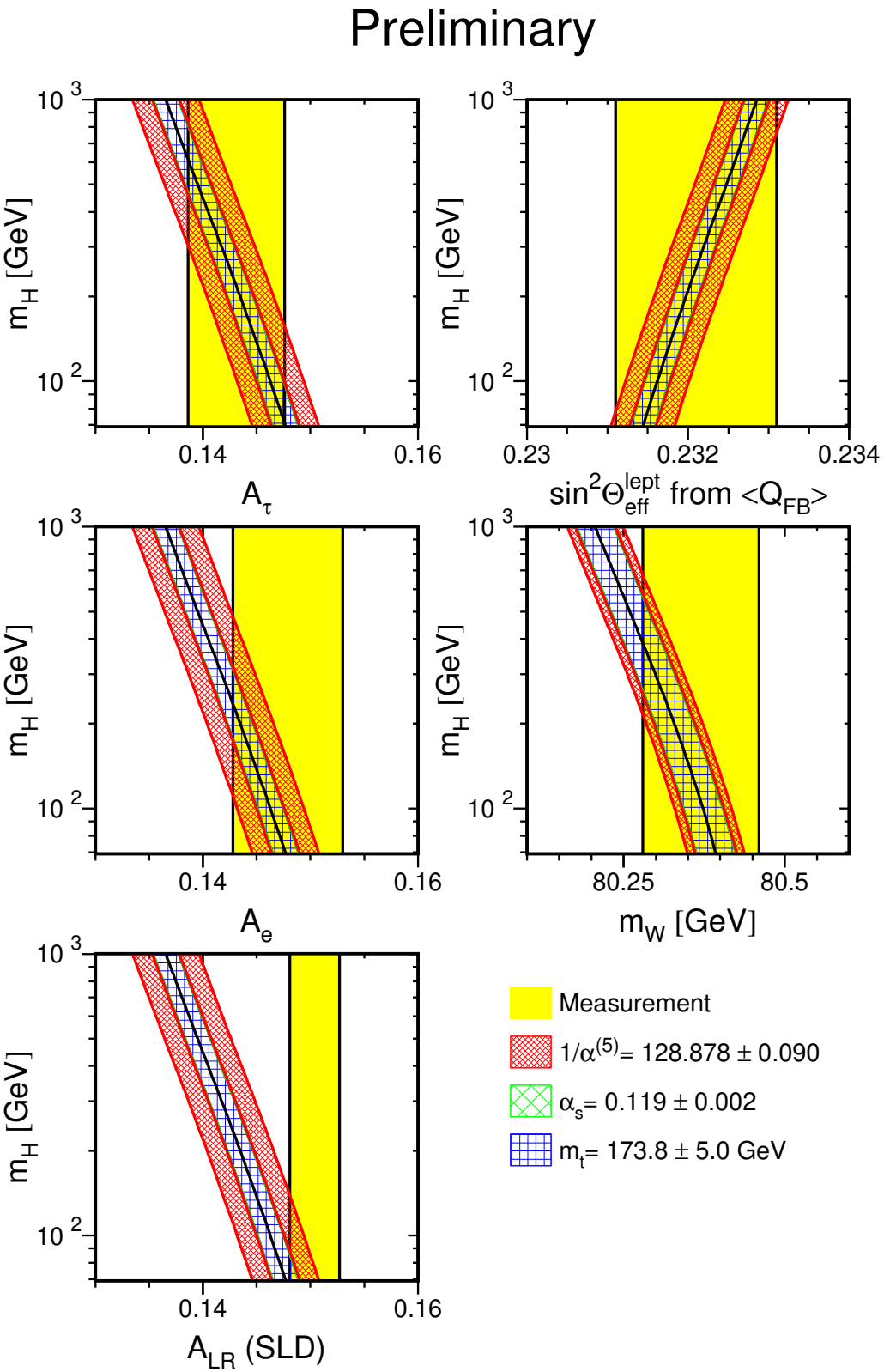


Figure 14: Comparison of LEP-I measurements with the Standard Model prediction as a function of $m_{\rm H}$ (*c.f.* Figure 13). Also shown is the comparison of the SLD measurement of $A_{\rm LR}$ with the Standard Model.

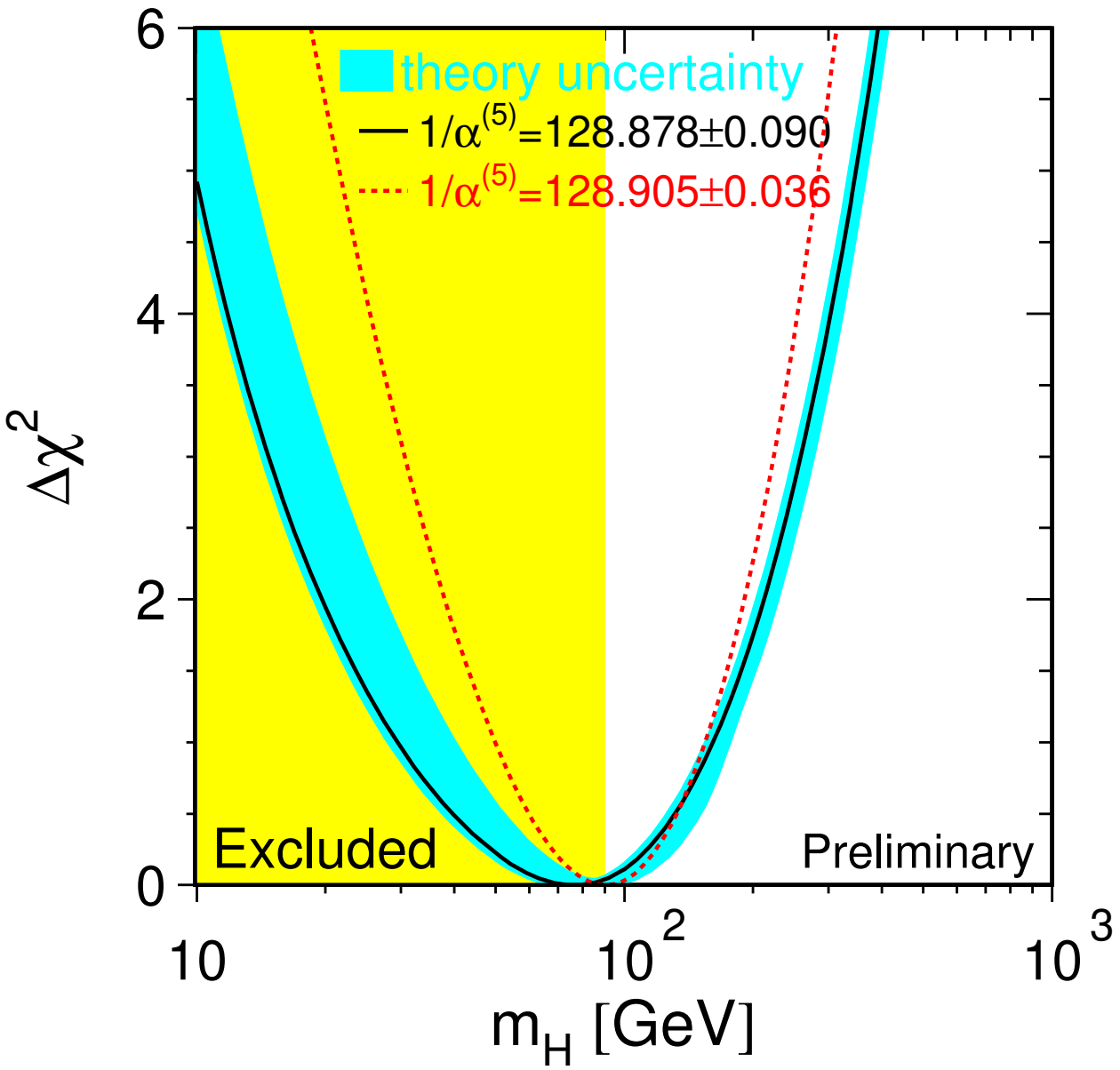


Figure 15: $\Delta\chi^2 = \chi^2 - \chi^2_{min}$ *vs.* $m_{\rm H}$ curve. The line is the result of the fit using all data (last column of Table 32); the band represents an estimate of the theoretical error due to missing higher order corrections. The vertical band shows the 95% CL exclusion limit on $m_{\rm H}$ from the direct search.

# Appendix

## A S-Matrix Fit Results

The full 16 parameter S-Matrix fits to the lineshape and asymmetry data taken at LEP-I and at LEP-II energies is summarised for each LEP experiment in Table 33. The average including the parameter mean values and errors and the correlation amongst them are given in Tables 34 and 35.

| | ALEPH | DELPHI | L3[a] | OPAL[a] |
|---|---|---|---|---|
| $m_Z$ (GeV) | 91.1951±0.0056 | 91.1841±0.0056 | 91.1867±0.0056 | 91.1874±0.0055 |
| $\Gamma_Z$ (GeV) | 2.4939±0.0044 | 2.4897±0.0041 | 2.5003±0.0043 | 2.4946±0.0044 |
| $r^{tot}_{had}$ | 2.966±0.010 | 2.957±0.010 | 2.972±0.010 | 2.962±0.010 |
| $r^{tot}_{e}$ | 0.14361±0.00076 | 0.1412±0.0010 | 0.14171±0.00088 | 0.1418±0.0011 |
| $r^{tot}_{\mu}$ | 0.14248±0.00062 | 0.14274±0.00069 | 0.14257±0.00083 | 0.14228±0.00066 |
| $r^{tot}_{\tau}$ | 0.14313±0.00067 | 0.14140±0.00097 | 0.1433±0.0011 | 0.14118±0.00088 |
| $j^{tot}_{had}$ | -0.18±0.27 | 0.36±0.28 | 0.30±0.28 | 0.03±0.27 |
| $j^{tot}_{e}$ | -0.007±0.041 | -0.037±0.045 | -0.011±0.045 | -0.123±0.060 |
| $j^{tot}_{\mu}$ | -0.018±0.030 | 0.052±0.030 | 0.028±0.036 | -0.012±0.037 |
| $j^{tot}_{\tau}$ | -0.012±0.032 | 0.017±0.037 | 0.042±0.039 | -0.003±0.042 |
| $r^{fb}_{e}$ | 0.00303±0.00072 | 0.00326±0.00096 | 0.0025±0.0013 | 0.0016±0.0010 |
| $r^{fb}_{\mu}$ | 0.00288±0.00048 | 0.00267±0.00053 | 0.00323±0.00067 | 0.00262±0.00050 |
| $r^{fb}_{\tau}$ | 0.00288±0.00055 | 0.00376±0.00075 | 0.00419±0.00094 | 0.00318±0.00066 |
| $j^{fb}_{e}$ | 0.861±0.058 | 0.813±0.073 | 0.644±0.080 | 0.778±0.068 |
| $j^{fb}_{\mu}$ | 0.826±0.036 | 0.759±0.034 | 0.838±0.046 | 0.724±0.036 |
| $j^{fb}_{\tau}$ | 0.846±0.041 | 0.745±0.047 | 0.788±0.057 | 0.727±0.042 |
| $\chi^2$/d.o.f. | 180/189 | 233/195 | 156/183 | 109/155 |

Table 33: S-Matrix parameters from 16-parameter fits to the data of the four LEP experiments, without the assumption of lepton universality.
[a]For the averaging procedure the L3 values of $m_Z$ and $\Gamma_Z$ are shifted by +0.3 MeV and the OPAL value of $m_Z$ by +0.5 MeV to account for the new energy calibration.

| Parameter | Average Value |
|---|---|
| $m_{\rm Z}$ (GeV) | 91.1884±0.0031 |
| $\Gamma_{\rm Z}$ (GeV) | 2.4945±0.0025 |
| $r^{\rm tot}_{\rm had}$ | 2.9637±0.0063 |
| $r^{\rm tot}_{\rm e}$ | 0.14229±0.00049 |
| $r^{\rm tot}_{\mu}$ | 0.14253±0.00036 |
| $r^{\rm tot}_{\tau}$ | 0.14247±0.00043 |
| $j^{\rm tot}_{\rm had}$ | 0.13±0.14 |
| $j^{\rm tot}_{\rm e}$ | -0.028±0.023 |
| $j^{\rm tot}_{\mu}$ | 0.013±0.016 |
| $j^{\rm tot}_{\tau}$ | 0.010±0.018 |
| $r^{\rm fb}_{\rm e}$ | 0.00270±0.00046 |
| $r^{\rm fb}_{\mu}$ | 0.00279±0.00027 |
| $r^{\rm fb}_{\tau}$ | 0.00329±0.00034 |
| $j^{\rm fb}_{\rm e}$ | 0.786±0.034 |
| $j^{\rm fb}_{\mu}$ | 0.780±0.019 |
| $j^{\rm fb}_{\tau}$ | 0.778±0.023 |

Table 34: Average S-Matrix parameters from the data of the four LEP experiments given in Table 33, without the assumption of lepton universality. The $\chi^2$/d.o.f. of the average is 54/48.

| | $m_{\rm Z}$ | $\Gamma_{\rm Z}$ | $r^{\rm tot}_{\rm had}$ | $r^{\rm tot}_{\rm e}$ | $r^{\rm tot}_{\mu}$ | $r^{\rm tot}_{\tau}$ | $j^{\rm tot}_{\rm had}$ | $j^{\rm tot}_{\rm e}$ | $j^{\rm tot}_{\mu}$ | $j^{\rm tot}_{\tau}$ | $r^{\rm fb}_{\rm e}$ | $r^{\rm fb}_{\mu}$ | $r^{\rm fb}_{\tau}$ | $j^{\rm fb}_{\rm e}$ | $j^{\rm fb}_{\mu}$ | $j^{\rm fb}_{\tau}$ |
|---|---|---|---|---|---|---|---|---|---|---|---|---|---|---|---|---|
| $m_{\rm Z}$ | 1.00 | -.10 | -.07 | -.03 | -.06 | -.05 | -.75 | -.25 | -.30 | -.28 | .04 | .11 | .09 | .01 | -.02 | -.01 |
| $\Gamma_{\rm Z}$ | -.10 | 1.00 | .80 | .51 | .51 | .43 | .16 | .03 | .07 | .06 | .00 | .00 | .00 | .02 | .05 | .04 |
| $r^{\rm tot}_{\rm had}$ | -.07 | .80 | 1.00 | .59 | .66 | .55 | .13 | .01 | .05 | .05 | .01 | .01 | .01 | .03 | .06 | .05 |
| $r^{\rm tot}_{\rm e}$ | -.03 | .51 | .59 | 1.00 | .42 | .35 | .09 | .04 | .04 | .04 | .03 | .00 | .00 | .05 | .04 | .03 |
| $r^{\rm tot}_{\mu}$ | -.06 | .51 | .66 | .42 | 1.00 | .46 | .10 | .01 | .14 | .04 | .01 | .03 | .01 | .03 | .10 | .04 |
| $r^{\rm tot}_{\tau}$ | -.05 | .43 | .55 | .35 | .46 | 1.00 | .09 | .01 | .04 | .13 | .01 | .01 | .03 | .02 | .04 | .09 |
| $j^{\rm tot}_{\rm had}$ | -.75 | .16 | .13 | .09 | .10 | .09 | 1.00 | .27 | .32 | .30 | -.04 | -.11 | -.09 | .00 | .03 | .01 |
| $j^{\rm tot}_{\rm e}$ | -.25 | .03 | .01 | .04 | .01 | .01 | .27 | 1.00 | .11 | .10 | .01 | -.04 | -.03 | .02 | .01 | .00 |
| $j^{\rm tot}_{\mu}$ | -.30 | .07 | .05 | .04 | .14 | .04 | .32 | .11 | 1.00 | .12 | -.01 | .00 | -.03 | .00 | .02 | .00 |
| $j^{\rm tot}_{\tau}$ | -.28 | .06 | .05 | .04 | .04 | .13 | .30 | .10 | .12 | 1.00 | -.01 | -.04 | .00 | .00 | .01 | .01 |
| $r^{\rm fb}_{\rm e}$ | .04 | .00 | .01 | .03 | .01 | .01 | -.04 | .01 | -.01 | -.01 | 1.00 | .01 | .01 | .09 | .00 | .00 |
| $r^{\rm fb}_{\mu}$ | .11 | .00 | .01 | .00 | .03 | .01 | -.11 | -.04 | .00 | -.04 | .01 | 1.00 | .03 | .00 | .17 | .00 |
| $r^{\rm fb}_{\tau}$ | .09 | .00 | .01 | .00 | .01 | .03 | -.09 | -.03 | -.03 | .00 | .01 | .03 | 1.00 | .00 | .00 | .16 |
| $j^{\rm fb}_{\rm e}$ | .01 | .02 | .03 | .05 | .03 | .02 | .00 | .02 | .00 | .00 | .09 | .00 | .00 | 1.00 | .00 | .00 |
| $j^{\rm fb}_{\mu}$ | -.02 | .05 | .06 | .04 | .10 | .04 | .03 | .01 | .02 | .01 | .00 | .17 | .00 | .00 | 1.00 | .00 |
| $j^{\rm fb}_{\tau}$ | -.01 | .04 | .05 | .03 | .04 | .09 | .01 | .00 | .00 | .01 | .00 | .00 | .16 | .00 | .00 | 1.00 |

Table 35: The correlation matrix for the set of parameters given in Table 34.

# B Heavy-Flavour Fit including Off-Peak Asymmetries

The full 17 parameter fit to the LEP and SLD data gave the following results:

$$
\begin{aligned}
R_{\mathrm{b}}^{0} &= 0.21656 \pm 0.00074 \\
R_{\mathrm{c}}^{0} &= 0.1736 \pm 0.0044 \\
A_{\mathrm{FB}}^{\mathrm{b\bar{b}}}(-2) &= 0.0553 \pm 0.0088 \\
A_{\mathrm{FB}}^{\mathrm{c\bar{c}}}(-2) &= -0.030 \pm 0.018 \\
A_{\mathrm{FB}}^{\mathrm{b\bar{b}}}(\mathrm{pk}) &= 0.0972 \pm 0.0022 \\
A_{\mathrm{FB}}^{\mathrm{c\bar{c}}}(\mathrm{pk}) &= 0.0643 \pm 0.0046 \\
A_{\mathrm{FB}}^{\mathrm{b\bar{b}}}(+2) &= 0.1081 \pm 0.0077 \\
A_{\mathrm{FB}}^{\mathrm{c\bar{c}}}(+2) &= 0.134 \pm 0.015 \\
\mathcal{A}_{\mathrm{b}} &= 0.867 \pm 0.035 \\
\mathcal{A}_{\mathrm{c}} &= 0.647 \pm 0.040 \\
\mathrm{BR}(\mathrm{b} \to \ell) &= 0.1087 \pm 0.0024 \\
\mathrm{BR}(\mathrm{b} \to \mathrm{c} \to \bar{\ell}) &= 0.0791 \pm 0.0039 \\
\overline{\chi} &= 0.1186 \pm 0.0048 \\
f(\mathrm{D}^{+}) &= 0.233 \pm 0.015 \\
f(\mathrm{D_s}) &= 0.118 \pm 0.024 \\
f(\mathrm{c_{baryon}}) &= 0.094 \pm 0.016 \\
\mathrm{P}(\mathrm{c} \to \mathrm{D}^{*+}) \times \mathrm{BR}(\mathrm{D}^{*+} \to \pi^{+}\mathrm{D}^{0}) &= 0.1588 \pm 0.0061
\end{aligned}
$$

with a $\chi^2$/d.o.f. of $41/(88-17)$. The corresponding correlation matrix is given in Table 36. The energy for the peak$-2$, peak and peak$+2$ results are respectively 89.55 GeV, 91.26 GeV and 92.94 GeV. Note that the asymmetry results shown here are not the pole asymmetries which have been shown in Section 4.2.1.

The results from the ALEPH [48] and OPAL [50] charm counting analyses in this combination still use an old value of $Br(\Lambda_c \to pK^-\pi^+)$, which has an error smaller by a factor of two than the most recent Particle Data Group value [95]. If the corrected results are used in the combination, $R_{\mathrm{c}}^{0}$ changes by about one tenth of a standard deviation, and its error increases by 2% relative. All the other electroweak quantities are unchanged, and the impact on the full electroweak fits would be negligible. There are also small changes to the charm hadron fractions, which become:

$$
\begin{aligned}
f(\mathrm{D}^{+}) &= 0.235 \pm 0.016 \\
f(\mathrm{D_s}) &= 0.122 \pm 0.025 \\
f(\mathrm{c_{baryon}}) &= 0.085 \pm 0.023
\end{aligned}
$$

| | 1) $R_{\rm b}$ | 2) $R_{\rm c}$ | 3) $A_{\rm FB}^{\rm b\bar{b}}$ (−2) | 4) $A_{\rm FB}^{\rm c\bar{c}}$ (−2) | 5) $A_{\rm FB}^{\rm b\bar{b}}$ (pk) | 6) $A_{\rm FB}^{\rm c\bar{c}}$ (pk) | 7) $A_{\rm FB}^{\rm b\bar{b}}$ (+2) | 8) $A_{\rm FB}^{\rm c\bar{c}}$ (+2) | 9) $\mathcal{A}_{\rm b}$ | 10) $\mathcal{A}_{\rm c}$ | 11) BR (1) | 12) BR (2) | 13) $\overline{\chi}$ | 14) $f(\mathrm{D}^+)$ | 15) $f(\mathrm{D_s})$ | 16) $f(c_{bar.})$ | 17) PcDst |
|---|---|---|---|---|---|---|---|---|---|---|---|---|---|---|---|---|---|
| 1) | 1.00 | −0.17 | −0.01 | −0.01 | −0.06 | 0.02 | −0.02 | 0.01 | −0.02 | 0.02 | −0.02 | 0.05 | −0.02 | −0.14 | −0.02 | 0.09 | 0.17 |
| 2) | −0.17 | 1.00 | 0.02 | 0.01 | 0.05 | −0.04 | 0.01 | −0.02 | 0.01 | −0.04 | 0.12 | 0.06 | 0.05 | −0.14 | 0.29 | 0.12 | −0.49 |
| 3) | −0.01 | 0.02 | 1.00 | 0.16 | 0.05 | 0.01 | 0.02 | 0.01 | 0.00 | 0.01 | 0.03 | −0.04 | 0.08 | 0.00 | 0.00 | 0.00 | −0.01 |
| 4) | −0.01 | 0.01 | 0.16 | 1.00 | 0.02 | 0.03 | 0.01 | 0.01 | 0.00 | 0.00 | 0.02 | −0.03 | 0.02 | 0.00 | 0.01 | 0.00 | 0.00 |
| 5) | −0.06 | 0.05 | 0.05 | 0.02 | 1.00 | 0.12 | 0.12 | 0.01 | 0.03 | 0.02 | 0.04 | −0.14 | 0.22 | 0.00 | 0.01 | 0.00 | −0.03 |
| 6) | 0.02 | −0.04 | 0.01 | 0.03 | 0.12 | 1.00 | 0.00 | 0.14 | −0.01 | 0.07 | 0.21 | −0.25 | 0.19 | 0.01 | −0.02 | −0.01 | 0.02 |
| 7) | −0.02 | 0.01 | 0.02 | 0.01 | 0.12 | 0.00 | 1.00 | 0.13 | 0.01 | 0.01 | 0.00 | −0.04 | 0.09 | 0.00 | 0.01 | 0.00 | 0.00 |
| 8) | 0.01 | −0.02 | 0.01 | 0.01 | 0.01 | 0.14 | 0.13 | 1.00 | 0.00 | 0.03 | 0.08 | −0.09 | 0.07 | 0.00 | −0.01 | 0.00 | 0.00 |
| 9) | −0.02 | 0.01 | 0.00 | 0.00 | 0.03 | −0.01 | 0.01 | 0.00 | 1.00 | 0.04 | −0.02 | 0.00 | 0.04 | −0.01 | 0.00 | 0.00 | −0.02 |
| 10) | 0.02 | −0.04 | 0.01 | 0.00 | 0.02 | 0.07 | 0.01 | 0.03 | 0.04 | 1.00 | 0.10 | −0.18 | 0.13 | −0.04 | −0.01 | 0.02 | 0.02 |
| 11) | −0.02 | 0.12 | 0.03 | 0.02 | 0.04 | 0.21 | 0.00 | 0.08 | −0.02 | 0.10 | 1.00 | −0.38 | 0.43 | −0.01 | 0.03 | 0.01 | −0.07 |
| 12) | 0.05 | 0.06 | −0.04 | −0.03 | −0.14 | −0.25 | −0.04 | −0.09 | 0.00 | −0.18 | −0.38 | 1.00 | −0.51 | 0.00 | 0.01 | 0.00 | −0.04 |
| 13) | −0.02 | 0.05 | 0.08 | 0.02 | 0.22 | 0.19 | 0.09 | 0.07 | 0.04 | 0.13 | 0.43 | −0.51 | 1.00 | 0.00 | 0.02 | 0.00 | −0.02 |
| 14) | −0.14 | −0.14 | 0.00 | 0.00 | 0.00 | 0.01 | 0.00 | 0.00 | −0.01 | −0.04 | −0.01 | 0.00 | 0.00 | 1.00 | −0.45 | −0.19 | 0.14 |
| 15) | −0.02 | 0.29 | 0.00 | 0.01 | 0.01 | −0.02 | 0.01 | −0.01 | 0.00 | −0.01 | 0.03 | 0.01 | 0.02 | −0.45 | 1.00 | −0.31 | −0.06 |
| 16) | 0.09 | 0.12 | 0.00 | 0.00 | 0.00 | −0.01 | 0.00 | 0.00 | 0.00 | 0.02 | 0.01 | 0.00 | 0.00 | −0.19 | −0.31 | 1.00 | −0.03 |
| 17) | 0.17 | −0.49 | −0.01 | 0.00 | −0.03 | 0.02 | 0.00 | 0.00 | −0.02 | 0.02 | −0.07 | −0.04 | −0.02 | 0.14 | −0.06 | −0.03 | 1.00 |

Table 36: The correlation matrix for the set of the 17 heavy-flavour parameters. BR(1) and BR(2) denote BR($\mathrm{b} \to \ell$) and BR($\mathrm{b} \to \mathrm{c} \to \bar{\ell}$) respectively, PcDst denotes P($\mathrm{c} \to \mathrm{D}^{*+}$) × BR($\mathrm{D}^{*+} \to \pi^+ \mathrm{D}^0$).

## The Measurements used in the Heavy-Flavour Averages

In the following 18 tables the results used in the combination are listed. In each case an indication of the data set used and the type of analysis is given. Preliminary results are indicated by the symbol "†". The values of centre-of-mass energy are given where relevant. In each table, the result used as input to the average procedure is given followed by the statistical error, the correlated and uncorrelated systematic errors, the total systematic error, and any dependence on other electroweak parameters. In the case of the asymmetries, the measurement moved to a common energy (89.55 GeV, 91.26 GeV and 92.94 GeV, respectively, for peak−2, peak and peak+2 results) is quoted as *corrected* asymmetry.

Contributions to the correlated systematic error quoted here are from any sources of error shared with one or more other results from different experiments in the same table, and the uncorrelated errors from the remaining sources. In the case of $\mathcal{A}_c$ and $\mathcal{A}_b$ from SLD the quoted correlated systematic error has contributions from any source shared with one or more other measurements from LEP experiments. Constants such as $a(x)$ denote the dependence on the assumed value of $x^{\text{used}}$, which is also given.

| | ALEPH | DELPHI | L3 | OPAL | SLD |
|---|---|---|---|---|---|
| | 92-95 [40] | 92-95† [41] | 94† [42] | 92-95 [43] | 93-98† [44] |
| $R_b^0$ | 0.2160 | 0.2163 | 0.2179 | 0.2176 | 0.2159 |
| Statistical | 0.0009 | 0.0007 | 0.0015 | 0.0011 | 0.0014 |
| Uncorrelated | 0.0007 | 0.0004 | 0.0014 | 0.0009 | 0.0013 |
| Correlated | 0.0007 | 0.0005 | 0.0019 | 0.0008 | 0.0006 |
| Total Systematic | 0.0010 | 0.0006 | 0.0023 | 0.0012 | 0.0014 |
| $a(R_c)$ | -0.0033 | -0.0041 | -0.0364 | -0.0122 | -0.0074 |
| $R_c^{used}$ | 0.1720 | 0.1720 | 0.1722 | 0.1720 | 0.1710 |
| $a(f(D^+))$ | -0.0010 | -0.0010 | -0.0087 | -0.0029 | -0.0004 |
| $f(D^+)^{used}$ | 0.2330 | 0.2330 | 0.2330 | 0.2380 | 0.2370 |
| $a(f(D_s))$ | -0.0001 | 0.0001 | -0.0005 | -0.0001 | -0.0002 |
| $f(D_s)^{used}$ | 0.1020 | 0.1030 | 0.1020 | 0.1020 | 0.1140 |
| $a(f(\Lambda_c))$ | 0.0002 | 0.0003 | 0.0008 | 0.0003 | -0.0004 |
| $f(\Lambda_c)^{used}$ | 0.0650 | 0.0630 | 0.0650 | 0.0650 | 0.0730 |

Table 37: The measurements of $R_b^0$. All measurements use a lifetime tag enhanced by other features like invariant mass cuts or high $p_T$ leptons.

| | ALEPH | | | DELPHI | | OPAL | | SLD |
|---|---|---|---|---|---|---|---|---|
| | 91-95 D-meson [45] | 91-95† c count [48] | 92-95 lepton [45] | 92-95† D-meson [46] | 92-95† c count [49] | 90-95 D-meson [47] | 91-94 c count [50] | 93-97† lifetime + mass [51] |
| $R_c^0$ | 0.1689 | 0.1756 | 0.1675 | 0.1673 | 0.1696 | 0.1799 | 0.167 | 0.1790 |
| Statistical | 0.0082 | 0.0048 | 0.0062 | 0.0166 | 0.0049 | 0.0098 | 0.011 | 0.0085 |
| Uncorrelated | 0.0077 | 0.0085 | 0.0102 | 0.0154 | 0.0068 | 0.0100 | 0.009 | 0.0059 |
| Correlated | 0.0028 | 0.0070 | 0.0010 | 0.0053 | 0.0104 | 0.0062 | 0.009 | 0.0015 |
| Total Systematic | 0.0082 | 0.0110 | 0.0103 | 0.0163 | 0.0124 | 0.0118 | 0.013 | 0.0061 |
| $a(R_b)$ | -0.0050 | | | | | | | -0.0239 |
| $R_b^{used}$ | 0.2159 | | | | | | | 0.2175 |

Table 38: The measurements of $R_c^0$. "c count" denotes the determination of $R_c^0$ from the sum of production rates of weakly decaying charmed hadrons. "D-meson" denotes any single/double tag analysis using exclusive and/or inclusive D-meson reconstruction.

| | ALEPH | | | | DELPHI | | L3 | OPAL | | |
|---|---|---|---|---|---|---|---|---|---|---|
| | 90-95 lepton [54] | 90-95 lepton [54] | 90-95 lepton [54] | 91-95 jet charge [58] | 91-95† lepton [55] | 92-95† D-meson [63] | 90-93† lepton [56] | 91-95 jet charge [61] | 90-95† lepton [57] | 90-95 D-meson [64] |
| $\sqrt{s}$ (GeV) | 88.380 | 89.380 | 90.210 | 89.430 | 89.430 | 89.540 | 89.560 | 89.440 | 89.490 | 89.490 |
| $A_{\rm FB}^{\rm bb}(-2)$ | -3.51 | 5.45 | 9.07 | 7.46 | 6.37 | 1.99 | 6.90 | 4.10 | 3.54 | -8.70 |
| $A_{\rm FB}^{\rm bb}(-2)$Corrected | 5.01 | | | 7.75 | 6.66 | 2.01 | 6.99 | 4.36 | 3.68 | -8.56 |
| Statistical | 1.80 | | | 1.78 | 3.86 | 10.48 | 3.50 | 2.10 | 1.73 | 10.80 |
| Uncorrelated | 0.04 | | | 0.19 | 0.16 | 1.12 | 0.34 | 0.25 | 0.16 | 2.53 |
| Correlated | 0.03 | | | 0.15 | 0.12 | 0.11 | 0.13 | 0.01 | 0.04 | 1.37 |
| Total Systematic | 0.05 | | | 0.24 | 0.19 | 1.12 | 0.37 | 0.25 | 0.16 | 2.88 |
| $a(R_{\rm b})$ | 0.0870 | | | -0.2430 | -0.7233 | | -1.5984 | -0.7300 | -0.1000 | |
| $R_{\rm b}^{\rm used}$ | 0.2192 | | | 0.2155 | 0.2170 | | 0.2160 | 0.2150 | 0.2155 | |
| $a(R_{\rm c})$ | 0.0333 | | | 1.4800 | 0.1221 | | 0.9126 | 0.0700 | 0.1000 | |
| $R_{\rm c}^{\rm used}$ | 0.1710 | | | 0.1726 | 0.1710 | | 0.1690 | 0.1730 | 0.1720 | |
| $a(A_{\rm FB}^{\rm c\bar{c}}(-2))$ | -0.186 | | | -0.2501 | | | -0.2684 | -0.3156 | | |
| $A_{\rm FB}^{\rm c\bar{c}}(-2)^{\rm used}$ | -2.34 | | | -2.70 | | | -2.96 | -2.81 | | |
| $a({\rm BR}({\rm b}\to\ell))$ | -0.236 | | | | -0.9706 | | -0.7770 | | 0.3406 | |
| ${\rm BR}({\rm b}\to\ell)^{\rm used}$ | 11.34 | | | | 11.00 | | 10.50 | | 10.90 | |
| $a({\rm BR}({\rm b}\to{\rm c}\to\bar{\ell}))$ | -0.102 | | | | 0.1580 | | -0.2464 | | -0.5298 | |
| ${\rm BR}({\rm b}\to{\rm c}\to\bar{\ell})^{\rm used}$ | 7.86 | | | | 7.90 | | 8.00 | | 8.30 | |
| $a(\overline{\chi})$ | 5.12 | | | | 2.0533 | | | | | |
| $\overline{\chi}^{\rm used}$ | 0.12460 | | | | 0.12100 | | | | | |

Table 39: The measurements of $A_{\rm FB}^{\rm b\bar{b}}(-2)$. All numbers are given in %.

| | ALEPH | | DELPHI | | | L3 | | OPAL | | |
|---|---|---|---|---|---|---|---|---|---|---|
| | 90-95 lepton [54] | 91-95 jet charge [58] | 91-95† lepton [55] | 92-95† D-meson [63] | 92-95† jet charge [59] | 94† jet charge [60] | 90-95 lepton [56] | 91-95 jet charge [61] | 90-95† lepton [57] | 90-95 D-meson [64] |
| $\sqrt{s}$ (GeV) | 91.210 | 91.250 | 91.260 | 91.235 | 91.260 | 91.220 | 91.260 | 91.210 | 91.240 | 91.240 |
| $A_{\rm FB}^{\rm b\bar{b}}$(pk) | 9.88 | 10.40 | 9.98 | 7.66 | 9.79 | 8.55 | 9.63 | 10.04 | 9.10 | 9.50 |
| $A_{\rm FB}^{\rm b\bar{b}}$(pk)Corrected | 9.97 | 10.42 | 9.98 | 7.71 | 9.79 | 8.63 | 9.63 | 10.13 | 9.14 | 9.54 |
| Statistical | 0.46 | 0.40 | 0.65 | 1.90 | 0.47 | 1.18 | 0.65 | 0.52 | 0.44 | 2.70 |
| Uncorrelated | 0.10 | 0.23 | 0.18 | 0.98 | 0.20 | 0.46 | 0.28 | 0.41 | 0.14 | 2.14 |
| Correlated | 0.16 | 0.22 | 0.19 | 0.12 | 0.04 | 0.32 | 0.22 | 0.20 | 0.15 | 0.50 |
| Total Systematic | 0.19 | 0.32 | 0.26 | 0.99 | 0.20 | 0.56 | 0.35 | 0.46 | 0.20 | 2.20 |
| $a(R_{\rm b})$ | -1.4613 | -0.2430 | -1.760 | | -0.1962 | -8.2916 | -2.0736 | -7.6300 | -0.7000 | |
| $R_{\rm b}^{\rm used}$ | 0.2192 | 0.2155 | 0.2170 | | 0.2158 | 0.2182 | 0.2160 | 0.2150 | 0.2155 | |
| $a(R_{\rm c})$ | 1.0474 | 1.4900 | 0.9351 | | 0.8200 | 1.0925 | 1.2506 | 0.4600 | 0.6000 | |
| $R_{\rm c}^{\rm used}$ | 0.1710 | 0.1726 | 0.1733 | | 0.1720 | 0.1707 | 0.1690 | 0.1730 | 0.1720 | |
| $a(A_{\rm FB}^{\rm c\bar{c}}$(pk)) | 0.5068 | 0.6345 | | | | 1.1185 | 0.6253 | 0.6870 | | |
| $A_{\rm FB}^{\rm c\bar{c}}$(pk)$^{\rm used}$ | 6.41 | 6.85 | | | | 6.21 | 6.70 | 6.19 | | |
| $a(\mathrm{BR}(\mathrm{b}\to\ell))$ | -1.3500 | | -2.8968 | | | | -1.5540 | | -0.3406 | |
| $\mathrm{BR}(\mathrm{b}\to\ell)^{\rm used}$ | 11.34 | | 11.12 | | | | 10.50 | | 10.90 | |
| $a(\mathrm{BR}(\mathrm{b}\to\mathrm{c}\to\bar{\ell}))$ | -0.1886 | | 0.7130 | | | | -0.0272 | | -0.3532 | |
| $\mathrm{BR}(\mathrm{b}\to\mathrm{c}\to\bar{\ell})^{\rm used}$ | 7.86 | | 8.03 | | | | 8.00 | | 8.30 | |
| $a(\overline{\chi})$ | 3.2930 | | 3.4053 | | | | | | | |
| $\overline{\chi}^{\rm used}$ | 0.12460 | | 0.12140 | | | | | | | |
| $a(f(\mathrm{D}^+))$ | | | | | 0.2310 | | | | | |
| $f(\mathrm{D}^+)^{\rm used}$ | | | | | 0.2310 | | | | | |
| $a(f(\mathrm{D_s}))$ | | | | | 0.0129 | | | | | |
| $f(\mathrm{D_s})^{\rm used}$ | | | | | 0.1100 | | | | | |
| $a(f(\Lambda_{\rm c}))$ | | | | | -0.0239 | | | | | |
| $f(\Lambda_{\rm c})^{\rm used}$ | | | | | 0.0630 | | | | | |

Table 40: The measurements of $A_{\rm FB}^{\rm b\bar{b}}$(pk). All numbers are given in %.

| | ALEPH | | | | DELPHI | | L3 | OPAL | | |
|---|---|---|---|---|---|---|---|---|---|---|
| | 90-95 lepton [54] | 90-95 lepton [54] | 90-95 lepton [54] | 91-95 jet charge [58] | 91-95† lepton [55] | 92-95† D-meson [63] | 90-93† lepton [56] | 91-95 jet charge [61] | 90-95† lepton [57] | 90-95 D-meson [64] |
| $\sqrt{s}$ (GeV) | 92.050 | 92.940 | 93.900 | 92.970 | 93.017 | 92.940 | 92.930 | 92.910 | 92.950 | 92.950 |
| $A_{\rm FB}^{\rm bb}(+2)$ | 3.91 | 10.56 | 9.00 | 9.24 | 15.44 | 5.70 | 10.80 | 14.60 | 10.70 | -2.10 |
| $A_{\rm FB}^{\rm bb}(+2)$Corrected | 10.00 | | | 9.21 | 15.36 | 5.70 | 10.98 | 14.63 | 10.69 | -2.11 |
| Statistical | 1.50 | | | 1.79 | 3.65 | 9.55 | 2.90 | 1.70 | 1.43 | 9.00 |
| Uncorrelated | 0.14 | | | 0.45 | 0.50 | 1.61 | 0.35 | 0.72 | 0.25 | 2.18 |
| Correlated | 0.22 | | | 0.26 | 0.41 | 0.11 | 0.15 | 0.06 | 0.28 | 1.59 |
| Total Systematic | 0.26 | | | 0.52 | 0.65 | 1.62 | 0.38 | 0.72 | 0.37 | 2.70 |
| $a(R_{\rm b})$ | -1.86 | | | -0.2430 | -2.8933 | | -1.5984 | -12.9000 | -0.8000 | |
| $R_{\rm b}^{\rm used}$ | 0.2192 | | | 0.2155 | 0.2170 | | 0.2160 | 0.2150 | 0.2155 | |
| $a(R_{\rm c})$ | 1.43 | | | 1.4900 | -0.9771 | | 0.9126 | 0.6900 | 0.8000 | |
| $R_{\rm c}^{\rm used}$ | 0.1710 | | | 0.1726 | 0.1710 | | 0.1690 | 0.1730 | 0.1720 | |
| $a(A_{\rm FB}^{\rm c\bar{c}}(+2))$ | 0.913 | | | 1.2018 | | | 1.1156 | 1.3287 | | |
| $A_{\rm FB}^{\rm c\bar{c}}(+2)^{\rm used}$ | 12.51 | | | 12.96 | | | 12.13 | 12.08 | | |
| $a({\rm BR}({\rm b}\to\ell))$ | -1.65 | | | | -3.2353 | | -0.4200 | | -1.3625 | |
| ${\rm BR}({\rm b}\to\ell)^{\rm used}$ | 11.34 | | | | 11.00 | | 10.50 | | 10.90 | |
| $a({\rm BR}({\rm b}\to{\rm c}\to\bar{\ell}))$ | -0.2410 | | | | 0.4740 | | -0.5280 | | 0.7064 | |
| ${\rm BR}({\rm b}\to{\rm c}\to\bar{\ell})^{\rm used}$ | 7.86 | | | | 7.90 | | 8.00 | | 8.30 | |
| $a(\overline{\chi})$ | 6.409 | | | | 4.8400 | | | | | |
| $\overline{\chi}^{\rm used}$ | 0.12460 | | | | 0.12100 | | | | | |

Table 41: The measurements of $A_{\rm FB}^{\rm b\bar{b}}(+2)$. All numbers are given in %.

| | ALEPH | DELPHI | OPAL | |
|---|---|---|---|---|
| | 91-95 D-meson [62] | 92-95† D-meson [63] | 90-95† lepton [57] | 90-95 D-meson [64] |
| $\sqrt{s}$ (GeV) | 89.370 | 89.540 | 89.490 | 89.490 |
| $A_{\rm FB}^{\rm c\bar{c}}(-2)$ | -1.10 | 0.20 | -6.90 | 3.90 |
| $A_{\rm FB}^{\rm c\bar{c}}(-2)$Corrected | -0.02 | 0.26 | -6.54 | 4.26 |
| Statistical | 4.30 | 5.19 | 2.44 | 5.10 |
| Uncorrelated | 1.00 | 0.55 | 0.43 | 0.80 |
| Correlated | 0.09 | 0.07 | 0.21 | 0.30 |
| Total Systematic | 1.00 | 0.55 | 0.48 | 0.86 |
| $a(R_{\rm b})$ | | | -3.4000 | |
| $R_{\rm b}^{\rm used}$ | | | 0.2155 | |
| $a(R_{\rm c})$ | | | 3.2000 | |
| $R_{\rm c}^{\rm used}$ | | | 0.1720 | |
| $a(A_{\rm FB}^{\rm b\bar{b}}(-2))$ | -1.3365 | | | |
| $A_{\rm FB}^{\rm b\bar{b}}(-2)^{\rm used}$ | 6.13 | | | |
| $a({\rm BR}({\rm b}\to\ell))$ | | | -1.7031 | |
| ${\rm BR}({\rm b}\to\ell)^{\rm used}$ | | | 10.90 | |
| $a({\rm BR}({\rm b}\to{\rm c}\to\bar{\ell}))$ | | | -1.4128 | |
| ${\rm BR}({\rm b}\to{\rm c}\to\bar{\ell})^{\rm used}$ | | | 8.30 | |

Table 42: The measurements of $A_{\rm FB}^{\rm c\bar{c}}(-2)$. All numbers are given in %.

| | ALEPH | DELPHI | | L3 | OPAL | |
|---|---|---|---|---|---|---|
| | 91-95 D-meson [62] | 91-95† lepton [55] | 92-95† D-meson [63] | 90-91 lepton [56] | 90-95† lepton [57] | 90-95 D-meson [64] |
| $\sqrt{s}$ (GeV) | 91.220 | 91.260 | 91.235 | 91.240 | 91.240 | 91.240 |
| $A_{\rm FB}^{\rm c\bar{c}}({\rm pk})$ | 6.20 | 7.70 | 6.58 | 7.84 | 5.95 | 6.30 |
| $A_{\rm FB}^{\rm c\bar{c}}({\rm pk})$Corrected | 6.39 | 7.70 | 6.70 | 8.02 | 6.05 | 6.40 |
| Statistical | 0.90 | 1.13 | 0.93 | 3.70 | 0.59 | 1.20 |
| Uncorrelated | 0.23 | 0.60 | 0.42 | 2.42 | 0.37 | 0.47 |
| Correlated | 0.17 | 0.34 | 0.05 | 0.60 | 0.38 | 0.28 |
| Total Systematic | 0.28 | 0.69 | 0.42 | 2.50 | 0.53 | 0.55 |
| $a(R_{\rm b})$ | | 2.6522 | | 4.3200 | 4.1000 | |
| $R_{\rm b}^{\rm used}$ | | 0.2170 | | 0.2160 | 0.2155 | |
| $a(R_{\rm c})$ | | -5.3434 | | -6.7600 | -3.8000 | |
| $R_{\rm c}^{\rm used}$ | | 0.1733 | | 0.1690 | 0.1720 | |
| $a(A_{\rm FB}^{\rm b\bar{b}}({\rm pk}))$ | -2.1333 | | | 6.4274 | | |
| $A_{\rm FB}^{\rm b\bar{b}}({\rm pk})^{\rm used}$ | 9.79 | | | 8.84 | | |
| $a({\rm BR}({\rm b}\to\ell))$ | | 3.753 | | 3.5007 | 5.1094 | |
| ${\rm BR}({\rm b}\to\ell)^{\rm used}$ | | 11.12 | | 10.50 | 10.90 | |
| $a({\rm BR}({\rm b}\to{\rm c}\to\bar{\ell}))$ | | -2.8373 | | -3.2917 | -1.7660 | |
| ${\rm BR}({\rm b}\to{\rm c}\to\bar{\ell})^{\rm used}$ | | 8.03 | | 7.90 | 8.30 | |

Table 43: The measurements of $A_{\rm FB}^{\rm c\bar{c}}({\rm pk})$. All numbers are given in %.

| | ALEPH | DELPHI | OPAL | |
|---|---|---|---|---|
| | 91-95 D-meson [62] | 92-95† D-meson [63] | 90-95† lepton [57] | 90-95 D-meson [64] |
| $\sqrt{s}$ (GeV) | 93.000 | 92.940 | 92.950 | 92.950 |
| $A_{\rm FB}^{\rm c\bar{c}}(+2)$ | 10.94 | 8.10 | 15.60 | 15.80 |
| $A_{\rm FB}^{\rm c\bar{c}}(+2)$Corrected | 10.89 | 8.10 | 15.57 | 15.77 |
| Statistical | 3.30 | 4.55 | 2.02 | 4.10 |
| Uncorrelated | 0.79 | 0.55 | 0.89 | 1.05 |
| Correlated | 0.18 | 0.15 | 0.37 | 0.21 |
| Total Systematic | 0.81 | 0.57 | 0.96 | 1.07 |
| $a(R_{\rm b})$ | | | 9.6000 | |
| $R_{\rm b}^{\rm used}$ | | | 0.2155 | |
| $a(R_{\rm c})$ | | | -8.9000 | |
| $R_{\rm c}^{\rm used}$ | | | 0.1720 | |
| $a(A_{\rm FB}^{\rm b\bar{b}}(+2))$ | -2.2398 | | | |
| $A_{\rm FB}^{\rm b\bar{b}}(+2)^{\rm used}$ | 12.08 | | | |
| $a({\rm BR}({\rm b}\to\ell))$ | | | 9.5375 | |
| ${\rm BR}({\rm b}\to\ell)^{\rm used}$ | | | 10.90 | |
| $a({\rm BR}({\rm b}\to{\rm c}\to\bar{\ell}))$ | | | -1.5894 | |
| ${\rm BR}({\rm b}\to{\rm c}\to\bar{\ell})^{\rm used}$ | | | 8.30 | |

Table 44: The measurements of $A_{\rm FB}^{\rm c\bar{c}}(+2)$. All numbers are given in %.

| | SLD | | |
|---|---|---|---|
| | 93-96† lepton [65] | 93-98† jet charge [67] | 94-95 $K^{\pm}$ [68] |
| $\sqrt{s}$ (GeV) | 91.280 | 91.280 | 91.280 |
| $\mathcal{A}_{\rm b}$ | 0.933 | 0.849 | 0.854 |
| Statistical | 0.058 | 0.026 | 0.088 |
| Uncorrelated | 0.032 | 0.031 | 0.106 |
| Correlated | 0.016 | 0.001 | 0.006 |
| Total Systematic | 0.035 | 0.031 | 0.106 |
| $a(R_{\rm b})$ | -0.2411 | | -0.0139 |
| $R_{\rm b}^{\rm used}$ | 0.2170 | | 0.2180 |
| $a(R_{\rm c})$ | 0.0578 | | 0.0060 |
| $R_{\rm c}^{\rm used}$ | 0.1733 | | 0.1710 |
| $a(\mathcal{A}_{\rm c})$ | | 0.0209 | -0.0112 |
| $\mathcal{A}_{\rm c}^{\rm used}$ | | 0.670 | 0.666 |
| $a({\rm BR}({\rm b}\to\ell))$ | -0.2780 | | |
| ${\rm BR}({\rm b}\to\ell)^{\rm used}$ | 11.12 | | |
| $a({\rm BR}({\rm b}\to{\rm c}\to\bar{\ell}))$ | 0.0925 | | |
| ${\rm BR}({\rm b}\to{\rm c}\to\bar{\ell})^{\rm used}$ | 8.03 | | |
| $a(\overline{\chi})$ | 0.3275 | | |
| $\overline{\chi}^{\rm used}$ | 0.12140 | | |

Table 45: The measurements of $\mathcal{A}_{\rm b}$.

| | SLD | | |
|---|---|---|---|
| | 93-96† lepton [65] | 93-97† D-meson [66] | 93-97† K+vertex [69] |
| $\sqrt{s}$ (GeV) | 91.280 | 91.280 | 91.280 |
| $\mathcal{A}_c$ | 0.696 | 0.633 | 0.651 |
| Statistical | 0.093 | 0.063 | 0.041 |
| Uncorrelated | 0.044 | 0.036 | 0.031 |
| Correlated | 0.040 | 0.006 | 0.002 |
| Total Systematic | 0.060 | 0.037 | 0.031 |
| $a(R_b)$ | 0.2170 | | |
| $R_b^{used}$ | 0.2170 | | |
| $a(R_c)$ | -0.5704 | | |
| $R_c^{used}$ | 0.1733 | | |
| $a(\mathcal{A}_b)$ | | -0.1122 | -0.0450 |
| $\mathcal{A}_b{}^{used}$ | | 0.935 | 0.900 |
| $a(BR(b \to \ell))$ | 0.4670 | | |
| $BR(b \to \ell)^{used}$ | 11.12 | | |
| $a(BR(b \to c \to \ell))$ | -0.6984 | | |
| $BR(b \to c \to \bar{\ell})^{used}$ | 8.03 | | |
| $a(\overline{\chi})$ | | | 0.0910 |
| $\overline{\chi}^{used}$ | | | 0.13000 |
| $a(f(D^+))$ | | | -0.0657 |
| $f(D^+)^{used}$ | | | 0.2300 |
| $a(f(D_s))$ | | | -0.0155 |
| $f(D_s)^{used}$ | | | 0.1150 |

Table 46: The measurements of $\mathcal{A}_c$.

| | ALEPH | DELPHI | L3 | OPAL |
|---|---|---|---|---|
| | 92-93† [70] | 94-95† [71] | 92-95† [72] | 92-95† [73] |
| $BR(b \to \ell)$ | 11.01 | 10.65 | 10.68 | 10.86 |
| Statistical | 0.10 | 0.11 | 0.11 | 0.08 |
| Uncorrelated | 0.21 | 0.24 | 0.36 | 0.30 |
| Correlated | 0.20 | 0.36 | 0.26 | 0.32 |
| Total Systematic | 0.29 | 0.43 | 0.44 | 0.44 |
| $a(R_b)$ | | | -9.2571 | 2.1090 |
| $R_b^{used}$ | | | 0.2160 | 0.2209 |
| $a(R_c)$ | | 0.3612 | | 0.3480 |
| $R_c^{used}$ | | 0.1734 | | 0.1580 |
| $a(BR(b \to c \to \bar{\ell}))$ | | | -1.1700 | |
| $BR(b \to c \to \bar{\ell})^{used}$ | | | 9.00 | |
| $a(\overline{\chi})$ | 0.2075 | | | |
| $\overline{\chi}^{used}$ | 0.12610 | | | |

Table 47: The measurements of $BR(b \to \ell)$. All measurements are a combination of lepton- and lifetime-tags. All numbers are given in %.

| | ALEPH | DELPHI |
|---|---|---|
| | 92-93† multi [70] | 94-95† multi [71] |
| $BR(b \to c \to \bar{\ell})$ | 7.68 | 7.91 |
| Statistical | 0.18 | 0.23 |
| Uncorrelated | 0.27 | 0.41 |
| Correlated | 0.41 | 0.57 |
| Total Systematic | 0.49 | 0.71 |
| $a(R_c)$ | | 0.3612 |
| $R_c^{used}$ | | 0.1734 |
| $a(\overline{\chi})$ | -0.5108 | |
| $\overline{\chi}^{used}$ | 0.12610 | |

Table 48: The measurements of $BR(b \to c \to \bar{\ell})$. All numbers are given in %.

| | ALEPH | DELPHI | L3 | OPAL |
|---|---|---|---|---|
| | 90-95 lepton [54] | 94-95† lepton [71] | 90-95 lepton [56] | 90-95† lepton [57] |
| $\overline{\chi}$ | 0.12461 | 0.12780 | 0.11870 | 0.11390 |
| Statistical | 0.00515 | 0.01300 | 0.00680 | 0.00540 |
| Uncorrelated | 0.00252 | 0.00352 | 0.00453 | 0.00306 |
| Correlated | 0.00398 | 0.00572 | 0.00257 | 0.00324 |
| Total Systematic | 0.00471 | 0.00672 | 0.00521 | 0.00446 |
| $a(R_b)$ | 0.0341 | | 0.0004 | |
| $R_b^{used}$ | 0.2192 | | 0.2160 | |
| $a(R_c)$ | 0.0009 | -0.0036 | 0.0003 | |
| $R_c^{used}$ | 0.1710 | 0.1734 | 0.1690 | |
| $a(BR(b \to \ell))$ | 0.0524 | | 0.0521 | 0.0170 |
| $BR(b \to \ell)^{used}$ | 11.34 | | 10.50 | 10.90 |
| $a(BR(b \to c \to \bar{\ell}))$ | -0.0440 | | -0.0427 | -0.0318 |
| $BR(b \to c \to \bar{\ell})^{used}$ | 7.86 | | 8.00 | 8.30 |

Table 49: The measurements of $\overline{\chi}$.

| | DELPHI | | OPAL |
|---|---|---|---|
| | 92-95† slow $\pi$ [46] | 91-94† D-meson [46] | 90-95 D-meson [47] |
| $P(c \to D^{*+}) \times BR(D^{*+} \to \pi^+ D^0)$ | 0.1560 | 0.1647 | 0.1516 |
| Statistical | 0.0085 | 0.0140 | 0.0096 |
| Uncorrelated | 0.0090 | 0.0113 | 0.0088 |
| Correlated | 0.0071 | 0.0030 | 0.0011 |
| Total Systematic | 0.0115 | 0.0117 | 0.0089 |
| $a(R_c)$ | -0.0009 | -0.0020 | |
| $R_c^{used}$ | 0.1720 | 0.1720 | |

Table 50: The measurements of $P(c \to D^{*+}) \times BR(D^{*+} \to \pi^+ D^0)$.

| | ALEPH | DELPHI | OPAL |
|---|---|---|---|
| | 91-95† c count [48] | 92-95† c count [49] | 91-94 c count [50] |
| $R_c f_{D^+}$ | 0.0404 | 0.0383 | 0.0393 |
| Statistical | 0.0013 | 0.0013 | 0.0050 |
| Uncorrelated | 0.0014 | 0.0023 | 0.0040 |
| Correlated | 0.0032 | 0.0025 | 0.0033 |
| Total Systematic | 0.0035 | 0.0034 | 0.0052 |

Table 51: The measurements of $R_c f_{D^+}$.

| | ALEPH | DELPHI | OPAL |
|---|---|---|---|
| | 91-95† c count [48] | 92-95† c count [49] | 91-94 c count [50] |
| $R_c f_{D_s}$ | 0.0205 | 0.0211 | 0.0161 |
| Statistical | 0.0033 | 0.0017 | 0.0042 |
| Uncorrelated | 0.0011 | 0.0019 | 0.0016 |
| Correlated | 0.0053 | 0.0054 | 0.0043 |
| Total Systematic | 0.0054 | 0.0057 | 0.0046 |

Table 52: The measurements of $R_c f_{D_s}$.

| | ALEPH | DELPHI | OPAL |
|---|---|---|---|
| | 91-95† c count [48] | 92-95† c count [49] | 91-94 c count [50] |
| $R_c f_{\Lambda_c}$ | 0.0176 | 0.0169 | 0.0107 |
| Statistical | 0.0018 | 0.0035 | 0.0050 |
| Uncorrelated | 0.0007 | 0.0020 | 0.0014 |
| Correlated | 0.0026 | 0.0045 | 0.0020 |
| Total Systematic | 0.0027 | 0.0049 | 0.0024 |

Table 53: The measurements of $R_c f_{\Lambda_c}$.

| | ALEPH | DELPHI | OPAL |
|---|---|---|---|
| | 91-95† c count [48] | 92-95† c count [49] | 91-94 c count [50] |
| $R_c f_{D^0}$ | 0.0966 | 0.0933 | 0.1016 |
| Statistical | 0.0029 | 0.0026 | 0.0070 |
| Uncorrelated | 0.0040 | 0.0054 | 0.0054 |
| Correlated | 0.0049 | 0.0023 | 0.0050 |
| Total Systematic | 0.0063 | 0.0059 | 0.0074 |

Table 54: The measurements of $R_c f_{D^0}$.

# References


[1] The LEP Collaborations ALEPH, DELPHI, L3, OPAL and the LEP Electroweak Working Group, and the SLD Heavy Flavour Group, *A Combination of Preliminary LEP Electroweak Measurements and Constraints on the Standard Model*, CERN-PPE/97-154.

[2] The LEP Collaborations ALEPH, DELPHI, L3, OPAL and the LEP Electroweak Working Group, *Combined Preliminary Data on* Z *Parameters from the LEP Experiments and Constraints on the Standard Model*, CERN-PPE/94-187.

[3] The LEP Experiments: ALEPH, DELPHI, L3 and OPAL, Nucl. Inst. Meth. **A378** (1996) 101.

[4] ALEPH Collaboration, D. Decamp *et al.*, Z. Phys. **C48** (1990) 365;
ALEPH Collaboration, D. Decamp *et al.*, Z. Phys. **C53** (1992) 1;
ALEPH Collaboration, D. Buskulic *et al.*, Z. Phys. **C60** (1993) 71;
ALEPH Collaboration, D. Buskulic *et al.*, Z. Phys. **C62** (1994) 539;
ALEPH Collaboration, *LEP I results on Z resonance parameters and lepton forward-backward asymmetries*, ALEPH 98-068 CONF 98-038, contributed paper to ICHEP 98 Vancouver **ICHEP'98 #284**.

[5] DELPHI Collaboration, P. Aarnio *et al.*, Nucl. Phys. **B367** (1991) 511;
DELPHI Collaboration, P. Abreu *et al.*, Nucl. Phys. **B417** (1994) 3;
DELPHI Collaboration, P. Abreu *et al.*, Nucl. Phys. **B418** (1994) 403;
DELPHI Collaboration, DELPHI Note 95-62 PHYS 497, contributed paper to EPS-HEP-95 Brussels, **eps0404**;
DELPHI Collaboration, DELPHI Note 97-130 CONF 109, contributed paper to EPS-HEP-97, Jerusalem, **EPS-463**.

[6] L3 Collaboration, B. Adeva *et al.*, Z. Phys. **C51** (1991) 179;
L3 Collaboration, O. Adriani *et al.*, Phys. Rep. **236** (1993) 1;
L3 Collaboration, M. Acciarri *et al.*, Z. Phys. **C62** (1994) 551;
L3 Collaboration, *Preliminary L3 Results on Electroweak Parameters using 1990-96 Data*, L3 Note 2065, March 1997, available via http://l3www.cern.ch/note/note-2065.ps.gz.

[7] OPAL Collaboration, G. Alexander *et al.*, Z. Phys. **C52** (1991) 175;
OPAL Collaboration, P.D. Acton *et al.*, Z. Phys. **C58** (1993) 219;
OPAL Collaboration, R. Akers *et al.*, Z. Phys. **C61** (1994) 19;
OPAL Collaboration, *Precision Measurements of the* $Z^0$ *Lineshape and Lepton Asymmetry*, OPAL Physics Note PN358, July 1998;
OPAL Collaboration, *Precision Luminosity for OPAL* $Z^0$ *Lineshape Measurements with a Silicon-Tungsten Luminometer*, OPAL Physics Note PN364, July 1998.

[8] A. Arbuzov, *et al.*, Phys. Lett. **B383** (1996) 238;
S. Jadach, *et al.*, Comp. Phys. Comm. **102** (1997) 229.

[9] B.F.L. Ward, S. Jadach, M. Melles and S.A. Yost, *New Results on the Theoretical Precision of the LEP/SLC Luminosity*, talk presented at ICHEP 98, Vancouver, B.C., Canada, 23-29 July, 1998, UTHEP-98-0501, hep-ph/9811245.

[10] The LEP Collaborations ALEPH, DELPHI, L3, OPAL and the LEP Electroweak Working Group, *Updated Parameters of the* Z *Resonance from Combined Preliminary Data of the LEP Experiments*, CERN-PPE/93-157.

[11] F.A. Berends et al., in *Z Physics at LEP 1, Vol. 1*, ed. G. Altarelli, R. Kleiss and C. Verzegnassi, (CERN Report: CERN 89-08, 1989), p. 89.
M. Böhm et al., in *Z Physics at LEP 1, Vol. 1*, ed. G. Altarelli, R. Kleiss and C. Verzegnassi, (CERN Report: CERN 89-08, 1989), p. 203.

[12] See, for example, M. Consoli *et al.*, in "Z Physics at LEP 1", CERN Report CERN 89-08 (1989), eds G. Altarelli, R. Kleiss and C. Verzegnassi, Vol. 1, p. 7.

[13] S. Jadach, *et al.*, Phys. Lett. **B257** (1991) 173.

[14] M. Skrzypek, Acta Phys. Pol. **B23** (1992) 135.

[15] G. Montagna, *et al.*, Phys. Lett. **B406** (1997) 243.

[16] W. Beenakker and G. Passarino, Phys. Lett. **B425** (1998) 199.

[17] LEP Energy Working Group note 96-07, E. Lancon and A. Blondel, *Determination of the LEP Energy Spread Using Experimental Constraints.*

[18] G. R. Wilkinson. The determination of the LEP energy in the 1995 $Z^0$ scan. In Z. Ajduk and A. K. Wroblewski, editor, *Proceedings of the 28$^{th}$ International Conference on High Energy Physics, Warsaw, Poland, 25-31 July 1996*, pages 1068–1071. World Scientific, 1997.

[19] LEP Energy Working Group, R. Assmann *et al.*, *Calibration of centre-of-mass energies at LEP1 for precise measurements of Z properties*, CERN-EP/98-40, CERN-SL/98-12, March 1998, submitted to Eur. Phys. Jour. C.

[20] The LEP Collaborations ALEPH, DELPHI, L3, OPAL the LEP Electroweak Working Group, and the SLD Heavy Flavour Group, *A Combination of Preliminary LEP Electroweak Measurements and Constraints on the Standard Model*, CERN-PPE/96-183.

[21] A. Borrelli, M. Consoli, L. Maiani, R. Sisto, Nucl. Phys. **B 333** (1990) 357;
R.G. Stuart, Phys. Lett. **B 272** (1991) 353.

[22] A. Leike, T. Riemann, J. Rose, Phys. Lett. **B 273** (1991) 513;
T. Riemann, Phys. Lett. **B 293** (1992) 451;
S. Kirsch, T. Riemann, Comp. Phys. Comm. **88** (1995) 89.

[23] ALEPH Collaboration, D. Buskulic et al., Phys. Lett. **B 378** (1996) 373;
ALEPH Collaboration, *Measurement of fermion pair production in* $e^+e^-$ *annihilation and interpretation in terms of new physics phenomena*, contributed paper to EPS 1997, Jerusalem, eps-hep-602.

[24] DELPHI Collaboration, *DELPHI results on the Measurement of Fermion-Pair Production at LEP energies from 130 GeV to 172 GeV*, DELPHI 97-132 CONF 110, contributed paper to EPS 1997, Jerusalem, eps-hep-464.

[25] L3 Collaboration, M. Acciarri et al., Phys. Lett. **B 370** (1996) 195;
L3 Collaboration, CERN preprint CERN-PPE/97-052;
L3 Collaboration, *Preliminary L3 Results on Z–Boson Parameters from 1990–96 Data*, L3 Note 2163, September 1997.

[26] OPAL Collaboration, K. Ackerstaff, *et al.*, Eur. Phys. J. **C2** (1998) 441;
OPAL Collaboration, *S-Matrix Fits to the OPAL LEP1 Lineshape and Asymmetry Data and the LEP2 Cross-Section Data*, OPAL Physics Note PN319, September 1997.

[27] The LEP experiments and the LEP Electroweak Working Group, CERN preprint CERN-PPE/95-172.

[28] L3 Collaboration, O. Adriani et al., Phys. Lett. **B 315** (1993) 637;
G. Isidori, Phys. Lett. **B 314** (1993) 139;
M.W. Grünewald, S. Kirsch, CERN preprint CERN-PPE/93-188.

[29] TOPAZ Collaboration, K. Miyabayashi et al., Phys. Lett. **B 347** (1995) 171.

[30] ALEPH Collaboration, D. Buskulic *et al.*, Zeit. Phys. **C69** (1996) 183.

[31] DELPHI Collaboration, P. Abreu *et al.*, Z. Phys. **C67** (1995) 183;
DELPHI Collaboration, *An updated measurement of tau polarisation*, DELPHI 96-114 CONF 42, contributed paper to ICHEP96, Warsaw, 25-31 July 1996, **PA07-008**.

[32] L3 Collaboration, M. Acciarri *et al.*, Phys. Lett. **B429** (1998) 387.

[33] OPAL Collaboration, G.Alexander *et al.*, Z. Phys. **C75** (1996) 365.

[34] The LEP Heavy Flavour Group, *Input Parameters for the LEP/SLD Electroweak Heavy Flavour Results for Summer 1998 Conferences* , LEPHF/98-01,
http://www.cern.ch/LEPEWWG/heavy/lephf9801.ps.gz.

[35] ALEPH Collaboration, D. Buskulic *et al.*, Z. Phys. **C62** (1994) 179.

[36] DELPHI Collaboration, P.Abreu et al., Z. Phys. **C66** (1995) 323.

[37] L3 Collaboration, *Measurement of $R_b$ and BR($b \to \ell X$) from b-quark semileptonic decays,* L3 Note 1449, July 16 1993;
L3 Collaboration, *L3 Results on $R_b$ and* BR($b \to \ell$) *for the Glasgow Conference,* L3 Note 1625.

[38] OPAL Collaboration, R. Akers *et al.*, Z. Phys. **C60** (1993) 199.

[39] L3 Collaboration, O. Adriani *et al.*, Phys. Lett. **B307** (1993) 237.

[40] ALEPH Collaboration, R. Barate *et al.*, Physics Letters **B 401** (1997) 150;
ALEPH Collaboration, R. Barate *et al.*, Physics Letters **B 401** (1997) 163.

[41] DELPHI Collaboration, *A precise measurement of the partial decay width ratio* $R_b^0 = \Gamma_{b\bar{b}}/\Gamma_{had}$ DELPHI 98-123 CONF 184, contributed paper to ICHEP 98 Vancouver **ICHEP'98 #123** .
Delphi notes are available at http://wwwcn.cern.ch/~pubxx/www/delsec/delnote/.

[42] L3 Collaboration, *Measurement of the Z Branching Fraction into Bottom Quarks Using Double Tag Methods,* L3 Note 2114, contributed paper to the EPS-HEP-97, Jerusalem, **EPS-489**.

[43] OPAL Collaboration, G. Abbiendi *et al.*, *A Measurement of $R_b$ using a Double Tagging Method,* CERN-EP/98-137, accepted by Eur. Phys. J. C.

[44] SLD Collaboration, SLAC-PUB-7585, contributed paper to EPS-HEP-97, Jerusalem, **EPS-118**;
V.Serbo, *Electroweak measurements with heavy quarks at SLD*, III International conference on Hyperons, Charm and Beauty Hadrons, Genova, Italy, June/30–July/3/1998.

[45] ALEPH Collaboration, R. Barate *et al.*, Eur. Phys. J. **C4** (1998) 557.

[46] DELPHI Collaboration, *Summary of $R_c$ measurements in DELPHI,* DELPHI 96-110 CONF 37 contributed paper to ICHEP96, Warsaw, 25-31 July 1996 **PA01-060**.

[47] OPAL Collaboration, K. Ackerstaff *et al.*, Eur. Phys. J. **C1** (1998) 439.

[48] ALEPH Collaboration, *Study of Charmed Hadron Production in Z Decays,* contributed paper to the EPS-HEP-97, Jerusalem, **EPS-623**.

[49] DELPHI Collaboration, *Measurement of the Z Partial Decay Width into* $c\bar{c}$ *and Multiplicity of Charm Quarks per b Decay* DELPHI 98-120 CONF 181, contributed paper to ICHEP 98 Vancouver **ICHEP'98 #122** .

[50] OPAL Collaboration, G. Alexander *et al.*, Z. Phys. **C72** (1996) 1.

[51] SLD Collaboration, *A Measurement of* $R_c$ *with the SLD Detector* SLAC–PUB–7880, contributed paper to ICHEP 98 Vancouver **ICHEP'98 #174** .

[52] D. Bardin *et al.*, Z. Phys. **C44** (1989) 493; Comp. Phys. Comm. **59** (1990) 303; Nucl. Phys. **B351**(1991) 1; Phys. Lett. **B255** (1991) 290 and CERN-TH 6443/92 (May 1992).

[53] D. Abbaneo *et al.*, Eur. Phys. J. **C4** (1998) 2, 185.

[54] ALEPH Collaboration, D. Buskulic *et al.*, Phys. Lett. **B384** (1996)414.

[55] DELPHI Collaboration, P.Abreu *et al.*, Z. Phys **C65** (1995) 569;
DELPHI Collaboration, *Measurement of the Forward-Backward Asymmetries of* $e^+e^- \to Z \to b\bar{b}$ *and* $e^+e^- \to Z \to c\bar{c}$ *using prompt leptons* DELPHI 98-143 CONF 204, contributed paper to ICHEP 98 Vancouver **ICHEP'98 #124** .

[56] L3 Collaboration, O. Adriani *et al.*, Phys. Lett. **B292** (1992) 454;
L3 Collaboration, M. Acciarri *et al.*, Phys. Lett. **B335** (1994) 542;
L3 Collaboration, *L3 Results on* $A_{\rm FB}^{\rm b\bar{b}}$, $A_{\rm FB}^{\rm c\bar{c}}$ *and* $\chi$ *for the Glasgow Conference,* L3 Note 1624;
L3 Collaboration, *Measurement of the* $e^-e^- \to Z \to b\bar{b}$ *Forward-Backward Asymmetry Using Leptons,* L3 Note 2112, contributed paper to the EPS-HEP-97, Jerusalem, **EPS-490**;
L3 Collaboration, *Measurement of the* $B^0 - \bar{B}^0$ *Mixing Parameter,* L3 Note 2113, contributed paper to the EPS-HEP-97, Jerusalem, **EPS-490**.

[57] OPAL Collaboration, G. Alexander *et al.*, Z. Phys. **C70** (1996) 357;
OPAL Collaboration, R. Akers *et al.*, *Updated Measurement of the Heavy Quark Forward-Backward Asymmetries and Average B Mixing Using Leptons in Multihadronic Events*, OPAL Physics Note PN226 contributed paper to ICHEP96, Warsaw, 25-31 July 1996 **PA05-007**
OPAL Collaboration, R. Akers *et al.*, *QCD corrections to the bottom and charm forward-backward asymmetries* OPAL Physics Note PN284.

[58] ALEPH Collaboration, R. Barate *et al.*, Phys. Lett. **B426**, (1998) 217.

[59] DELPHI Collaboration, *Measurement of* $A_{FB}^{\rm b\bar{b}}$ *in Hadronic Z Decays using a Jet Charge Technique* DELPHI 98-103 CONF 171, contributed paper to ICHEP 98 Vancouver **ICHEP'98 #125** .

[60] L3 Collaboration, *Afb(bb) using a jet-charge technique on 1994 data,* L3 Note 2129.

[61] OPAL Collaboration, K.Ackerstaff *et al.*, Z. Phys. **C75** (1997) 385.

[62] ALEPH Collaboration, R. Barate *et al.*, *The Forward-Backward Asymmetry for Charm Quarks at the Z Pole* CERN EP/98-101 subm. to Phys. Lett. B.

[63] DELPHI Collaboration, P.Abreu *et al.*, Z. Phys **C66** (1995) 341;
DELPHI Collaboration, *Measurement of the forward backward asymmetry of c and b quarks at the Z pole using reconstructed D mesons* DELPHI 98-121 CONF 182, contributed paper to ICHEP 98 Vancouver **ICHEP'98 #126** .

[64] OPAL Collaboration, G. Alexander *et al.*, Z. Phys. **C73** (1996) 379.

[65] SLD Collaboration, SLAC–PUB–7637, contributed paper to EPS-HEP-97, Jerusalem, **EPS-124**;
S. Fahey, *Measurements of Quark Coupling Asymmetries at the SLD* , talk presented at ICHEP 98 Vancouver.

[66] S. Fahey, *Measurements of Quark Coupling Asymmetries at the SLD* , talk presented at ICHEP 98 Vancouver.

[67] SLD Collaboration, *Measurement of $\mathcal{A}_b$ at the Z resonance using a Jet-Charge Technique* SLAC–PUB–7886, contributed paper to ICHEP 98 Vancouver **ICHEP'98 #179** .

[68] SLD Collaboration, SLAC-PUB-7630, contributed paper to EPS-HEP-97, Jerusalem, **EPS-123**;
S. Fahey, *Measurements of Quark Coupling Asymmetries at the SLD* , talk presented at ICHEP 98 Vancouver.

[69] SLD Collaboration, *An Improved Inclusive Measurement of $\mathcal{A}_c$ using the SLD Detector* SLAC–PUB–7879, contributed paper to ICHEP 98 Vancouver **ICHEP'98 #175** .

[70] ALEPH Collaboration., D. Buskulic *et al.*, *Measurement of the semileptonic b branching ratios from inclusive leptons in Z decays*, Contributed Paper to EPS-HEP-95 Brussels, **eps0404**.
This note may be found at http://alephwww.cern.ch/ALPUB/oldconf/HEP95/HEP95.html.

[71] DELPHI Collaboration, *Measurement of the semileptonic b branching ratios and $\bar{\chi}_b$ from inclusive leptons in Z decays* DELPHI 98-122 CONF 183, contributed paper to ICHEP 98 Vancouver **ICHEP'98 #129** .

[72] L3 Collaboration, M. Acciarri *et al.*, Z Phys. **C71** 379 (1996).

[73] OPAL Collaboration, OPAL Collaboration, *Measurement of the semileptonic branching fraction of inclusive b-hadrons* OPAL Physics Note PN334/98, contributed paper to ICHEP 98 Vancouver **ICHEP'98 #370** .

[74] P. Gagnon, *Semileptonic B decays at the $Z^0$* , talk presented at ICHEP 98 Vancouver.

[75] ALEPH Collaboration, D. Decamp *et al.*, Phys. Lett. **B259** (1991) 377.

[76] ALEPH Collaboration, ALEPH-Note 93-041 PHYSIC 93-032 (1993);
ALEPH Collaboration, ALEPH-Note 93-042 PHYSIC 93-033 (1993);
ALEPH Collaboration, ALEPH-Note 93-044 PHYSIC 93-035 (1993).

[77] ALEPH Collaboration, D. Buskulic *et al.*, Z. Phys. **C71** (1996) 357.

[78] DELPHI Collaboration, P. Abreu *et al.*, Phys. Lett. **B277** (1992) 371.

[79] DELPHI Collaboration, *Measurement of the Inclusive Charge Flow in Hadronic Z Decays,* DELPHI 96-19 PHYS 594.

[80] L3 Collaboration, *Forward-Backward charge asymmetry measurement on 91-94 data*, L3 Note 2063.

[81] OPAL Collaboration, P. D. Acton *et al.*, Phys. Lett. **B294** (1992) 436.

[82] OPAL Collaboration, *A determination of $\sin^2\theta_W$ from an inclusive sample of multihadronic events,* OPAL Physics Note PN195 (1995).

[83] T. Sjöstrand, Comp. Phys. Comm. **82** (1994) 74.

[84] G. Marchesini *et al.*, Comp. Phys. Comm. **67** (1992) 465.

[85] SLD Collaboration, K. Baird, *Measurements of $A_{\rm LR}$ and $A_\ell$ from SLD*, talk presented at ICHEP 98, Vancouver, B.C., Canada, 23-29 July, 1998.

[86] Calibration Working Group, contributed paper to the 29th International Conference on High-Energy Physics (ICHEP 98), LEP Energy Note 98/02.

[87] ALEPH Collaboration, *Measurement of the W Mass in $e^+e^-$ Collisions at 183 GeV*, ALEPH note 98-058 CONF-98-030.

[88] DELPHI Collaboration, *Measurement of the W boson mass and width in $e^+e^-$ collisions at $\sqrt{s}$ = 183 GeV*, DELPHI note 98-85 CONF 153.

[89] L3 Collaboration, *Measurement of the Mass and Width of the W Boson in $e^+e^-$ Interactions at LEP*, L3 note 2277.

[90] OPAL Collaboration, *Measurement of the mass of the W-boson from direct reconstruction*, OPAL Physics Note PN331.

[91] ALEPH Collaboration, *WW cross section and W branching ratios at $\sqrt{s}$ = 183 GeV*, ALEPH note 98-019 CONF-98-009.

[92] DELPHI Collaboration, *W-pair Production cross-section and W branching ratios in $e^+e^-$ interactions at 183 GeV*, DELPHI note 98-80 CONF 148.

[93] L3 Collaboration, *Measurement of W-Pair Cross Sections and W-Decay Branching Fractions at LEP*, L3 note 2276.

[94] OPAL Collaboration, *Measurement of the W-pair production cross section and triple gauge boson couplings at LEP*, OPAL Physics Note PN354.

[95] The Particle Data Group, C. Caso et al., E. Phys. J. **C3** (1998) 1.

[96] ALEPH Collaboration, *Measurement of $|V_{cs}|$ in hadronic W decays with the ALEPH detector* , ALEPH note 98-011 CONF-98-001.

[97] DELPHI Collaboration, *Measurement of $|V_{cs}|$ using W-decays at LEP 2*, DELPHI note 98-107 CONF 174.

[98] L3 Collaboration, *Measurement of $W \to cs$ and direct determination of $|V_{cs}|$* , L3 note 2232.

[99] OPAL Collaboration, *Measurement of $R_c^W$ in $e^+e^- \to W^+W^-$ at $\sqrt{s} \approx$ 183 GeV*, OPAL Physics Note PN355.

[100] K. Gaemers and G. Gounaris, Z. Phys. **C 1** (1979) 259.

[101] K. Hagiwara, S. Ishihara, R. Szlapski, and D. Zeppenfeld, Phys. Lett. **B 283** (1992) 353;
K. Hagiwara, S. Ishihara, R. Szlapski, and D. Zeppenfeld, Phys. Rev. **D 48** (1993) 2182.

[102] M. Bilenky, J. L. Kneur, F. M. Renard and D. Schildknecht, Nucl. Phys. **B 409** (1993) 22;
M. Bilenky, J. L. Kneur, F. M. Renard and D. Schildknecht, Nucl. Phys. **B 419** (1994) 240.

[103] I. Kuss and D. Schildknecht, Phys. Lett. **B 383** (1996) 470.

[104] G. Gounaris and C. G. Papadopoulos, Eur. Phys. J. **C2** (1998) 365.

[105] G. Gounaris *et al.*, in *Physics at LEP 2*, Report CERN 96-01 (1996), eds G. Altarelli, T. Sjöstrand, F. Zwirner, Vol. 1, p. 525.

[106] The DELPHI Collaboration, P. Abreu *et al.*, Phys. Lett. **B 397** (1997) 158;
The DELPHI Collaboration, P. Abreu *et al.*, Phys. Lett. **B 423** (1998) 194;
The DELPHI Collaboration, DELPHI 98-94/CONF 162.

[107] The L3 Collaboration, M. Acciari *et al.*, Phys. Lett. **B 398** (1997) 223;
The L3 Collaboration, M. Acciari *et al.*, Phys. Lett. **B 413** (1998) 176;
The L3 Collaboration, *Measurement of the Triple Gauge Couplings of the W Boson at LEP* L3 Note 2302, July 1998.

[108] The OPAL Collaboration, K. Ackerstaff *et al.*, Phys. Lett. **B 397** (1997) 147;
The OPAL Collaboration, K. Ackerstaff *et al.*, Eur. Phys. J. **C 2** (1998) 597;
The OPAL Collaboration, *Measurement of the W-pair cross section and triple gauge boson couplings at LEP,* OPAL physics note PN354, July 1998.

[109] The ALEPH Collaboration, R. Barate *et al.*, Phys. Lett. **B 422** (1998) 369;
The ALEPH Collaboration, ALEPH 98-012 CONF 98-002;
The ALEPH Collaboration, ALEPH 98-023 CONF 98-013.

[110] The DØ Collaboration, S. Abachi *et al.*, Phys. Rev. **D 58** (1998) 3102.

[111] L. Maiani and P. M. Zerwas, *W Static ELM Parameters*, Memorandum to the LEP Electroweak Working Group, Aug 1998.

[112] O. Klein, *On the Theory of Charged Fields*, Proceedings, Warsaw 1938.

[113] CHARM II Collaboration, P. Vilain *et al.*, Phys. Lett. **B335** (1994) 246.

[114] UA2 Collaboration, J. Alitti *et al.*, Phys. Lett. **B276** (1992) 354.

[115] CDF Collaboration, F. Abe *et al.*, Phys. Rev. Lett. **65** (1990) 2243;
CDF Collaboration, F. Abe *et al.*, Phys. Rev. **D43** (1991) 2070.

[116] CDF Collaboration, F. Abe *et al.*, Phys. Rev. Lett. **75** (1995) 11;
CDF Collaboration, F. Abe *et al.*, Phys. Rev. **D52** (1995) 4784.
A. Gordon, talk presented at XXXIInd Rencontres de Moriond, Les Arcs, 16-22 March 1997, to appear in the proceedings.

[117] DØ Collaboration, S. Abachi *et al.*, Phys. Rev. Lett. **77** (1996), 3309;
K. Streets, talk presented at Hadron Collider Physics 97, Stony Brook, to appear in the proceedings.

[118] Y.K. Kim, talk presented at the Lepton-Photon Symposium 1997, Hamburg, 28 July - 1 Aug, 1997, to appear in the proceedings.

[119] CDF Collaboration, W. Yao, *t Mass at CDF*, talk presented at ICHEP 98, Vancouver, B.C., Canada, 23-29 July, 1998.

[120] DØ Collaboration, B. Abbott *et al.*, Phys. Rev. **D58** (1998) 052001.

[121] R. Partridge, *Heavy Quark Production and Decay (t and b Onia)*, talk presented at ICHEP 98, Vancouver, B.C., Canada, 23-29 July, 1998.

[122] CCFR/NuTeV Collaboration, K. McFarland *et al.*, Eur. Phys. J. **C1** (1998) 509.

[123] NuTeV Collaboration, K. McFarland, talk presented at the XXXIIIth Rencontres de Moriond, Les Arcs, France, 15-21 March, 1998, hep-ex/9806013. The result quoted is a combination of the NuTeV and CCFR results.

[124] S. Eidelmann and F. Jegerlehner, Z. Phys. **C67** (1995) 585.

[125] M. Steinhauser, Phys. Lett. **B429** (1998) 158.

[126] *Reports of the working group on precision calculations for the Z resonance*, eds. D. Bardin, W. Hollik and G. Passarino, CERN Yellow Report 95-03, Geneva, 31 March 1995.

[127] G. Degrassi, S. Fanchiotti and A. Sirlin, Nucl. Phys. **B351** (1991) 49;
G. Degrassi and A. Sirlin, Nucl. Phys. **B352** (1991) 342;
G. Degrassi, P. Gambino and A. Vicini, Phys. Lett. **B383** (1996) 219;
G. Degrassi, P. Gambino and A. Sirlin, Phys. Lett. **B394** (1997) 188.

[128] A. Czarnecki and J. Kühn, Phys. Rev. Lett. **77** (1996) 3955;
R. Harlander, T. Seidensticker and M. Steinhauser, Phys. Lett. **B426** (1998) 125.

[129] Electroweak libraries:
ZFITTER: see Reference 52;
BHM (G. Burgers, W. Hollik and M. Martinez): W. Hollik, Fortschr. Phys. **38** (1990) 3, 165; M. Consoli, W. Hollik and F. Jegerlehner: Proceedings of the Workshop on Z physics at LEP I, CERN Report 89-08 Vol.I,7 and G. Burgers, F. Jegerlehner, B. Kniehl and J. Kühn: the same proceedings, CERN Report 89-08 Vol.I, 55;
TOPAZ0 Version 4.0i: G. Montagna, O. Nicrosini, G. Passarino, F. Piccinni and R. Pittau, Nucl. Phys. **B401** (1993) 3; Comp. Phys. Comm. **76** (1993) 328.
These computer codes have upgraded by including the results of [126] and references therein. ZFITTER and TOPAZ0 have been further updated using the results of references 127 and 128. See, D. Bardin and G. Passarino, *Upgrading of Precision Calculations for Electroweak Observables*, CERN-TH/98-92, hep-ph/9803425.

[130] T. Hebbeker, M. Martinez, G. Passarino and G. Quast, Phys. Lett. **B331** (1994) 165;
P.A. Raczka and A. Szymacha, Phys. Rev. **D54** (1996) 3073;
D.E. Soper and L.R. Surguladze, Phys. Rev. **D54** (1996) 4566.

[131] M. L. Swartz, Phys. Rev. **D53** (1996) 5268.

[132] A.D. Martin and D. Zeppenfeld, Phys. Lett. **B345** (1994) 558.

[133] H. Burkhardt and B. Pietrzyk, Phys. Lett. **B356** (1995) 398.

[134] R. Alemany, *et al.*, Eur. Phys. J. **C2** (1998) 123.

[135] M. Davier and A. Höcker, Phys. Lett. **B419** (1998) 419.

[136] J.H. Kühn and M. Steinhauser, *A theory driven analysis of the effective QED coupling at* $m_{\rm Z}$, hep-ph/9802241.

[137] J. Erler, Phys. Rev. **D59**, (1999) 054008.

[138] P. McNamara, *The Search for the Standard Model Higgs Boson at LEP*, talk presented at ICHEP 98, Vancouver, B.C., Canada, 23-29 July, 1998.